Study of the murine Stem Cell E3 Ubiquitin ligase Lin41 in Development and Postnatal stages through the characterization of Lin41 Gene Trap and conditional Knockout models

Inaugural-Dissertation
to obtain the academic degree
Doctor rerum naturalium (Dr. rer. nat.)
submitted to the Department of Biology, Chemistry and Pharmacy of
Freie Universität Berlin.

by
Elisa Cuevas García
from Madrid, Spain.

Berlin, 2013

1. Gutachter: Dr. F. Gregory Wulczyn

2. Gutachter: Prof. Dr. Stephan Sigrist

Disputation am: 02.12.2013

Acknowledgments

I want to thank my supervisor, Dr. Gregory Wulczyn, for giving me the opportunity to join his lab and develop this great project. Thank you for the discussions, the constant questions, and for not giving up when it got hard. It was worth it.
Thanks to former and present AG Wulczyn: Heiko, Aga, Marlis, Daniel, Ele, Fred, Anna and Duong. I could not wish for a better group to share these years in the lab. Thanks for listening and having always a word to support my project, but more for the bench time, the laughter, the mensas, and the parties. Anna, thank you for always having the time, the patience to come with a cup of coffee and deal with my German allergy. For being a great friend.
Thanks to all people in the Institute of Cell and Neurobiology for making it a great place to spend all this time, for helping out in seminars, in small talks and in nights out. Olaf and Thorsten, thanks for always having time (and patience) to discuss Southern blots and the give me good advises. Thanks, of course, to our collaborators, in particular to Dr. Geert Michel and Ellen Na, for their implication and enthusiasm. I want to thank as well the members of the GRK 1123 for funding and support, and for all the friends I found there.

Gracias a toda la gente que me ha ayudado, querido, recordado y soportado durante todos estos años: a mis chicas de Pontevedra, a mi gente de Madrid y del CIB. Gracias a Isa por prestarme Berlín y a Pao por enseñármelo. No me cabéis todos, pero sabéis quiénes sois. Gracias a mis primeros mentores: Samartín, mi primo Miguel, Antón Masa. A toda mi familia por quererme y apoyarme tanto, en especial a mi hermana, mi padre, y sobre todo a mi madre: sin tu cariño y tu apoyo nunca, nunca hubiese conseguido llegar hasta aquí.

A mi tía Teresa.

Nacho, gracias por haber estado ahí durante estos años. Tantos trenes, aviones, tantos kilómetros y tantos planes que al final se han ido cumpliendo uno a uno. Por todos los planes que aún nos quedan. Gracias por ser mi compañero, mi sensei, mi amigo y mi media langosta. Esta tesis es para esa estantería que me prometiste.

Index

Abbreviations

^{32}P	Phosphorus-32
aa	Amino acid
amp^R	Ampicilin resistance
ATP	Adenosine-5'-triphosphate
bp	Base pair
BrdU	Bromodeoxyuridine
BSA	Bovine serum albumin
C. elegans	*Caenorhabditis elegans*
Ci	Curie
cKO	Conditional knockout
Cm	Chloramphenicol
CNS	Central nervous system
DABCO	1,4-diazabicyclo[2.2.2]octane
DAPI	4',6-diamidino-2-phenylindole
DCX	Doublecortin
DMEM	Dulbecco's modified Eagle's medium
DNA	Deoxyribonucleic acid
DNA	Deoxyribonucleic acid
dNTPS	Deoxynucleotidetriphosphat
D. melanogaster	*Drosophila melanogaster*
E. coli	*Escherichia coli*
EGF	Epidermal growth factor
EpC	Ependymal culture
EUCOMM	European Conditional Mouse Mutagenesis Program
FACS	Fluorescence-Activated Cell Sorter
FBS	Fetal bovine serum
FGF	Fibroblast growth factor
g	Gram
GFAP	Glial fibrillary acidic protein
gt	Gene Trap
h	Hour
HEK	Human Embryonic Kidney 293 cell line
ICC	Immunocytochemistry
ICM	Inner cell mass
IHC	Immunohistochemistry
ISH	In situ hybridization
Kan^R	Kanamycin (prokaryotes) resistance
kDa	Kilo dalton
l	Liter
L/A Switch	Larva to adult switch
Lin41	Lineage 41
M	Molar
MEFs	Mouse embyonic fibroblasts
mES cells	Mouse embryonic stem cells
MilliQ	Ultrapure water
min	Minute

miRISC	Micro RNA induced silencing complex
miRNA	MicroRNA
mRNA	Messenger RNA
Neo^R	Neomycin (eukaryotes) resistance
nm	Nanometer
NSCs	Neural Stem Cells
NSPs	Neurospheres
nt	Nucleotide
O/N	Over night
OB	Olfactory bulb
P19	Mouse embryonic carcinoma cell line
PBS	Phospate Buffered Saline
PCR	Polymerase chain reaction
PFA	Paraformaldehyde
PolyA	Polyadenylation signal
Pre-miRNA	Precursor miRNA
Pri-miRNA	Primary miRNA
PSA-NCAM	Polysialylated neuronal cell adhesion molecule
R/T	Room temperature
RMS	Rostral Migratory Stream
RNA	Ribonucleic acid
rpm	Revolutions per minute
RT-PCR	Reverse transcription PCR
SDS	Sodium dodecyl sulfate
sec	Second
SGZ	Subgranular Zone
Shh	Sonic Hedgehog
ß-Gal	ß-Galactosidase
SSC	Solution of sodium chloride and sodium citrate
SVZ	Subventricular Zone
TBE	Tris/Borate/EDTA buffer
TBE	Tris-borate-EDTA buffer
TEMED	N,N,N',N'-Tetramethylethylenediamine
Tris	Tris- hydroxymethyl- aminomethane
Tris	Tris(hydroxymethyl)aminomethane
U	Units
Ub	Ubiquitin
UTR	Untranslated region
UV	Ultraviolet light
v	Volume
V	Volts
VZ	Ventricular zone
w	Weight
µ	Micro

Abstract

Lin41 gene encodes a member of the Trim-NHL protein sub-family, discovered in *C. elegans* as a master regulator of development. *Lin41* is a target of the microRNA let-7, and this regulatory relationship is conserved throughout bilateral animals. Like other Trim-NHL proteins, LIN41 was shown to be an E3 ubiquitin ligase influencing the microRNA biogenesis, although its function in other biological contexts remains largely unknown.

The present dissertation focused on the study of the mouse ortholog of *Lin41* in different contexts, mainly using a *Lin41* gene trap line as a genetic model.

Using this gene trap line, I characterized the expression pattern of *Lin41* during mid-gestational stages of the mouse embryo. In accordance to subsequently published studies, I described *Lin41* ubiquitous expression at E8.5, which becomes restricted to structures like neuroepithelium and limb buds between E10.5 and E12.5, and is progressively lost at E13.5. In the absence of functional LIN41, mouse embryos fail to properly develop the neural tube and die around E9.5. I am the first to reveal Lin41 expression in the adult central nervous system (CNS), where is restricted to the ependymal cells of the lateral ventricle, and show its expression in an ependymal primary culture model. Due to the relationship of these cells with the subventricular zone (SVZ) neurogenic niche, the pluripotency-related LIN41 protein might be of relevance for the process of adult neurogenesis.

As a new tool for the study of *Lin41* in pluripotency and neural differentiation, mouse embryonic stem (mES) cell lines were derived from the gene trap mouse line. Using *Lin41* null ES cells, I uncover that *Lin41* is dispensable for self-renewal and pluripotency factor profile maintenance. Additionally, to achieve *Lin41* mutation in a precise spatial-temporal manner, and to circumvent the embryonic lethality, we have generated the first known conditional knockout mouse model. In combination with Cre-expression under active promoters in development and adult ependymal cells we will be able to specify the importance of *Lin41* in the mammalian organism. This conditional knockout provides a new, versatile tool in addition to the mES cell lines to perform developmental and postnatal specific studies of *Lin41*.

Zusammenfassung

Das *Lin41*-Gen kodiert für ein Protein der Trim-NHL-Familie und wurde erstmals in *Caenorhabditis elegans* als elementarer Faktor für dessen Entwicklung beschrieben. *Lin41* ist zudem das Zielgen der let-7 miRNA und diese regulatorische Beziehung ist durch das gesamte bilaterale Tierreich hinweg konserviert. Wie auch andere Mitglieder der Trim-NHL-Proteinfamilie besitzt LIN41 eine E3-Ubiquitinligase-Aktivität durch welche es direkt die miRNA-Funktion beeinflussen kann. Im Bezug auf andere biologische Fragestellungen ist seine Funktion hingegen noch ungeklärt.

Die hier vorliegende Dissertation konzentriert sich auf die Untersuchung des *Lin41*-Mausorthologs in verschiedenen Kontexten und verwendet hierzu hauptsächlich eine *Lin41*-„Gene-Trap-Knock-out"-Mauslinie. Mit Hilfe dieses genetischen Modells wurde die *Lin41*-Expression in mittleren embryonalen Entwicklungsstadien der Maus untersucht. In Übereinstimmung mit später publizierten Studien konnte *Lin41*-Expression im gesamten Embryo bis Embryonaltag (E) 8.5 gezeigt werden. Im weiteren Verlauf der Entwicklung, zwischen E10.5 und E12.5, ist die Expression auf das Neuroepithel und die Extremitätenanlagen begrenzt und bis zum E13.5 vollständig verschwunden. Mausembryonen ohne funktionelles LIN41 besitzen ein fehlgebildetes Neuralrohr und sterben am E9.5. Es konnte zudem erstmals *Lin41*-Expression im adulten zentralen Nervensystem (ZNS) gezeigt werden. Hier ist es in Ependymazellen der Lateralventrikelwand exprimiert und auch in einem ependymalen Zellkulturmodell konnte *Lin41*-Expression nachgewiesen werden. Aufgrund der Nähe der Ependymazellen zu Zellen der adulten Stammzellnische der Subventrikulärzone (SVZ) könnte das pluripotenz-assoziierte LIN41-Protein einen Einfluss auf die adulte Entstehung von Neuronen haben.

Als zusätzliche Möglichkeit *Lin41s* Einfluss auf Pluripotenz sowie neuronale Differenzierung zu untersuchen, wurden embryonale Stammzelllinien (ES) der „Gene-Trap"-Mauslinie etabliert. Mit Hilfe dieser „Knock-out"-ES Zellen konnte gezeigt werden, dass *Lin41* keinen Einfluss auf die Zellvermehrung oder die Level von Pluripotenzfaktoren hat. Um die embryonale Lethalität der „Knock-out"-Mäuse zu umgehen und das Fehlen von *Lin41* an verschiedenen Zeitpunkten und Orten zu charakterisieren, wurde das bisher erste konditionale „Knock-out"–Mausmodell

erstellt. In Kombination mit Cre-Rekombinase-Expression unter der Kontrolle verschiedener Promotoren, die während der Entwicklung aktiv sind, und durch die adulten Ependymazellen wird es möglich sein, die Funktion *Lin41s* im Säugetier besser zu verstehen.

Die konditionale Deletion des *Lin41*-Allels bietet in Ergänzung zu den ES-Zelllinien vielfältige Möglichkeiten *Lin41* während der Entwicklung und im adulten Organismus zu untersuchen.

1 Introduction

1.1 Discovery of miRNAs and heterochronic genes

1.1.1 *C. elegans*: heterochronic gene pathways during larval development

The control of adequate growth and development of multicellular organisms depends on a tight regulation in time and space of genes involved in cell cycle control, proliferation, differentiation and morphogenesis. Genes that regulate the correct timing of developmental pathways are called heterochronic genes (Vella et al. 2004; Ambros & Horvitz 1984; Reinhart et al. 2000), and are of great importance not only at single organism level, but also in the evolutionary events that lead to origination of new species (Slack et al. 2000; Moss 2007; Ambros & Horvitz 1984; Vella et al. 2004).

The nematode *Caenorhabditis elegans* (*C. elegans*) development divides in discreet and defined larval (L1 to L4) and adult stages. This characteristic makes it a valuable model for the study of heterochronic genes, compared to the more complex and continuous changing pattern of vertebrates. The study of developmental mutations in *C. elegans* led to the identification of the heterochronic genes, their expression patterns, and the pathways in which they interact.

Four heterochronic genes were first identified in a screen performed by Ambros and colleagues: *lin-4*, *lin-14*, *lin-28*, and *lin-29*. Their misexpression resulted in failures in specific postembryonic program events known as the “larva-to-adult switch” (L/A switch), which comprise cell division, formation of the adult cuticle, cell fusion, and cessation of the molting cycle. These mutants display either late juvenile (blocking of maturation events) or precocious mature phenotypes (early execution of differentiation programs), depending on the program affected (Figure 1) (Ambros 1989).

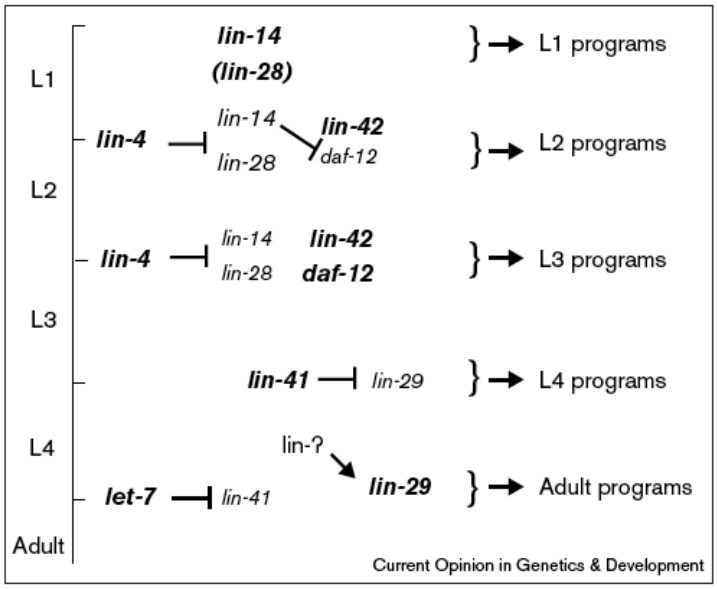

Figure 1. Heterochronic genes network in *C. elegans* development. *C. elegans* has four defined larval stages, each one determined by a specific molecular program, as well as the larva to adult transition. From Ambros *et al.* 2000.

Lin-14 and *lin-28* are key regulators during the first three larval stages (L1 to L3). Their expression is high in early L1 stage, but is progressively downregulated during the transition to L2. In the same time frame *lin-4* expression is upregulated, repressing both *lin-14* and *lin-28*. This tight control is essential in the switches of both L1/L2 and L2/L3 phases: *lin-28* and *lin-14* null mutants display precociously specialized characteristics that correspond to L4 phase, while deletions in *lin-4* produce a reiterative phenotype of juvenile features (Moss et al. 1997; Ambros 2000; L. P. Lim, Lau, et al. 2003b; Wightman et al. 1993). A second network regulates the late developmental to adult events: it involves *lin-29* (a transcription factor that promotes adult identity), *lin-41*, and *let-7*. *Lin-41* negatively regulates *lin-29*, and at L4 stage let-7 represses *lin-41* mRNA translation, thereby promoting the final L/A specification (Ambros 2000). This way, increasing *let-7* levels indirectly promotes *lin-29* transcription factor through *lin-41* repression, to trigger the last maturation events. Experiments involving *lin-41* null mutations showed high levels of LIN-29 protein abnormally early, at L3 or even L2, accompanied by a precocious expression of adult fates. In parallel, *lin-41* mutation rescued the phenotype of *let-7* defective mutants (that display a late juvenile phenotype), indicating a direct regulation of *lin-41* by *let-7*, as explained in more detail in section 1.1.3.2 (Figure 2) (Slack et al. 2000).

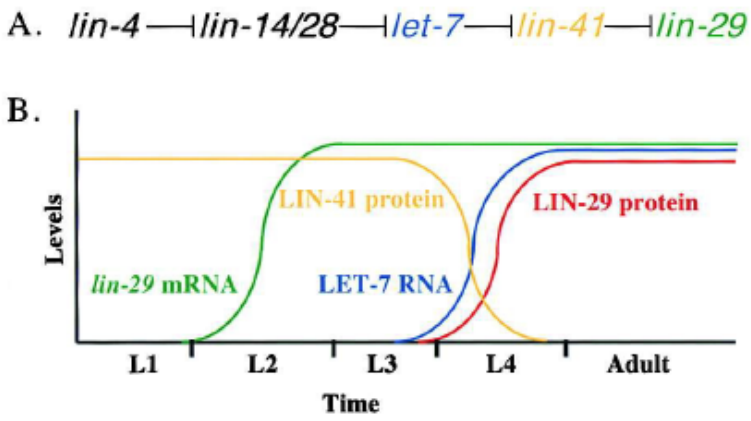

Figure 2. Heterochronic gene expression as a function of developmental stage. A. Model of heterochronic genes interactions. B. Expression of heterochronic genes mRNA and protein products, suggesting time-frames of post-transcriptional regulation. From Slack *et al.* 2000.

1.1.2 MicroRNAs: *Lin-4* and *let-7*

MicroRNAs (miRNAs) are small, non coding RNAs of about 22 nucleotides (nt) length, with a major role in post-transcriptional regulation. Identified during the study of the heterochronic pathways in *C. elegans*, their discovery established a new paradigm in post-transcriptional gene regulation.

Research on *lin-4* involved the study of the mutant phenotypes, as well as the cloning of the gene for molecular characterization. Surprisingly, the gene product was not a protein or peptide, but two RNA sequences (of 21 and 61 nt), named *lin-4*S (small) and *lin-4*L (large). *Lin-4*S showed a non-perfect complementarity to the 3' untranslated region (3'UTR) of *lin-14* and *lin-28* genes, suggesting an interaction region mediating the repression (R. Lee et al. 2004; R. C. Lee et al. 1993). In fact, two different deletion mutations in the 3'UTR of *lin-14* resulted in an abnormal high level of protein after L2 stage, indicating a failure in the downregulation of the gene (Wightman et al. 1991).

For several years *lin-4* was the only known small RNA with this type of regulatory function, and it was considered an exceptional case. It was not until 2000 when *let-7*, previously identified as responsible for the regulation of the L/A switch in *C. elegans* development, was shown to have similar characteristics. The gene product is a ~ 21 nt RNA, complementary to elements in the 3'UTR sequences of

the genes *lin-14*, *lin-28*, *lin-41*, *lin-42* and *daf-12*, an indication of a possible regulation by *let-7* via direct RNA-RNA interaction (Reinhart et al. 2000).

The publication of this second small RNA, let-7, and its regulatory function in *C. elegans* in addition to lin-4, led to the idea of miRNA activity as a major mechanism for post-transcriptional regulation in animals. Following publications reported the high conservation of *let-7* across species, including mouse and human (Pasquinelli et al. 2000); soon afterwards numerous new miRNAs were identified, not only in the developmental context, but directing genetic programs in disparate physiological processes: cell proliferation, apoptosis, tissue differentiation, and metabolism (L. P. Lim, Glasner, et al. 2003a; Ambros 2004; Plasterk 2006; Valencia-Sanchez et al. 2006). MiRNAs constitute between 1 and 2% of genes in invertebrates and humans (Bartel 2009). As each of them might target the mRNA of more than one gene, their regulatory potential is vast: more than 60% of protein-coding genes are computationally predicted to be miRNA targets, based on conserved base-pairing between the 3′ UTR and the sequence of nt 2-8 in the 5’ of the miRNA 5′ region of the miRNA, called the seed sequence (Friedman et al. 2009).

1.1.2.1 MicroRNA biogenesis pathway

Molecular processing of miRNAs from the gene to the mature, active form comprises several steps in nucleus and cytoplasm. Two intermediate molecules are generated, and their processing requires the coordinated activity of two protein complexes. A scheme of this biogenesis is summarized in Figure 3.

Transcription

Around half of the miRNAs are located close to other miRNAs in the genome, forming clusters. Most are found in intergenic regions, thereby belonging to autonomous transcriptional units that generate polycistronic products. They also can be exonic miRNA in non-coding transcription units; intronic miRNAs in non-coding transcription units or intronic miRNAs in protein-coding transcription units. Regardless of their location, miRNAs are transcribed from RNA polymerase II, although it is possible that other polymerases transcribe a small number of miRNAs. The transcript generated may be several kbp long and contains a stem-

loop structure; it has 5'CAP and polyadenylation (polyA) tail, and is named pri-miRNA (Bartel 2004).

Maturation

Pri-miRNAs are subjected to a first processing step in the nucleus; the nuclear RNAseIII Drosha, together with DGCR8, form a molecular complex called Microprocessor, which trims both strands of the duplex RNA at the base of the stem loop, producing a hairpin intermediate structure called pre-miRNA (Y. Lee et al. 2003).

The pre-miRNA molecule is exported to the cytoplasm through the nuclear pores, in an energy-consuming process mediated by Exportin-5 (Lund et al. 2004). Afterwards, the cytoplasmic RNAse III endonuclease Dicer, associated to either TRBP or PACT, recognizes the double strand and cleaves it two helical turns from the base of the stem loop, generating a ~22 nucleotide duplex. The duplex is formed by the future mature miRNA, and a semi-complementary sequence called miRNA* (Y. Lee et al. 2003; Winter et al. 2009).

RISC Assembly

After these maturation processes, the activity of miRNAs is similar to other known post-transcriptional gene silencing mechanisms like RNA interference (RNAi). Following the Dicer processing step, the RNA duplex is loaded in a multi-protein aggregate forming the miRISC (microRNA-induced silencing complex). The core component of RISC is always a member of the Argonaute (*Ago*) protein family; mammals have 4 *Ago* genes (*Ago1-4*), but AGO2 is the only one with both RNA binding domain for single and double strand (PAZ,) and endonuclease domain (PIWI) activity (Hammond et al. 2001). Other components of RISC vary among species, but might be TNRC6 (also known as GW182) in mammals, heat shock proteins, or putative helicases like MOV10 (Cook et al. 2004). RISC proteins separate the two strands and load the functional one. Usually, the miRNA mature form is loaded, and miRNA* is the so-called passenger strand that is discarded and degraded. The miRISC uses the sequence of the loaded strand as a guide to identify and bind the target mRNA and execute translational repression (Figure 3) (Zamore 2002). The seed sequence, generally recognizes a sequence of the 3'UTR in the target mRNA, and execute downregulation via translational

repression or mRNA decay, depending on the degree of identity between the two sequences or modifications like adenylation (Zeng et al. 2003; C.-Y. A. Chen et al. 2009; Huntzinger & Izaurralde 2011). Reviews of miRNA biogenesis and function: (V. N. Kim 2005; Bartel 2004; Winter et al. 2009).

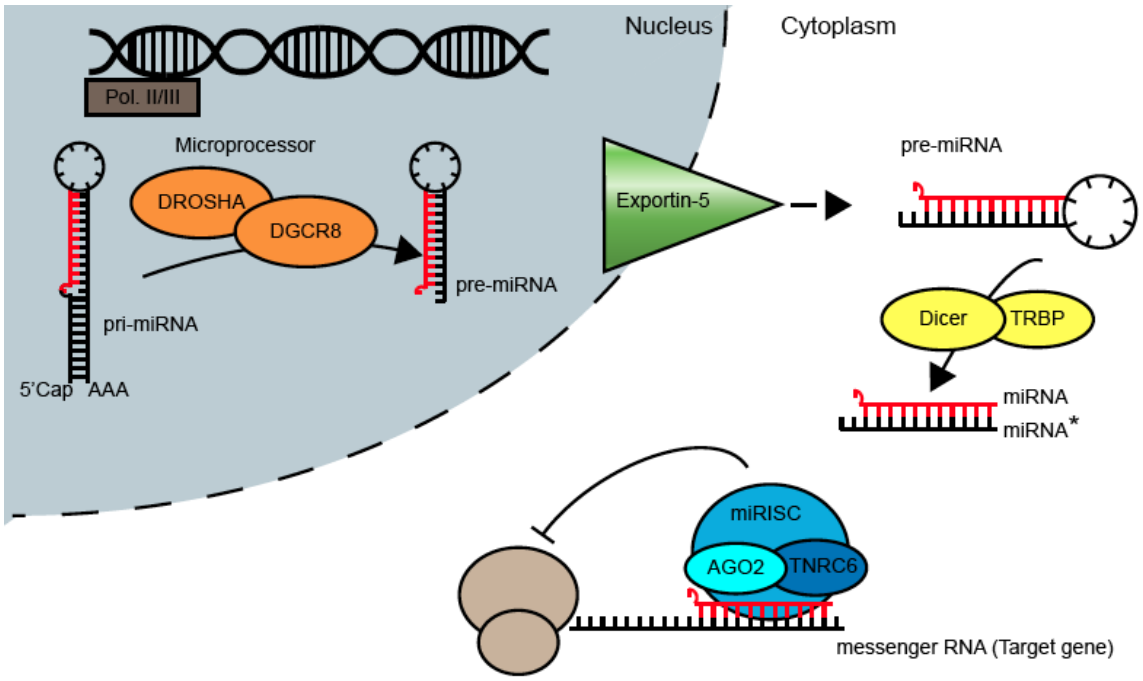

Figure 3. Scheme of miRNA biogenesis pathway. Adapted from Winter *et al*. 2009.

1.1.3 Evolutionary conservation of *let-7*, *lin-41* and their regulation.

1.1.3.1 *Let-7* miRNAs

Let-7 microRNA receives its name from the phenotype *let*hal-*7* in the mutant *C. elegans*, where it was first identified. It is one of the miRNAs with strongest conservation across animal species, suggesting a high relevance of its functions. Vertebrates, ascidians, hemichordates, mollusks, annelids and arthropods have one or more copies of *let-7*, while is absent from basal metazoans, like cnidarians and poriferans, as well as plants or unicellular organisms (Pasquinelli et al. 2000). *Let-7* is often present in numerous copies throughout the genome, and is a key regulator of physiological processes from cell cycle regulation to neural specification or cancer disease (Roush & Slack 2008).

Let-7 family members are defined by the seed sequence, essential for recognition and repression of the target gene. This sequence is conserved within the family of

each miRNA, and the different isoforms may vary in the rest of the nucleotides. To distinguish them, a letter follows the miRNA name of members, and when one isoform is present in a different genomic location, a number follows the letter. For example, vertebrates have let-7a to let7-k members, and let-7a has three precursors that produce identical mature miRNAs let-7a (let-7a-1, let-7a-2, let-7a-3) (Roush & Slack 2008). *C. elegans* has nine members of the let-7 family: *let-7*, *mir-48*, *mir-84*, *mir-241*, *mir-265*, *mir-793*, *mir-794*, *mir-795* and *mir-1821* (Pasquinelli et al. 2000; Pasquinelli et al. 2003; Ambros 2004; Valencia-Sanchez et al. 2006; Roush & Slack 2008). Single mutants of closely related family members *mir-48*, *mir-84*, and *mir-241* show similar features, but with low penetrance, that increases in double and triple mutations, an indication of possible functional redundancy (Abbott et al. 2005).

As mentioned above, the last stage of larval development or transition to adult in *C. elegans* is triggered by the activity of *lin-29* gene. Let-7 is necessary for *lin-29* upregulation and successful adult transition. *Let-7* complementary sites found in the *lin-41* 3'UTR suggests that *let-7* influences specific expression of LIN-29 protein in the L/A switch by downregulating *lin-29* repressor *lin-41* at the mRNA level(Slack et al. 2000). *Let-7* mutations cause reiteration of L4 stage cell lineages and a highly penetrant lethal vulva bursting phenotype at the L4/adult molt, presumably because of temporal misspecification of hypodermal tissues (Reinhart et al. 2000). The *lin-41* mutations caused recessive precocious heterochronic expression of an adult-specific hypodermal cell fate. On the contrary, animals carrying a higher than normal dosage of *lin-41*, showed a retarded phenotype in the hypodermis, and in some cases, the animals died by bursting through the vulva, resembling the lethality caused by loss of *let-7* function. This epistatic relationship, partial rescue of the *let-7* mutant phenotype by *lin-41* disruption is indicative of a genetic interaction, with *lin-41* acting downstream *let-7* (Reinhart et al. 2000).

Drosophila melanogaster (*D. melanogaster*) has only one *let-7* gene, located next to *miR-125* (a *lin-4* ortholog) and other miRNAs in a polycistronic locus. They maintain a temporal hierarchy during develolpment, *miR-125* is expressed first, followed by *let-7*, that is expressed in pulses from the third larval instar

(developmental stage) on. *Let-7* depletion causes behavioral defects in the adult, affecting flight, motility and fertility. Some studies consider the possibility of transcription of precursor and mature forms of *let-7* to be under control of the developmental hormone ecdysone, which is expressed in pulses that coincide with each peak of *let-7* expression (Büssing et al. 2008; Sokol et al. 2008; Caygill & Johnston 2008; Sempere et al. 2002; Sempere et al. 2003). In zebrafish, let-7 is detectable between 24-48 h after fertilization, persisting throughout adulthood (Pasquinelli et al. 2000). In vertebrate embryos, embryonic stem cells or embryocarcinoma lines *miR-125* and *let-7* mature active forms are largely absent, and they start to be expressed upon differentiation. Like in *C. elegans* and zebrafish, temporal hierarchy is maintained, and *miR-125* expression precedes *let-7* (Y. S. Lee et al. 2005; Schulman et al. 2005). In general, vertebrate let-7 miRNA family members are found in cells undergoing differentiation or highly differentiated, like neurons. In addition, reduced levels of let-7 are found in a number of human cancers, reinforcing the idea of *let-7* as a regulator of post-mitotic and specification events (Esquela-Kerscher & Slack 2006; Hatfield & Ruohola-Baker 2008; Büssing et al. 2008).

1.1.3.2 *Lin-41* as *let-7* target

Let-7 and other miRNAs have coevolved with their target genes from *C. elegans* to humans, reinforcing the evolutionary relevance of these pathways and regulatory mechanisms (Nimmo & Slack 2009). In particular, there is a notable conservation in the targeting of *lin-41* and *lin-28* by miRNA let-7, and the role of these two proteins in undifferentiated cells and early stages of development (Y. S. Lee et al. 2005; Yokoyama et al. 2008; L. Wu & Belasco 2005; Yang & Moss 2003). LIN-41 is a member of the large Trim protein family (Reymond et al. 2001). This protein family is named after the Tri-partite Motif characteristic of their members, comprised of an N-terminal RING finger (a zinc-binding domain thought to be involved in protein–and/or protein–nucleic acid interactions), one or two B-boxes (additional zinc binding domains) (Freemont 1993), and a Coiled-coil domain. LIN-41 contains a C-terminal domain called NHL, consisting on six copies of a 44 aa motif that forms a ß-propeller structure. The NHL domain was named after the three first proteins where it was identified: NCL-1 (Frank & Roth 1998), HT2A (Fridell et al. 1995), and LIN-41 proteins (Slack & Ruvkun 1998). This domain is

often found associated with Trim proteins, forming the Trim-NHL protein sub-family (Meroni & Diez-Roux 2005).

Lin-41 orthologs have been identified in human, mouse, rat and zebrafish (Lancman et al. 2005), although the gene nomenclature has been subject to several variations: *lin-41* was used in nematode and zebrafish, while for mouse the names *mLin-41* or *mLin41*, and *Trim71* (tripartite motif 71) were preferred, and the latter one was also used for the human ortholog. In the rest of this study I refer to the mouse gene as *Lin41*, to maintain consistency and emphasize its evolutionary conservation.

C. elegans lin-41 gene has 15 exons, and is predicted to encode two nearly identical proteins, LIN-41A and LIN-41B, that differ in 3 aa. The 3'UTR contains six potential let-7 binding sites, where the post-transcriptional regulation by RNA-RNA interaction occurs, although two sites have been shown to be necessary and sufficient for downregulation of *Lin-41* 3'UTR reporter constructs (Reinhart et al. 2000; Slack et al. 2000; Vella et al. 2004). *Lin-41* expression in *C. elegans* is prominent in neurons, body wall and pharyngeal muscles from embryogenesis to adulthood and in the lateral hypodermal seam cells until L4, when its expression reduces due to a surge in let-7 expression at the L/A switch. It is predominantly expressed in the cytoplasm, and its detailed function has not yet been unraveled, although the mutant phenotypes suggest a role in cell proliferation control (Slack et al. 2000).

Lin41 regulation by miRNAs was investigated in chicken initially by bioinformatic approaches, revealing that binding sites for let-7 and other miRNAs, like the lin-4 ortholog miR-125b, are conserved in the 3'UTR. Northern blot analysis of the limb extracts showed reciprocal expression of these miRNA species and *Lin41* mRNA, although this does not directly prove these miRNAs are necessary or sufficient for *Lin41* regulation (Lancman et al. 2005). Simultaneously, a second work reproduced *Lin41* expression pattern in mouse limbs during embryogenesis, with a drastic reduction after E11.0, when let-7 and miR-125 expression peak in this tissue, suggesting that, just like in nematodes, miRNA regulation is the responsible for temporal control of *Lin41* (Schulman et al. 2005). Let-7 regulation of *Lin41*

mRNA via 3'UTR binding sites was also demonstrated in zebrafish (Lin et al. 2007).

Using *C. elegans* genes with let-7 complementarity in the 3'UTR, some groups screened the human genome to identify conserved target genes. Human ortholog of *Lin41*, *Trim71*, was shown to be a target of let-7, although no specific function has yet been reported for it (Lin et al. 2007). In addition, Johnson and colleagues showed that let-7 regulates human RAS oncogenes (orthologs to *C. elegans* let-60/RAS). In addition, abnormal low levels of let-7 and high levels of RAS were identified in lung cancer samples, suggesting a role for this regulatory mechanism in cancer control (Johnson et al. 2005).

Taken together, these publications provide strong evidence of a developmental time hierarchy, and moreover, of a regulatory mechanism involving let-7 miRNA and its target *Lin41*, conserved throughout evolution (Lin et al. 2007).

1.2 *Lin41* in vertebrates

1.2.1 Embryonic expression pattern in chick and mouse limb development

The conservation of miRNAs and their targets across animal species raised the question of whether the entire *C. elegans* heterochronic regulatory pathway might be maintained in complex systems, such as vertebrate embryonic development.

Two papers published in parallel in 2005 addressed the expression of *Lin41* in embryonic development in chicken and mouse, in particular during limb specification.

In wild type CD-1 mouse embryos, strong *Lin41* expression was found from embryonic day 8.5 (E8.5) on, gradually decreasing until E11.5, and undetectable afterwards. This temporal pattern was inversely correlated to miR-125 and let-7 miRNAs, that commence at E9.5 and 10.5 respectively, and peak around E12.5, remaining stably expressed afterwards; this suggests a regulatory relationship in embryogenesis between *Lin41* and miRNAs, equivalent to the one displayed by *C. elegans* (Schulman et al. 2005). In particular, *Lin41* is almost ubiquitously expressed by E8-9.5, with exception of the heart tissue. From that time on expression declines and is restricted to areas like the branchial arches, facial

prominence, tail bud, dorsal root ganglia and eyes, besides the dynamic expression of hind and forelimbs. Limb formation involves three stages: in the first one thickened mesoderm protrudes from the body wall, and *Lin41* is highly and evenly expressed. In the second stage, *Lin41* becomes restricted to the distal posterior area of the limb; interestingly, let-7 was reported to be expressed on the opposite side, anteriorly, at the same time (Mansfield et al. 2004; Lancman et al. 2005). In the third stage, *Lin41* is only detectable in the very distal tip of the limb, before the signal disappears. This presumable downregulation by the miRNA occurs first in forelimbs, but happens also in hindlimbs with a slight delay (Lancman et al. 2005). Interestingly, this pattern matches the *in situ hybridization* (ISH) data for *Lin41* mRNA probe (Maller Schulman et al. 2008).

ISH analysis of chicken embryos showed a very similar pattern: pharyngeal arches, somites, frontal-nasal mass and all limbs in formation were positive for *Lin41* mRNA. This expression shows in all cases a temporal regulation, which points to specific developmental function. As well, LIN41 protein is detectable at high levels both in wing and leg, in correspondence to three phases in developmental events: ubiquitously in the mesoderm in phase one, then reducing to the distal portion, and in the third phase exclusively in the posterior distal portion of the developing digits. Two deficient models, affecting different programs in the limb development, were shown to alter *Lin41* expression. The proximal-distal axis, governed by fibroblast growth factor (FGF) signaling, and anterior-posterior axis, under Sonic Hedgehog (*Shh*) regulation, showed alterations, with *Lin41* rapidly retracting in *Shh* deficient *limbless* chicks, and only maintained at very basal levels in mouse double mutants for *Fgf4* and *Fgf6* (Sun et al. 2002; Lancman et al. 2005).

1.2.2 *Lin41* is essential in mouse, zebrafish and frog development

Prior to the first study in mouse, the zebrafish was used to study the role of *Lin41* in vertebrate development. *Lin41* was silenced by siRNA and morpholino injection, causing severely defective embryos after 24h, that displayed short trunk, deformed yolk, S-shaped tail phenotype, and perished after 48 h (Lin et al. 2007). Just like in *C. elegans*, this phenotype resembles the one of *let-7* overexpression, when injected in one-cell stage embryos of zebrafish, as well as in the frog *Xenopus tropicalis*. In addition, they demonstrated in *Xenopus* let-7 regulation of *Lin41* 3'UTR reporter constructs (Kloosterman et al. 2004).

Lin41 expression in mouse was first assessed using ISH, as mentioned in section 1.2.1. Mid-developmental embryos show a prominent *Lin41* mRNA signal in limb and tail buds, branchial arches, somites and developing neuroepithelium, which is restricted over time until disappearing at E12.5 (Schulman et al. 2005). To address the consequences of *Lin41* loss in mouse, Schulmann and colleagues generated a gene trap mouse model. This means the *Lin41* locus, located in chromosome 9, is disrupted after the first exon with a cassette that contains a *LacZ* gene together with a splice acceptor and a polyA signal, in order to force the end of transcription after the integration site. In addition to disrupting the gene, promoter activity can be traced using ß-Galactosidase (ß-Gal) activity encoded in the *LacZ* gene, via X-Gal staining. Heterozygous mice, containing one copy of the wild type allele and one of the trapped one, were used to investigate *Lin41* promoter activity: the pattern largely resembles that of the mRNA previously described. Other than the ß-Gal expression, these mice were morphologically indiscernible from their wild type littermates. However, the homozygous knockout mice without functional copy of *Lin41* displayed a very characteristic phenotype of neural tube closure defect, and embryonic lethality, manifesting from E9.5 on. Some mutant embryos could still be retrieved as late as E14.5, before being reabsorbed. A second independent mouse line, with a protein product only 24 aa shorter than the wild type, was shown to have a similar phenotype in null animals, with a slight variation in the penetrance (Maller Schulman et al. 2008).

1.2.3 *Lin41* in mouse embryonic stem cells

The limitations of a mutant phenotype with such an early lethality make cell lines a valuable tool for the study of *Lin41*. Specifically, some mammalian stem cells, like mouse embryocarcinoma (EC) P19 line or embyonic stem cells (mES cells) have been shown to express *Lin41* when maintained in the undifferentiated state (Rybak 2009).

In P19 cells, *Lin41* was demonstrated to be expressed during the proliferative, multipotent state, and to be lost upon commitment to neural differentiation. Neural progenitor cells are *Lin41* positive, but post-mitotic neuroblasts show a decrease on its levels, accompanied by miRNA *let-7* upregulation. Once again, a tight control by miRNAs seems to control this switch, emulating the heterochronic pathway. In particular, mutual regulation between the pluripotency molecules

Lin28 and *Lin41* and the miRNA biogenesis pathway was shown to comprise a double negative autoregulatory loop governing neural differentiation of stem cells. This mechanism will be explained in detail in the next chapter (Rybak et al. 2008; Rybak et al. 2009).

1.3 *Lin41* as E3 ubiquitin ligase: role in NSCs and in miRNA biogenesis

1.3.1 Trim proteins as E3 ubiquitin ligases

Lin41 is a member of the Trim-NHL protein sub-family, named after the conserved domains in the N-terminus (Trim) and the C-terminus (NHL). The conservation of these structural domains suggests a certain parallelism in their activity. Therefore, it is not surprising that after the identification E3 ubiquitin ligase activity for the RING domain, an increasing number of Trim family members have been postulated and in many cases confirmed as E3 ligases. This section describes the characteristics of this protein family, focusing on each domain, followed by an overview of some particular members in insects and mammals.

Trim proteins receive their name for their characteristic N-terminal Tripartite Motif; this consists in one RING domain, one or two B-box motifs and one Coiled-coil domain. Due to the initial of each motif name, they are alternatively called RBCC proteins (Torok & Etkin 2001; Meroni & Diez-Roux 2005). The RING domain is a zinc-binding domain. It was first identified in the protein Ring1 (really interesting new gene 1) and its canonical sequence is: Cys-X2-Cys-X(9-39)-Cys-X(1-3)-His-X(2-3)-Cys-X2-Cys-X(4-48)-Cys-X2–Cys. There are two subtypes of RING domains, C2 and H2, depending on the presence of cysteine or histidine residue in the fifth coordination site (Freemont 2000). The conserved cysteine and histidine are stabilized by two atoms of zinc in the core of the domain, that unlike the zinc fingers presents a rigid, globular-like structure, referred to as the “cross-brace” motif, for protein-protein interactions (Freemont et al. 1991; Deshaies & Joazeiro 2009; Meroni & Diez-Roux 2005). The RING domain has been shown to mediate the transfer of ubiquitin units to substrate molecules, and therefore this motif constitutes a signature of many E3 ubiquitin ligases (Joazeiro & Weissman 2000). This aspect will be discussed in detail together with the mechanisms of ubiquitination in section 1.3.1 and 1.3.2.

The B-boxes are, like the RING, zinc-binding modules. There are two types of B-boxes, 1 and 2, that slightly differ in their canonical sequence; although similar, there are some differences in the cysteine and histidine residues positions that conform the second coordination site (Reymond et al. 2001; Borden 1998). When both are present, B-box 1 always precedes B-box 2; when there is only one, it is always type 2. This kind of domain has only been found within the Trim family members, and its function has not yet been clarified (Reymond et al. 2001; Meroni & Diez-Roux 2005).

Following the B-boxes there is one Coiled-coil domain that extends for about 100 residues; the hydrophobic ones like leucine are highly conserved, due to their importance for the packing pattern. Deletion constructs used in pull-down experiments demonstrated that this element mediates protein interactions, to build high molecular weight complexes that define subcellular compartments where Trim protein accumulates (Reymond et al. 2001).

All Trim proteins display high conservation not only of the domains that comprise the tripartite motif, but also of the relative distances between domains, a feature that helps maintaining a constant tertiary structure. This points to a conservation of the biochemical mechanism, carried out by an integrated functional structure rather than by a sequence of independently active modules (Meroni & Diez-Roux 2005).

When present, the Filamin domain is always found after the Coiled-coil domain and before the C-terminus, but so far no function has been identified for this domain in the context of Trim members, although in Filamin proteins its ß-barrel conformation interacts with actin, among other proteins (Zhou et al. 2010).

The C-terminus of Trim proteins is variable; it may define a sub-family, among the most common ones are RFP-like (also called B30.2) motifs, NHL and PHD-BROMO. It also may be an uncharacterized sequence, that does not match any known domain, or be absent, meaning the protein ends after the Coiled-coil domain (Meroni & Diez-Roux 2005).

1.3.2 Ubiquitination mechanism

Ubiquitination is a mechanism of post-translational modification of proteins, with vast importance in cellular and organismal regulation. For example, in humans more than 600 genes are predicted to encode ubiquitin ligases, in comparison to the more than 500 with protein kinase domains (Wulczyn et al. 2011). Briefly, a target protein is tagged with one or more units of ubiquitin (Ub), a small 8.3 kDa protein that covalently bonds its C-terminal glycine to a certain lysine of the target protein. The signaling pattern (characterized by the length and linkage of the Ub chains), will determine the fate of the protein; for example, oligoubiquitination utilizing the Lys48 of Ub residues are used to tag the protein for degradation in the 26S proteasome (Thrower et al. 2000), while mono or polyubiquitination in the Lys63, are signals for non-proteolytic processes, like DNA repair, intracellular localization or signal transduction (Hicke et al. 2005) (Figure 4).

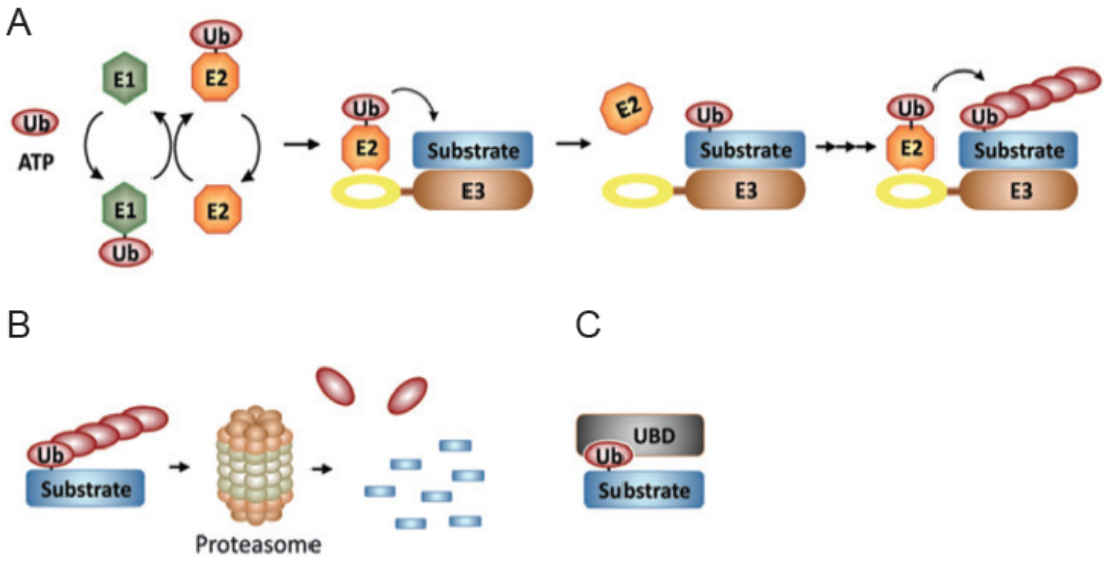

Figure 4. Schematic of Ubiquitination. A. A ubiquitin monomer is covalently linked to an E1 activating enzyme. Interaction of the E1 with an E2 conjugating enzyme results in transfer of the primed ubiquitin to an E2 conjugating enzyme. E2 directly interacts with the RING of E3 ubiquitin ligases. In general, the E3 attracts substrates via additional interaction surfaces such as the Coiled-coil or NHL domains. Construction of polyubiquitin chains requires iterative cycles of E2 binding and ubiquitin ligation. Ubiquitin is covalently attached via an isopeptide bond between the C-terminal glycine of ubiquitin and a substrate lysine. B. The classical pathway depicted here shows linear chains of at least four residues, connected at Lys48 of ubiquitin. This linkage is specifically recognized by the 26S proteasome, resulting in ubiquitin release for recycling and proteolytic degradation of the tagged substrate. C. Alternatively to the classical pathway, monoubiquitination can support protein binding with a partner containing a ubiquitin binding domain (UBD), allowing dynamic regulation analogous to protein phosphorylation. From Wulczyn *et al.* 2010.

The ubiquitination process involves three different types of enzymes (E1-E3) that cooperate to covalently attach Ub units to a substrate. First, an E1 enzyme incorporates an activated unit of Ub in an ATP-consuming step. Then this Ub is transferred to the active site of an E2 conjugating enzyme. Finally, an E3 ubiquitin ligase acts as intermediary between E2~Ub and the substrate protein, that will bind covalently one Ub moiety to a substrate lysine.

Six E1 enzymes have been described, from which only two use Ub (the others recognize similar proteins, like SUMO – Small Ubiquitin-like MOdifier), and around 40 E2's. The specificity is defined by the E3 affinity to the substrate protein, that induces a physical proximity between the substrate and the Ub loaded E2, facilitating the Ub transfer (Wulczyn et al. 2011).

1.3.3 *Lin41*, let-7 and AGO2 in neural stem cell differentiation

Lin41 is a well-studied target of the let-7 miRNA. As discussed above, the 3'UTR of *Lin41* mRNA has binding sites for let-7 that are conserved among species, suggesting that this regulation is as well maintained (Vella et al. 2004; Slack et al. 2000; Schulman et al. 2005; Lin et al. 2007; O'farrell et al. 2008). In the mammalian embryocarcinoma cell line P19, *Lin41* is highly expressed under proliferative conditions; during neural differentiation *let-7* induction leads to a decrease of Lin41 levels by binding to the mRNA 3'UTR, impairing translation and promoting degradation. Moreover, the negative correlation is reciprocal, as Lin41 is a negative regulator of the miRNA biogenesis pathway, and thus affects let-7 activity. The RING domain of the protein has E3 ubiquitin ligase activity, and is capable of self-ubiquitination *in vitro* and *in vivo*. Furthermore, when *Lin41* is transfected in HEK cells together with *Ago2*, AGO2 is tagged with a Ub chain and is subject to enhanced proteasomal degradation. LIN41 acts as Ubiquitin ligase to AGO2, the central element of the miRISC complex that mediates miRNA-mRNAs silencing (see Figure 3). Thus, *Lin41* and let-7 comprise a double negative, auto-regulatory loop controlling pluripotency and neural lineage commitment. In the pluripotent state Lin41 prevails with high levels and let-7 activity is low. Differentiation triggers a rebalancing, with high let-7 activity suppressing Lin41 expression (Figure 5) (Rybak et al. 2009).

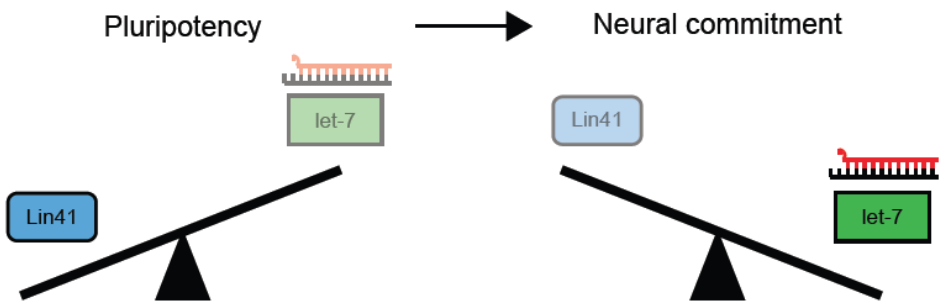

Figure 5. Scheme of Lin41 and let-7 regulation in neural commitment. In pluripotent stem cells, *Lin41* expression prevails, downregulating miRNA let-7 activity; upon neural differentiation, let-7 expression increases and targets the 3'UTR of *Lin41* mRNA, preventing translation into functional protein. Adapted from Rybak *et al*. 2009.

1.3.4 Other Trim-NHL proteins: E3 ubiquitin ligase activity, miRNA interaction and neurogenic roles

The characteristic feature of the *Lin41* protein sub-family is the NHL repeat in the C-terminus. Trim-NHL proteins are found from *C. elegans* to humans, and in many cases they have shown E3 ubiquitin ligase activity roles in development and neurogenesis, as well as interaction with the miRNA pathway (Figure 6).

1.3.4.1 Brat, Mei-P26, Abba, and Wech in Drosophila

Brat (*Bra*in *T*umor, for the mutant phenotype in larval brain) is considered the ortholog of mammalian Trim-NHL member*Trim32*, and has major implications in development, from regulation of body axis to correct brain and ovary formation, by controlling stem cell proliferation (Stegmüller & Bonni 2010; Sonoda 2001). In larval brain, neuroblasts divide asymmetrically, and the daughter cell containing Brat will eventually stop self-renewal and differentiate; the cell that did not receive the protein will remain proliferative (Betschinger et al. 2006). Brat binds to Ago1, although the consequences of that interaction are not yet known (Neumüller et al. 2008).

Like *Brat*, *Mei-P26* is a *Trim32* ortholog, a putative E3 ligase that also promotes ovarian germline differentiation; it interacts physically with Ago1, and has been confirmed as a miRNA pathway regulator (Neumüller et al. 2008). Moreover, Mei-p26 binds and regulates miRNA pathway components, and is as well subject to miRNA regulation in the *D. melanogaster* wing tissue, in an auto-regulatory mechanism (Herranz et al. 2010). *Abba* is an ortholog of *C. elegans* NHL-1 and of mammalian *Trim2* and *Trim3*. Was also suggested to be an E3 ubiquitin ligase,

and is expressed from mid-development onwards in muscle tissue. *Wech* was also described as Dappled, and is the *Lin41* ortholog gene in *D. melanogaster*. Wech is a tumor suppressor gene involved in the eye and muscle development; like Brat, it lacks the Ring domain, and was proven to be regulated by let-7 (Löer et al. 2008; O'farrell et al. 2008).

1.3.4.2 *Trim32, Trim2* and *Trim3* in mammals

Trim32 was the first mammalian member of the Trim-NHL family cloned, and to be identified as an E3 ubiquitin ligase. Mutations in *Trim32* have been liked to a number of diseases, including skin carcinogenesis or the Limb-Girdle Muscular Dystrophy Type 2H (LGMD2H), due to a failure in interaction with E2 ligases (Frosk et al. 2002; Horn 2003; Kudryashova et al. 2009; Kudryashova et al. 2005). Moreover, *Trim32* seems to influence the miRNA pathway in a positive fashion: during mouse corticogenesis, TRIM32 protein is asymmetrically inherited by the daughter cell of a progenitor division that will differentiate into a neuron. Trim32 was shown to interact with and increase activity of a subset of miRNAs, including let-7a, that promote neuronal differentiation (Schwamborn et al. 2009).

Trim2 and *Trim3* are very similar to each other, and both have been confirmed as E3 ubiquitin ligases. They are highly but not exclusively present in the central nervous system (CNS) (Hung et al. 2010; Balastik et al. 2008), and both have been shown to interact with Myosin V via their NHL motifs. Through this interaction, *Trim3* is involved in endosomal trafficking (Yan et al. 2005), but also in postsynaptic density morphology and dendritic regulation, by ubiquitination of GKAP scaffold protein (Hung et al. 2010). On the other hand, *Trim2* is responsible for axon establishment in neuronal specification *in vitro*, and its deletion results in a neurodegenerative phenotype *in vivo*, due to a failure in ubiquitination and subsequent proteasomal degradation of neurofilament light chain, which results in toxic accumulation (Khazaei et al. 2011; Balastik et al. 2008). More recently, it has also been described as an agent in ischemic neuroprotection (Thompson et al. 2011).

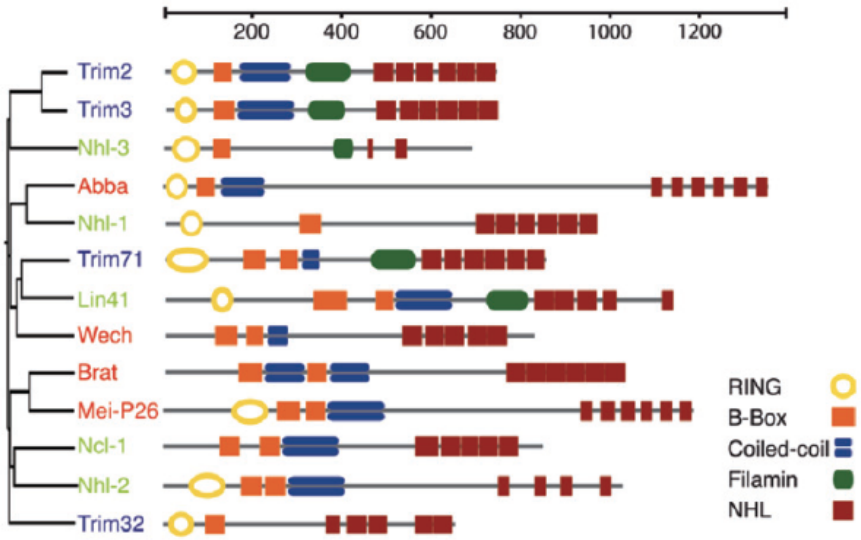

Figure 6. Trim-NHL proteins. Family tree generated by ClustalW alignment of the C-terminal sequences. Mammalian genes are depicted in blue, *C. elegans* in green and *D. melanogaster* in red. From Wulczyn *et al* 2010.

1.4 Mammalian neurogenesis in development and adulthood

1.4.1 Developmental neurogenesis: neuroepithelium and radial glia

The mammalian brain is a highly complex organ that develops following a tight spatial and temporal pattern to give rise to all the different cells and structures required for its function. This wide variety in tissue formation derives originally from a single cell layer that forms the neural plate. The neural plate is a sheet that folds and fuses, forming a cavity filled with cerebrospinal fluid, the future ventricular system. This primordial layer of cells is called the neuroepithelium, and is formed by columnar neuroepithelial cells that elongate to contact both the basal and apical surfaces (pia and ventricle, respectively). During the cell cycle the nuclei of these cells move along the apical-basal axis in a process called interkinetic nuclear migration, what confers the tissue the appearance of a pseudostratified epithelium (Sauer 1935; Gilbert 2005). The neuroepithelium changes over time and generates new cells by undergoing different patterns of division. First, there is a series of symmetric, proliferative divisions that increase the total number of cells, and therefore the size of the tissue. Between embryonic day 10 and 12, neural stem cells acquire glial identity; although morphologically identical to neuroepithelial cells, they express the molecular markers GLAST and S100ß, and receive the name of radial glia (Götz & Huttner 2005). Radial glia cells remain contacting the pial surface, while their nuclei conform the ventricular zone (VZ), and they originate a vast majority of the neurons and glia in the brain. The

subventricular zone (SVZ) is immediately below this layer, and is a second proliferative zone that contains basal progenitors dividing symmetrically (Malatesta et al. 2003; Anthony et al. 2004). In the VZ, the type of each cell division is determined by the cleavage plane orientation; thus, a vertical division yields two identical daughter cells that remain proliferative stem cells. When the division is horizontal, though, the most basal cell will lose contact to the ventricular cavity, and become an intermediate progenitor that can divide once more to generate only two post-mitotic neurons, or glial cells in the case of glial progenitors; the apical daughter cell will remain a stem cell (McConnell 1995).

Neurons organize in six layers in the cortex, from pial – external - surface to the ventricles. They reach their final position by using radial glia processes as guidance. Those originated earlier in time will migrate further, forming the first layers, and the ones born later, will migrate less and stay closer to the ventricular surface. In mice, this process starts at embryonic developmental day 12.5 (layer I/II) and is complete by birthdate (Götz & Huttner 2005; Merkle & Alvarez-Buylla 2006).

1.4.2 Adult neural stem cell niches: hippocampal SGZ and ventricular SVZ

After birth, the production of new neurons continues in many vertebrates, including mammals and humans. Two neurogenic niches have been described in the adult mammal brain, the subgranular zone (SGZ) of the hippocampus and the subventricular zone (SVZ) of the lateral ventricles. Although a number of works pointed to postnatal neurogenesis in rodents and apes from the 1950's, it was not until the 1990 decade that the scientific community accepted this fact, discarding the dogma of neurogenesis stopping around birthdate (Gross 2000):

"Acabada la evolución, secáronse irrevocablemente las fuentes del crecimiento y regeneración de axones y dendritas. Preciso es reconocer que en los centros adultos, las vías nerviosas son algo acabado, fijo, inmutable. Todo puede morir, nada renacer" (Once development was ended, the founts of growth and regeneration of the axons and dendrites dried up irrevocably. In adult centers the nerve paths are something fixed, ended, immutable. Everything may die, nothing may be regenerated). Santiago Ramón y Cajal, Estudios sobre la degeneración del sistema nervioso. Volume II, p.391.1913-1914.

In the hippocampus, the neural progenitors lay next to an area of compacted neurons in the granular zone, known as the subgranular zone (SGZ). They produce intermediate progenitors and neuroblasts that will mature into granular and perigranular neurons and infiltrate the inner molecular layer. These adultborn hippocampal neurons integrate into pre-existing circuits, and they play unique roles related to learning and memory. For example, neurogenesis is potentiated by enriched environments and learning tasks, while disruption of this neurogenetic program leads to a reduction in some hippocampal-dependent task performance, like trace conditioning (reviewed in (Zhao et al. 2008)) (Deng et al. 2010; Eriksson et al. 1998).

The subventricular zone (SVZ) of the lateral walls is the largest neurogenic compartment in adult mammals, and generates new neurons that migrate through the rostral migratory stream (RMS) to reach the olfalctory bulb (OB), where they integrate and mature as granular and periglomerular neurons. Neural stem cells (NSCs) from the SVZ reside in a complex three-dimensional niche in close relationship with other cells. The ependymal cells are cuboidal, multiciliated cells that directly contact the ventricular lumen. They produce the cerebrospinal fluid and the beating of their cilia assure its correct flow. Below the ependymal layer that covers the ventricular walls lay the NSCs, also called type B cells, able to re-enter the cell cycle and divide to generate new neurons. They have astrocytic identity, expressing markers such as GFAP and Nestin. Neurogenesis is highly dependent on the NSCs microenvironment: Shh signaling is detected by an apical primary cilium that project to the ventricular cavity. Basally, NSCs extend processes to interact with a specialized perivascular niche that has been defined as a key component of SGZ and SVZ neurogenic region (Han et al. 2008; Shen et al. 2008; Alvarez-Buylla & D. A. Lim 2004; Tavazoie et al. 2008).
B cells divide asymetrically, maintaining the cell pool and generating transient amplifiers or intermediate progenitors (C cells), which continue to divide while starting to migrate in the RMS. Type C cells express the marker double cortin (DCX); as they head the RMS they undertake one or more division cycles to increase the cell pool. C cells give rise to type A cells, called neuroblasts (precursors of neurons) that express PSA-NCAM. They will finish the migration, reach the OB, and finally integrate and differentiate in the granule cell layer of the

olfactory bulb (Figure 7) (Merkle & Alvarez-Buylla 2006) and reviews (Zhao et al. 2008; Alvarez-Buylla & D. A. Lim 2004).

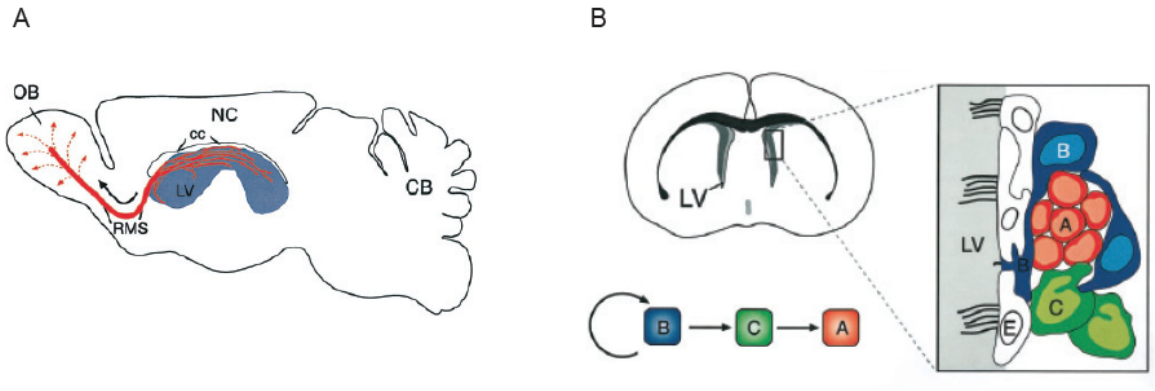

Figure 7. Adult neurogenic niches in mouse. A. Sagittal view of a mouse adult brain. Neural progenitors generate daughter cells that migrate through the rostral migratory stream (RMS) to reach the olfactory bulb and differentiate in granular or periglomerular cells. B. Architecture of the lateral wall of the lateral ventricle. Neural stem cells (B cells) lay underneath the ependymal layer (white cells) contacting the ventricle with a monocilium. They differentiate in transient amplifiers (C cells) that give rise to neuroblasts (A cells), which migrate to the OB and maturate in young neurons. Adapted from Alvarez-Buylla and García-Verdugo, 2002.

1.4.3 Architecture of the Subventricular Zone: relevance of ependymal cells

The SVZ is a large neurogenic repository sitting in the lateral walls of the lateral ventricles in mammals. NSCs have astrocytic identity and express markers like GFAP, vimentin and Nestin among others (Garcia et al. 2004; Doetsch et al. 1999; del Valle et al. 2010), or more controversially Prominin1 (CD133) (Coskun et al. 2008). Despite the numerous studies in the last years, it has been impossible to find a unique, specific marker to identify and isolate these cells. It is well known that neural stem cells are highly dependent on the interaction with their environment, both in SVZ and SGZ. They are in direct contact to blood vessels and they receive signals from them that stimulate self renewal through the Notch signaling pathway (Shen et al. 2008; Shen et al. 2004). In hippocampal progenitors, Smoothened ablation, essential for Shh signaling, results in failure of neurogenesis (Han et al. 2008; Breunig et al. 2008).

In this context, the importance of the ependymal cells, largely ignored, has been the object of recent studies. Ependymal cells are typically cuboidal and multiciliated, and they conform the interface between the ventricular lumen and the brain parenchyma (Spassky et al. 2005). They also have tight lateral cell-cell junctions, to regulate cerebrospinal fluid infiltration in the brain tissue (Brightman &

Palay 1963). The defective assembly or function of cilia leads to a range of diseases called ciliopathies. Ciliopathies can range from embryonic axis malformation or neural tube defects in case of the primary (non-motile) cilia, to chronic respiratory infections or sterility phenotypes in case of the motile cilia (Ibañez-Tallon et al. 2003).

The multicilia in the apical side of the ependymal cells are responsible for the unidirectional and synchronized movement of the cerebrospinal fluid through the ventricular system. Defects in these organelles lead to cerebrospinal fluid accumulation and enlargement of the ventricle cavities, a condition known as hydrocephaly (Paez-Gonzalez et al. 2011; Ibañez-Tallon et al. 2004). During development, ependymal cells are born from radial glia progenitors, between embryonic day 14 and 18, but it is not until the second postnatal week that they start to differentiate and produce multicilia on their apical surface (Spassky et al. 2005).

Recently, the structure of the subventricular germinal niche has been described in detail, highlighting its three-dimensional complexity, where the neural stem cells situate in the center of a pinwheel structure, surrounded by ependymal cells (E1), and contacting the ventricle with a primary cilium. An additional population of presumed immature ependymal cells with fewer cilia was also identified (E2) (Mirzadeh et al. 2008) (Figure 8).

Unlike the beating multiclia with 9+2 microtubule distribution present in ependymal cells, the NSCs primary cilium has 9+0 microtubule and is non-motile, just like those in hippocampal progenitors, and it is very likely to mediate both Shh and Wnt signaling (Gerdes et al. 2007; Corbit et al. 2005; J. Kim et al. 2009).

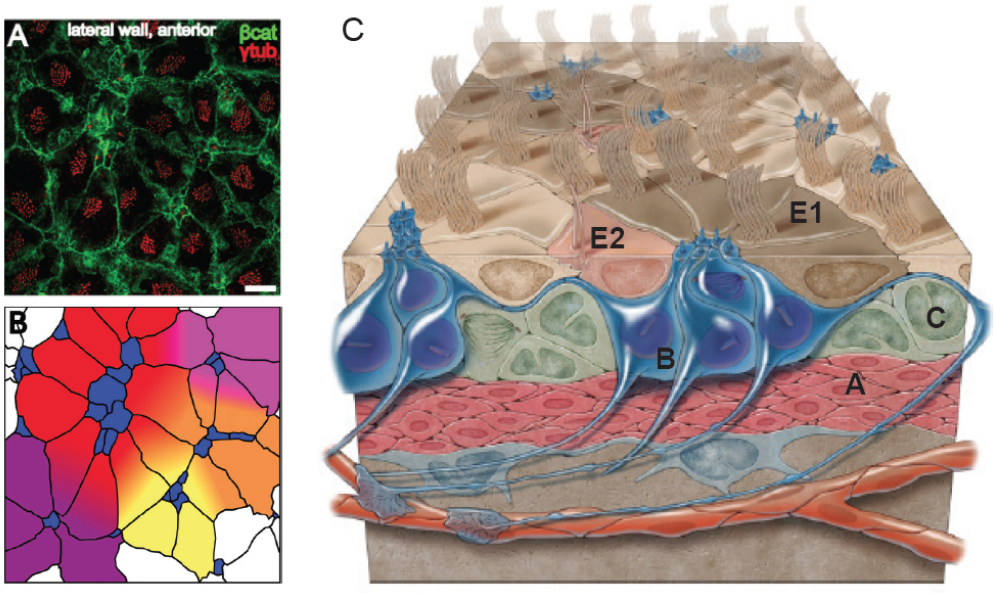

Figure 8. Pinwheel configuration of the neural stem cells niche in the SVZ. A. Immunostaining of whole mount pinwheel. ß-Catenin (green) labels cell-cell contact and γ-tubulin (red) the basal bodies of cilia. B. Schematic of the pinwheel, with ependymal (yellow, red or purple) cells surrounding B cells (blue). C. Three dimensional schematic of the SVZ niche: Mature ependymal cells (E1, brown) are arranged in a pinwheel structure surrounding the neural stem cells (B, blue) contacting the ventricle with primary cilia, as well as blood vessels (orange) with basal processes. E2, light brown, are immature, less ciliated ependymal cells. C, green: transient amplifiers, A, red: neuroblasts. Adapted from Mirzadeh *et al*. 2008.

Germinal pinwheels are not homogeneously distributed along the lateral wall, but are more frequently located in the posterior dorsal and the anterior ventral regions, meaning these are areas of high concentration of NSCs. The correct development of the ependymal layer has been shown to be essential in maintaining the ability of NSCs to form new neurons in the adult rodent brain. The proper assembly in pinwheels depends on Ankyrin3 (*Ank3*), which directs lateral membrane specializations and is expressed in progenitors that will become ependymal cells. *Ank3* expression is controlled by the transcription factor *FoxJ1* (also called *HFH*-4) responsive to Shh signaling, and an essential coordinator of the genetic program for multicilia formation, required for ependymal specialization. When the ependymogenesis fails, the pinwheel structures around NSCs are not properly assembled and adult neurogenesis is impaired (Cruz et al. 2010; X. Yu et al. 2008; Jacquet et al. 2009; Paez-Gonzalez et al. 2011; Nishimura et al. 2006).

1.5 Aims of this Thesis

- Description of *Lin41* expression pattern in mouse, during development and in postnatal stages, using a gene trap model.
- Design and generation of a conditional knockout mouse model for *Lin41* to overcome the limitations of the gene trap and achieve controlled deletion of the gene product.
- Study of *Lin41* in embryonic stem cells using a homozygous mutant cell line: implications in pluripotency and self-renewal.
- Characterization of *Lin41* in postnatal central nervous system: characterization of ependymal tissue and possible implications for the neural stem cell niche.

2 Materials and Methods

2.1 MATERIALS

2.1.1 Reagents

Name	Cat. Number	Company	Use
Agarose SeaKem® LE	50004	Lonza	Agarose gel - DNA electrophoresis
GeneRuler High Range DNA Ladder	SM1351	Thermo Scientific	Agarose gel - DNA electrophoresis
100 bp-DNA-Ladder extended	T835.1	Roth	Agarose gel - DNA electrophoresis
1 kbp DNA-Ladder	Y014.1	Roth	Agarose gel - DNA electrophoresis
2,2,2-Tribromoethanol	T48402	Sigma	Avertin - sedative
tert-Amyl Alcohol	A730-1	Fisher	Avertin - sedative
Whatman 3MM Chr sheets, 46 x 57 cm	3030-917	Whatman	Blotting
Oligo(dT) primer	SO132	Thermo Scientific	cDNA synthesis
RiboLock RNase Inhibitor	EO0381	Thermo Scientific	cDNA synthesis
RevertAid™ Reverse Transcriptase	EP0733	Fermentas	cDNA synthesis
dNTP Mix, 10 mM	R0192	Thermo Scientific	cDNA synthesis
0.05% Trypsin-EDTA (1x)	25300-054	Gibco	Cell culture
2-Mercaptoethanol 50mM	31350-010	Gibco	Cell culture
DMEM (1x)	21969-035	Gibco	Cell culture
EGTA	E-4378	Sigma	Cell culture
GlutaMAX 100x	35050-038	Gibco	Cell culture
KnockOut™ DMEM (1x)	10829-018	Gibco	Cell culture
Penicillin-Streptomycin, Liquid	15140-122	Gibco	Cell culture
Sodium Pyruvate	11360-039	Gibco	Cell culture
Foetal Bovine Serum GOLD	A15-151	PAA	Cell culture
L-Cysteine	C7352	Sigma	Cell culture - enzymatic solution
Papain	3119	Worthington	Cell culture - enzymatic solution
Leibovitz's L-15	11415-064	Gibco	Cell culture - Ependymal cells
Poly-L-Lysine	P1524	Sigma	Cell culture - Ependymal cells
ESGRO® (LIF)	ESG1106	Millipore	Cell culture - ESCs
LIF	GSR-7001	GlobalStem	Cell culture - ESCs
Gelatin 2%	G1393	Sigma	Cell culture - ESCs
N-2 Supplement	17502-048	Gibco	Cell culture - ESCs differentiation
KnockOut™ Serum Replacement	10828010	ambion	Cell culture - ESCs differentiation
MEM NEAA	11140-035	Gibco	Cell culture - MEFs
Mitomycin C	M0503	Sigma	Cell culture - MEFs inactivation
Bovine Albumin Fraction V Sol (7.5%)	15260-037	Gibco	Cell culture - NSPs
NeuroCult™ Proliferation Kit (Mouse)	5702	StemCell Tech.	Cell culture - NSPs
Recombinant Human EGF	AF-100-15	Peprotech	Cell culture - NSPs
Recombinant Human FGF-basic	100-18B	Peprotech	Cell culture - NSPs
BD Matrigel™	356231	BD Biosciences	Cell culture - NSPs
Cell Titer 96®	G358C	Promega	Cell prolifferation assay
Phusion™ Hot Start DNA Polymerase	F-540L	NEB	Cloning PCR

T4 DNA Ligase	M0202L	NEB	DNA ligation
GlycoBlue™	AM9515	ambion	DNA/RNA carrier
Paraformaldehyde	P6148	Sigma	Fixation
DirectPCR-Tail	31-102-T	peqlab	Genotype - gDNA isolation
Proteinase K	3115836001	Roche	Genotype - gDNA isolation
GoTaq® DNA Polymerase	M3178	Promega	Genotype PCR
Goat serum	G9023-10ML	Sigma	IF Blocking
DRAQ5 (5mM)	DR50200	Biostatus	IF Nuclei staining
KaryoMAX	15212-012	Gibco	Karyotype
EndoFree Plasmid Maxi Kit	12362	QIAGEN	Maxi preps
NucleoBond® Xtra Midi	740410100	Macherey Nagel	Midi preps
PXE 0.2 Thermal Cycler	HBPXE02	Thermo Scientific	PCR
dATP 100 mM	272-050	Pharmacia Biotech	PCR
dCTP 100 mM	272-060	Pharmacia Biotech	PCR
dTTP 100 mM	272-080	Pharmacia Biotech	PCR
dGTP 100 mM	272-070	Pharmacia Biotech	PCR
Bio-Rad Protein Assay Dye Reagent	500-0006	BIO-RAD	Protein measure
Standard Cuvettes (PS) and (PMMA)	67740	Sarstedt	Protein measure
Berthold LB 122	21509	Labexchange	Radioactivity monitor
TRIzol Reagent	15596026	ambion	RNA isolation - RT-PCR
Dimethyl sulfoxide	A994.2	Roth	Solvent
Amersham Hybond-N+	RPN303B	GE Healthcare	Southern blot
Hybond-N+	RPN303B	GE Healthcare	Southern blot
Guanosine	51050	Sigma - FLUKA	Southern blot - gel
Prime-It II Random Primer Labelling Kit	300385	Stratagene	Southern blot - probe labeling
Exo (-) Klenow Polymerase	300385-55	Agilent	Southern probe synthesis
OCT COMPOUND	3808610E	Leica	Tissue embedding
Lipofectamine® 2000	11668-019	Invitrogen	Transfection
Opti-MEM® I 1x	31985-047	Gibco	Transfection
Albumin Fraction V	8076.2	Roth	Western blot blocking
Milk powder	T145.2	Roth	Western blot blocking
PageRulerTM Protein Ladder Plus	SM1811	Fermentas	Western blot
Immobilon-P Transfer Membrane	IPVH00010	Millipore	Western blot
Ponceau S solution	P7170	Sigma	Western blot
Amersham Hyperfilm ECL	521572	GE Healthcare	Blot development
Clarity Western ECL Substrate	170-5060	BIO-RAD	Western blot development
30% Acrylamide/Bis Solution 29:1	161-0156	BIO-RAD	Western blot gel
TMED	T-8133	Sigma	Western blot gel
Cellscraper 25 cm	831830	Sarstedt	Western blot lysates
Protease Inhibitor Cocktail Set I	539131-10VL	Calbiochem	Western blot lysates
Bovine Serum Albumin Standard	23209	Pierce	Western blot standar curve
Potassium ferricyanide ($K_3Fe(CN)_6$	P8131	Sigma	X-Gal staining
Potassium ferrocyanide ($K_4Fe(CN)_6$-$3H_20$	P9287	Sigma	X-Gal staining
X-Gal UltraPure	B-1690	Invitrogen	X-Gal staining
Glutaraldehyde solution Grade II, 25%	G6257-100ML	Sigma	X-Gal staining
Glycerol	1040921000	Merk	

2.1.2 Restriction enzymes

Enzyme	Cat. Number	Buffer	Company
BamHI	R0136	NEBuffer 3	NEB
BamHI-HF™	R3136	NEBuffer 4	NEB
DrdI	R0530	NEBuffer 4	NEB
EcoRI	R0101	NEBuffer EcoRI	NEB
EcoRI-HF™	R3101	NEBuffer 4	NEB
HindIII	R0104	NEBuffer 2	NEB
HindIII-HF™	R3104	NEBuffer 4	NEB
NcoI	R0193	NEBuffer 3	NEB
NcoI-HF™	R3193	NEBuffer 4	NEB
NotI	R0189	NEBuffer 3	NEB
NotI-HF™	R3189	NEBuffer 4	NEB
PspXI	R0656	NEBuffer 4	NEB
SacI	R0156	NEBuffer 4	NEB
SacI-HF™	R3156	NEBuffer 4	NEB
SpeI	R0133	NEBuffer 4	NEB
SpeI-HF™	R3133	NEBuffer 4	NEB
XhoI	R0146	NEBuffer 4	NEB
BSA	10 mg/ml (100x)		NEB

2.1.3 Bacterial strains

Bacteria Strain	Genotype	Source
E. coli DH5α	F- φ80dlacZΔM15 Δ(lacZYA-argF)U169, deoR, recA1, endA1, hsdR17(rk-, mk+), phoA, supE44, λ-, thi-1, gyrA96, relA1	Invitrogen
E. coli XL10Gold	endA1 glnV44 recA1 thi-1 gyrA96 relA1 lac Hte Δ(mcrA)183Δ(mcrCB-hsdSMR-mrr)173 tetR F'[proAB lacIqZΔM15 Tn10(TetR Amy CmR)]	Stratagene
E. coli TOP10	F- mcrA Δ(mrr-hsdRMS-mcrBC) Φ80lacZΔM15 lacX74 recA1 deoR araD139 Δ(araleu)7697 galU galK rpsL (StrR) endA1 nupG	Invitrogen
E. coli DY380	F- mcrA Δ(mrr-hsdRMS-mcrBC) Φ80dlacZ M15 ΔlacX74 deoR recA1 endA1 araD139 Δ(ara, leu) 7649 galU galK rspL nupG [λcI857 (cro-bioA) <> tet]	Copeland (Liu et al. 2003)
E. coli EL250	DY380 [(cro-bioA) <> araC-PBADflpe]	Copeland
E. coli EL350	DY380 [(cro-bioA) <> araC-PBADcre]	Copeland

2.1.4 Antibiotics

Antibiotic	Stock Concentration	Work Concentration
Ampicillin	100 mg/ml in H_2O	50-100 ug/ml
Kanamycin	12,5 mg/ml in H_2O	25 ug/ml
Chloramphenicol	34 mg/ml in Ethanol	12,5-20 ug/ml

2.1.5 Plasmids

Plasmid	Comments, source
pDTA	Based on pBSK, contains MCS DT-A (Diphteria Toxin Fragment A). Gen under the control of HSV-TK promoter. Gift from Dr. Trimbuch
pNeo	From Liu et al. 2003{Liu:2003vn}. Gift from Dr. Trimbuch
pWu	Based on pEGFP-C1

2.1.6 Primers

Name	Sequence	Ann. Temp	Product
Genotype			
Intron2 Fw	TTCTGCATCCAGAGTGCAAC		
Intron2 Rev	CTTCCTCTGACCTTTGCTGG	66ºC	457bp in WT
GeneTrap Rev	ACCAGCTGTGCGCATAGTG	66ºC	600bp in GT
5'Arm Fw 2	GTGTGAGTGAGAGAGAGAGAGAT	66ºC	670 bp in WT
3'Arm Rev	GCCCCTGAGGTAAAAAGACC		
LacZ Fw	AACGTCGTGACTGGGAAAAC	65ºC	218 bp
LacZ Rev	GACAGTATCGGCCTCAGGAA		
Conditional Knockout Vector			
A_SpeI_Ret_Fw	TGGTTGACTAGTAGCTAGCAAGCATTGGTTTTTGTTG	72ºC	302 bp
B_HindIII_Ret_Rev	TGGTTGCAAGCTTCAGGCAAGAAGACTTAACATCCATC		
Y_HindIII_Ret_Fw	TGGTTGCAAGCTTTGGAAAACGCTGCCATCTGCTGGCC		303 bp
Z_XhoI_Ret_Rev	TGGTTCTCGAGCTCCAGTTTGGGAGGATCTGGGCAT		
C_XhoI_LoxP1_Fw	TGGTTCTCGAGAGCCCGGGGAGCCAGGAAGGCTGGG		235 bp
D_EcoRI_5'LoxP1_Rev	GTTGCGAATTCGGCTACAATGCTGTACGGTAGGAGT		
E_NotI_LoxP1_Fw	TGGTTGCTGGGGCGGCCGCTTTCTGGTTATGTGTCCTCTACCCA		303 bp
F_SacI_Loxp1_Rev	TGGTTGAGCTCAAACTCCAGATCTAGAGGGGTCCTA		
G_XhoI_Loxp2_Fw	TGGTTCTCGAGATACTGTGTTTATGTGGGGTTAGGT		225 bp
H_HindIII_5'LoxP_Rev	TGGTTGCAAGCTTATTTGCTTGGGATGTCTTGTGTCAA		
I_NotI_SpeI_LoxP2_Fw	TGGTTGCTGGGGCGGCCGCATAGTTTCTTCCCAGTTTGCTAAGAAACTC		308 bp
J_SacI_LoxP2_Rev	TGGTTGAGCTCTGTGCTTCTCAAATCAAAGCTATCC		
Conditional Knockout Insertions PCR			
loxP G Fw	AAGCCATCTTTGCTTGAGGA	65ºC	575 bp in Vector.
loxP J Rev	CTTGAGGTCTGCCTCCACTC		
loxP C Fw	AGCCCGGGGAGCCAGGAAGGCTGGG	69ºC	2582 bp in Vector
loxP F Rev	AAACTCCAGATCTAGAGGGGTCCTA		
Lin41 3'UTR cloning			
3' UTR_EcoRI Fw	TTGAATTCAGGGTGTGCATGTGTGTGTCTC	72ºC	1383 bp
3' UTR_BamHI Rev	TTGGATCCCACTTCCTGTTGGGTGGTTTGG		
Southern Blot probes			
Neo Fw	ATGATTGAACAAGATGGATT	57ºC	795 bp
Neo Rev	GAAGAACTGCTCAAGAAGACT		
Neo' Fw	GAAATCTCGTGATGGCAGGT	64ºC	871 bp
Neo' Rev	GAGGATCGTTTCGCATGATT		
WT 1 5'Int Fw (E_NotI_LoxP1)	TGGTTGCTGGGGCGGCCGCTTTCTGGTTATGTGTCCTCTACCCA	66ºC	957 bp
WT 1 5'Int Rev (Intron3)	GCCCCTGAGGTAAAAAGACC		
WT 2 Fw	CTGTCTCCACTCTGTTCACACCC	65ºC	479 bp
WT 2 Rev	ACCCAAACGGCTAAAGAAGA		
3' Ext Fw	ATTAGAATGGACCCCCAACC	65ºC	406 bp
3' Ext Rev	GGGGACCCAATGTCCTATTT		

3' Int Fw	AAAATCGGGGGCTAGGAGTA	66ºC	987 bp
3' Int Rev	TGCAGAACTGGACACAGGAG		
RT-PCR			
Lin41 E2-RT Fw	CTGTGACACCTGCTCTGTCC	56ºC	420 bp
Lin41 E2-RT Rev	GAAAGACCGCGAAGAGTTTG		
ß-actin Fw	GGCTGTATTCCCCTCCATCG	62ºC	154 bp
ß-actin Rev	CCAGTTGGTAACAATGCCATGT		

2.1.7 Antibodies

Name	Species	Company	Cat. Number	Use IF	Use WB
Lin41 peptide	Rabbit			1:50	
Lin41 serum	Rabbit				1:4000
ß-Galactosidase	Chicken	Abcam	ab9361	1:400	
FoxJ1	Mouse	eBioscience	14-9965	1:750	
CD24	Rat	Abcam	ab64064	1:250	
CD133	Rat	eBioscience	14-1331	1:500	
S100ß	Mouse	Sigma	S2532	1:600	
ß-Catenin	Mouse	BD	610154	1:200	
γ-tubulin	Mouse	Sigma	T6557	1:500	
α-tubulin	Mouse	Abcam	ab11304	1:500	
Oct4	Mouse	Santa Cruz	sc-5279	1:100	1:1000
Sox2	Mouse	Cell Signaling	4900	1:50	1:1000
Nanog	Mouse	Cell Signaling	8600		1:1000
Cdkn1a (p21)	Rabbit	Santa Cruz	sc-397		1:1000
Tuj1	Mouse	Millipore	MAB5564	1:1000	
Nestin	Mouse	DSHB		1:1000	
GFAP	Mouse	Sigma	G3893	1:400	1:1000
Alexa 568	Rabbit anti-rat	Invitrogen	A21211	1:1000	
Alexa 568	Goat anti-chicken	Invitrogen	A11041	1:1000	
Alexa 568	Goat anti-mouse	Invitrogen	A11031	1:1000	
Alexa 488	Donkey anti-rabbit	Invitrogen	A21206	1:1000	
Alexa 488	Rabbit anti-rat	Invitrogen	A21210	1:1000	
Alexa 488	Goat anti-mouse	Invitrogen	A11029	1:1000	
FITC	Goat anti-chicken	Abcam	ab6873	1:500	

2.1.8 Equipment

Name	Company	Use
Microscope Olympus BX51 with MagnaFire Image acquisition	Olympus	Microscopy
Confocal equipment TCS SL (Leica Microsystem)	Leica	Microscopy
Eppendorf Thermomixer® compact	Eppendorf	Equipment
Environmental Shaker-Incubator ES-20	Grant-bio	Equipment
Centrifuge 5415 D	Eppendorf	Equipment
Centrifuge 5417 R	Eppendorf	Equipment
Owl* EasyCast* B1 and B2 Mini Gel Electrophoresis Systems	Thermo Scientific	DNA electrophoresis
SGU-2626T-02	CBS Scientific Co.	DNA electrophoresis
Shake 'n' Stack* Hybridization Oven 6242	Thermo Scientific	Hybridization

ChemiDoc™ XRS+ System 170-8265	BIO-RAD	Western blot development
Plate reader ELX 800	Biotech Instruments	Proliferation assay
Berthold LB 122 21509	Labexchange	Radioactivity monitor
GS Gene Linker® UV Chamber	BIO-RAD	Southern blot
Mini Trans-Blot® Cell 170-3930	BIO-RAD	Western blot transfer
Nanophotometer 1374	IMPLEN	Equipment
BD FACSCanto II flow cytometer	BD	FACS
Leica CM1900 Cryostat	Leica	Histology

2.1.9 Software

Microsoft Office 2011 for Mac
Adobe Illustrator CS4
Adobe Photoshop CS4
Adobe Acrobat 8.3
Papers2 from Mekentosj
SeqBuilder (DNASTAR) Lasergene 10
Fiji 1.0
Prism 5 for MacOS
EnzimeX
Ensembl genome browser (http://www.ensembl.org/index.html)
BLAST (http://www.ncbi.nlm.nih.gov/BLAST/)
Leica Confocal Software v. 2.61 Build 1537
Magnafire
NCBI database (http://www.ncbi.nlm.nih.gov/)
Primer3 program (http://frodo.wi.mit.edu/)
TargetScan software (http://genes.mit.edu/targetscan)
Image Lab – BioRad
Flow Jo vX for Mac
DNA molar ratio calculator ((http://www.insilico.uni-duesseldorf.de/Lig_Input.html))
Primer Bank (http://pga.mgh.harvard.edu/primerbank/)

2.1.10 Buffers and solutions

2.1.10.1 Agarose gel electrophoresis

PBS 10x (1L) pH 7.4	80g NaCl, 0.2g KCl , 14.4g Na_2HPO_4 • 2 H_2O, 0.2g KH_2PO_4
TBS 10 x pH 7.4	Tris base --- 0.5 M, NaCl --- 1.5 M
DNA 10x Loading buffer	50 g Sucrose, 0.25 g Bromphenol blue, 100 ml in 1x TBE
TBE 10x (1L)	0.45M Trisbase, 0.45 M Boric Acid, 10 mM EDTA 0.5M (pH 8.0)

Etidium Bromide 5 mg/ml solution in H_2O

2.1.10.2 Embryo yolk sack lysis buffer for genotype by PCR

gDNA extraction buffer from embryo

Lysis buffer	25mM NaOH, 0.2mM EDTA
Neutralisation buffer	40mM Tris pH5.0

2.1.10.3 X-Gal Staining

0.1 M Phosphate buffer (PB) pH 7.3	70 mM Na_2HPO_4, 30 mM NaH_2PO_4
Wash buffer. In 500 ml PB	2mM $MgCl_2$ (1ml 1M)
Fix buffer. In 200 ml wash buffer	5mM EGTA, 0.2% Glutaraldehyde
Staining buffer. In 100 ml wash buffer	5mM $K_4Fe(CN)_6$, 5mM $K_3Fe(CN)_6$. X-Gal 1mg/ml

2.1.10.4 Animal sedation and tissue fixative (Immunostaining)

Avertin Stock solution	25 grams avertin (2, 2, 2-Tribromoethanol) 15. 5 ml tert-Amyl Alcohol (2-methyl-2-butanol)
Working solution (20 mg/ml)	0.5 ml Avertin stock 39.5 ml 0.9% saline (NaCl)
PFA 4% (w/v) in PB	

2.1.10.5 Western blot

8% Separating gel	ml/10 ml	10% Separating gel	ml/10 ml
H2O	4,6	H2O	4,0
30% acrylamide mix	2,7	30% acrylamide mix	3,3
1.5 M Tris (pH 8.8)	2,5	1.5 M Tris (pH 8.8)	2,5
10% SDS	0,1	10% SDS	0,1
10% ammonium persulfate	0,1	10% ammonium persulfate	0,1
TEMED	0,006	TEMED	0,004

5% Stacking gel	ml/2ml
H2O	1.4
30% acrylamide mix	0.33
1.0 M Tris (pH 6.8)	0.25
10% SDS	0.02
10% ammonium persulfate	0.02
TEMED	0.002

Protein lysis buffer TNN	50mM Tris pH7.4, 150 mM NaCl , 0.5% NP-40 (Igepal), 5mM EDTA, Protease Inhibitor Cocktail Set I 1x
10x Electrophoresis buffer	25 mM Tris, 200 mM glycin, 1% SDS
10x Blotting buffer 2 l	25 mM Tris, 150 mM mM glycin (15% MeOH in 1x buffer)
Ponceau-S	0.1 % Ponceau S , 5% acetic acid
PBST	PBS, 0.05% Tween 20
Western blot stripping buffer	0,2M Glycin pH2.5, 0.05%Tween

2.1.11 Cell culture Media

2.1.11.1 Adult mouse neurospheres

Enzymatic solution

Component	Catalog number	Amount
Papain	Worthington 3119	0.9mg/ml
L-Cystein	Sigma C-8277	0.2mg/ml
EDTA	Sigma E-6511	0.2mg/ml
HBSS	Gibco 24020-091	

Complete Adult NeuroCult™ Proliferation Medium

Component	Catalog number	Volume
NeuroCult® NSC Basal Medium	StemCell Technologies 05700	450 ml
NeuroCult® NSC Prolif. Supplements	StemCell Technologies 05701	50 ml
EGF human, recombinant	Peprotech AF-100-15	20ng/ml
bFGF human, recombinant	Peprotech 100-18B	20ng/ml
Heparin	Sigma H3149	0.7 U/ml
Penicillin-Streptomycin	Gibco 15140-122	1%

Adult NeuroCult™ Differentiation Medium

Component	Catalog number	Amount
NeuroCult® NSC Basal Medium	StemCell Thechnologies 05700	450 ml
FBS	PAA A15-151	2%
Penicillin-Streptomycin	Gibco 15140-122	1%

2.1.11.2 Ependymal primary culture

Enzymatic digestion solution

Component	Catalog number	Amount
3 ml DMEM 10% FBS 1% P/S		3 ml
90 µl Papain	Worthington 3119	10 mg
DNAse I (1% w/v)	Worthington 2139	45 µl
L-Cystein (12mg/ml)	Sigma C7352	72 µl

Stop Solution

Component	Catalog number	Amount
Liebovitz's L-15 medium	Gibco 11415	9 ml
FBS	PAA A15-151	1 ml
DNAse I (1% w/v)	Worthington 2139	45 µl
L-Cystein (12mg/ml)	Sigma C7352	72 µl

Proliferation medium

Component	Catalog number	Amount
DMEM Glutamax-I	GIBCO 31966	450 ml
Decomplemented FBS	PAA A15-151	50 ml
Penicillin-Streptomycin	Gibco 15140-122	1%

2.1.11.3 Embryonic Stem Cells culture

MEF Feeder cells medium

Component	Catalog number	Amount
DMEM	Gibco 21969	450 ml
FBS	PAA A15-151	50 ml (10%)
L-Glutamin	Gibco 25030	200mM (1%)

NEAA (100x)	Gibco 11140	5.7 ml
Penicillin-Streptomycin	Gibco 15140-122	1%

Embryonic Stem Cells proliferating medium

Component	Catalog number	Amount
Knockout DMEM	Gibco/Invitrogen 10829-018	500 ml
FBS for ESCs	PANSera 2602-P272405	75 ml (15%)
L-Glutamin	Gibco 25030	200 mM (1%)
ESGRO (LIF) or	Chemicon ESG 1107 or	57.5 µl or
LIF	GlobalStem GSR-7001	5 µg/ml (1000U/ml)
Penicillin-Streptomycin	Gibco 15140-122	1%

2.1.12 Southern blot

10x TBE buffer with 2,83 g/l guanosin (10 mM)

Denaturing buffer	NaCl 1.5M, NaOH 0.5M
Neutralization buffer	Tris-HCl pH 7.4 1M, NaCl 1.5M
20xSSC (1l) pH to 7,0	175.32 g NaCl, 88.23 g NaCitrat-Dihydrat.
Hybridization buffer	250mM Na2HPO4 pH 7.2, 7% SDS, 1 mM EDTA pH 8.0, 1% BSA

2.2 METHODS

2.2.1 Animals

All experiments were conducted according to the European and German laws, following the Animal Welfare Act and the European legislation Directive 86/609/EEC, followed by Directive 2010/63/EU from 2010 on and updated in 2013. The number of sacrificed animals and their stress or discomfort was kept to the minimum.

Mouse strains:

C57BL/6J

Lin41$^{Gt(lacZ\text{-}neo)fgw}$

(http://www.informatics.jax.org/javawi2/servlet/WIFetch?page=alleleDetail&key=91390#imsr)

2.2.2 Molecular Biology general methods

2.2.2.1 Agarose gel electrophoresis

Agarose (Lonza, 50004) was melted in Tris/Borate/EDTA (TBE) buffer at 1 to 2.5 %, and casted in Owl* EasyCast* B1 and B2 Mini Gel Electrophoresis Systems with 1 µl EtBr solution/10 ml. 10x Loading buffer was added to DNA prior loading. 10 µl of appropriate DNA ladder was loaded in the first well to evaluate DNA size resolution.

2.2.2.2 DNA restriction digestion

Restriction enzymes from NEB (New England Biolabs, section 2.1.2) were used according to manufacturer's instructions. DNA was digested from 30 min to O/N at 37°C, and enzymes were thermally inactivated when required for subsequent procedures, like ligation. When optimal digestion buffer was not common to two enzymes, subsequent digestions followed by purification were performed.

2.2.2.3 Mini, Midi, Maxi preparations

Bacterial cultures were grown in LB medium O/N at 37ºC unless otherwise indicated (lambda induced recombination, see conditional knockout overview 2.2.6). Cells were pelleted at 4ºC and plasmid DNA extracted with NucleoBond® Xtra Midi (Macherey Nagel, 740.410.100) according to manufacturer's instructions.

2.2.2.4 gDNA from biopsies

Tail clips from adult mice (> 3 weeks old) were mixed with a solution of 200 µl of DirectPCR-Tail reagent (Peqlab, 31-102-T) with Proteinase K (Roche, 3115836001) at 0.2 mg/ml final concentration. The tissue was digested O/N at 55ºC in a thermoblock (Eppendorf Thermomixer® compact). Next day, enzymatic activity was inactivated by 45 min incubation at 85ºC, residual tissue is spin down 2 min at 10000 rpm and 1 µl of the supernatant is used as template for PCR.

Yolk sacs from embryos were isolated, washed in iced cold PBS, and digested with 200 µl lysis buffer per sample, incubated them 65ºC 20 min, and twice at 98ºC 8 min, with mixtures by vortex between each step. After 2 min on ice, 200 µl of neutralization buffer was added, and 1 µl used as PCR template.

2.2.2.5 PCR DNA amplification

PCR was performed using a PXE 0.2 Thermal Cycler (Thermo Scientific), in 0.2 ml tubes. Unless otherwise is specified, 25 µl reaction is prepared as follows:

Reagent	Volume (µl)	Final concentration
Water MilliQ	17.25	
5x Phusion HF Buffer or 5x GoTaq Green Buffer	5	1x
10mM dNTPs	0.5	200 µM each
Primer A	0.5	1 µM
Primer B	0.5	1 µM
Template DNA	1	
Phusion Hot Start or GoTaq	0.25	0.02 U/µl

GoTaq enzyme was used for genotyping reactions, as well as semi-quantitative PCR. Phusion HF was used for cloning purposes.

2.2.2.6 RNA isolation

RNA was isolated from cells or tissue using TRIzol reagent (ambion, 15596026) according to manufacturer's instructions, and stored at -80°C.

2.2.2.7 cDNA synthesis

Reaction: 5 µg RNA, 1 µl OligodT, dNTP 10 mM, MilliQ up to 12.5 µl, 4µl 5x RT buffer, 0.5 µl Thermo S. Ribolock RNAse inhibitor, 1 µl RevertAid™ Premium Reverse Transcriptase. Total 20 µl reaction incubated 30 min at 50˚C and inactivated 5 min at 85˚C.

2.2.2.8 DNA Cloning

Antartic Phosphatase (M0289M, NEB) treatment was used after enzymatic digestion to prevent self-ligation of the DNA fragments.

Reagent	Volume (µl)
Restiction digest	50
Antartic phosphatase	1
Antartic buffer	5.5

Reaction was incubated at 37ºC 15 to 30 min and then at 65ºC 10 min to inactivate the enzyme prior to cloning.

Cloning was performed using T4 DNA ligase (EL0014, Fermentas) as follows:

Reagent	Amount
Linear vector DNA	20-100 µg
Insert DNA	1:3 to 1:5 molar ratio
10x T4 DNA Ligase Buffer	2 µl
T4 DNA Ligase	1U (0.2 µl)
MilliQ	Up to 20µl

The reaction was incubated 10 min at 22ºC and T4 Ligase subsequently inactivated at 65ºC 10 min.

2.2.2.9 Transformation

Transformation of plasmids was performed in XL-Gold *E. coli* bacterial chemicompetent strain. A vial of cells was thawed on ice, and 50 µl per condition

were transferred to pre-cooled 1.5 ml tubes. 50 µg of DNA was mixed with the cells and incubated 10 min on ice. Reaction was performed in Thermoblock 45 sec at 42ºC and immediately transfer to ice for 5 min. Transformed cells were then transferred to 500 µl of LB medium pre-warmed at 37ºC, and incubated 1 h with gentle shaking (50 rpm). Cells were then spread in agar plates containing the appropriate antibiotic, and incubated O/N at 37ºC, unless otherwise indicated. Individual colonies were picked for mini-preparation and subsequent enzymatic digestion evaluation.

2.2.2.10 FACS analysis

Astrocytes were washed with PBS and treated with trypsin to detach them from the plate. Then, they were centrifuged at 1000 rpm 5 min and after aspirating supernatant, resuspended in PBS and immediately used for analysis. Flow Cytometry assays were performed using BD Biosciences FACSCanto II flow cytometer. Results were analyzed with Flow Jo vX for Mac software.

2.2.2.11 Immunocytochemistry

Cells were cultured in 15 mm coverslips inserted in p24 well plates and coated when necessary (gelatin 0.2% solution in PBS for mES cells and BD Matrigel™ 1:20 in complete medium for NSPs). Cells were washed once with PBS, then fixed with PFA 4% 10 min at R/T and washed three times with PBS, 5 min each. Then they were blocked for unspecific bindings in blocking buffer containing 1xPBS, 5% normal goat serum and 0.2% Triton-X to allow permeable cell membranes, one hour at R/T.

Cells were incubated with primary antibodies diluted in blocking buffer O/N at 4°C, washed 3 times with PBS 1x and then incubated with the secondary antibodies in the same buffer for one hour at R/T, protected from light for the rest of the protocol. After washing 3 times in PBS the coverslips were mounted in a slide with DAPI or Drak5 to counterstain the nuclei and fluoro-protective mounting medium, and let dry at R/T horizontally. Images were acquired with microscopes Olympus software Magnafire or Confocal SL and processed using Adobe Photoshop CS4 for Mac.

2.2.2.12 Intracardiac perfusion for postnatal brain immunohistochemistry

Mice were administered a lethal dose of Avertin solution (1 ml - 20 mg - per adult mouse) via intra-peritoneal injection. When the animal was deeply anesthetized, was placed facing up, fixed and rib cage opened to expose the heart. A butterfly

needle was pinched into the left ventricle, the right atrium was cut and PB solution was perfused with a pump (2 ml/min flow) until liver color clears. Then, the solution is replaced by 30 ml PFA 4%. After perfusion, brain was removed and post fixed in PFA 4% solution O/N at 4ºC, and then treated for cryoprotection in a 30% sucrose solution in PBS O/N at 4ºC. Then the brain was embedded in O.C.T. compound and frozen using dry ice. Tissue blocks were stored at -80ºC and transferred to a Leica Cryostate at -20ºC to section 12 µm thick slides.

2.2.2.13 Immunohistochemistry from cryo-preserved tissue

Tissue sections in glass slides were let to dry at R/T when stored at -80°C or after cryosectioning, when the sample was previously fixed. Edges of the slide were profiled with a hydrophobic pen to contain the liquid; Tissue was post fixed with PFA 4% 10 min at R/T and then washed three times with PBS, 5 min. Then they were permeabilized and blocked for unspecific bindings in blocking buffer containing 1xPBS, 5% normal goat serum and 0.2% Triton-X, one hour at R/T. Sections were incubated with primary antibodies diluted in blocking buffer O/N at 4°C, covered with parafilm and in a wet chamber to avoid evaporation. Next day they were washed 3 times with PBS 1x and then with the secondary antibodies in the same buffer for one hour at R/T. After washing 3 times in PBS the sections were mounted in a slide with DAPI or Drak5 to counterstain the nuclei fluoro-protective mounting medium, covered with a glass coverslip and let dry at R/T horizontally, protected from the light.

For co-staining of Prominin-1 (antibody made in rat) with Lin41 (made in rabbit), the protocol was performed in two cycles: first, incubation of rabbit anti-Lin41 followed by secondary antibody goat anti-rabbit. Second, incubation of rat anti-Prominin-1 and secondary rabbit anti-rat. This way, cross-reaction between the secondary antibodies, of goat anti-rabbit binding rabbit anti-rat was avoided. For long-term storage, edge of the coverslips were sealed with colorless nail polish and slides were stored at 4°C. Images were acquired and processed like in immunocytochemistry procedure (section 2.2.2.11).

2.2.2.14 Whole embryo processing

E9.5 to E12.5 decidua were isolated from uterus branches in ice cold PBS, yolk sac was removed and used for genotyping and embryos were immediately fixed in PFA 4% (RNAse free) or X-Gal fixative, for 20 to 30 min at 4ºC.

2.2.2.15 Brain lateral ventricle wall whole mount preparation

The protocol was performed as described in (Mirzadeh, Doetsch, et al. 2010b). Briefly, adult mouse brains were isolated, and sectioned in two halves that separate the hemispheres. A coronal cut is made posteriorly to expose the hippocampus, which is later pulled away revealing the lateral wall that lays over the striatum. The superior cortex and corpus callosum are then cut away, to facilitate the section of the ventricular wall in a uniform thickness, necessary to mount it between a slide and a coverslip (Figure 9). This preparation can be used for immunofluorescence and other techniques, like X-Gal staining. Therefore, the tissue was fixed and treated accordingly to each purpose, using the standard protocol of IHC or X-Gal staining. A jellifying and flouro-protective mountain medium like DABCO was necessary to provide consistency, due to the thickness of the preparation, and the sample was let to settle at least O/N before imaging.

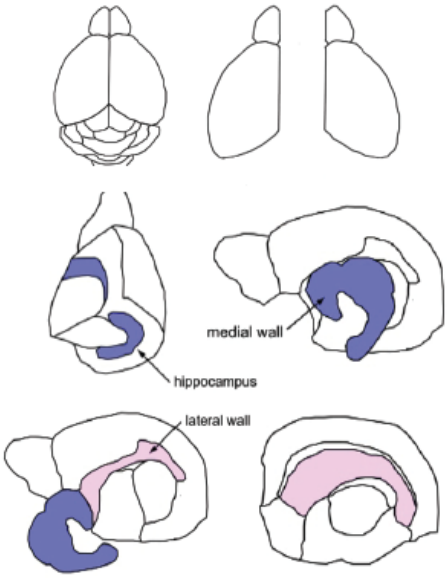

Figure 9. Scheme of ventricle lateral wall whole mount preparation. Hemispheres of the brain are dissected and hippocampus removed to expose the lateral wall. Adapted from Mirzadeh *et al*. 2010.

2.2.2.16 X-Gal staining

The same reagents were used to perform X-Gal staining in cells, sections, and whole mount like embryos or lateral walls. The time of fixation and enzymatic reaction was adapted to each preparation:

Step	Cells and Sections	E9.5 - E12.5 Whole mount
Fixation	10 min	20-60 min
Washing	3x 5 min	3x 15 min
Staining	2-4 hours	O/N
Washing	3x 5 min	3x 15 min

Staining reaction was performed at 37ºC protected from light. After the staining, the tissue is dehydrated in MeOH/PBS series (25, 50, 75 and 100%, 30 min to 1 hour each), and then rehydrated, to reduce the background and increase the staining intensity.

2.2.2.17 Immunoblotting. Western blot

Embryos were snap frozen in liquid nitrogen and reduced with a mortar and pestle; resulting powder was resuspended in TNN lysis buffer using aprox. 1ml buffer/mg of tissue. Cells were washed twice with ice cold PBS and then scraped in 500 µl PBS using a cell scraper. Lysate was centrifuged 5 min at 14000 rpm 4ºC, PBS aspirated and pellet resuspended in appropriate volume of TNN lysis buffer.

Tissue or cells were intensively resuspended in the buffer, using a 26G needle if necessary, and then incubated 20 min on ice. Afterwards the protein was separated from the rest of the cells by centrifuging 20 min at 4ºC and 14000 rpm and transferred the supernatant to a fresh tube.

Bradford assay

To measure the protein concentration, a reference of already known concentrations was used as a standard curve. BSA was diluted in lysis buffer to the following concentrations (0, 0.25, 0.50, 1 µg/ml). In addition, 1 µl of every sample to be measured was diluted in 9 µl of lysis buffer. 10 µl of the standard curve dilutions or the samples to be measured were dissolved in 1 ml Bio-Rad Protein Assay Dye Reagent working solution (a 1:5 solution in H_2O) and after 5 min incubation, and optic densitometry was measured at 595 nm.

To extrapolate the protein concentration, the values of the standard curved were plotted in a chart, with the known protein concentration in the X-axis versus the absorbance in the Y-axis. Then, the values of the absorbance corresponding to the samples (Y) were projected in the X-axis, obtaining the concentration of 1/10 dilution of the samples.

i) SDS-PAGE (Sodium Dodecyl Sulfate PolyAcrylamide Gel Electrophoresis) 8 or 10% gels were used to separate proteins according to their molecular weight. The appropriate volume 4x loading buffer was added to 20 to 30 µg of protein, and samples were boiled at 98ºC 3 min prior to loading, to denaturate the tertiary structure. 7 µl of PageRulerTM Prestained Protein Ladder Plus were loaded in the first well to monitor protein size resolution. Gels were run 25 min at 70 V and then another 90 min at 135 V.

ii) Wet transfer system Mini Trans-Blot® Cell was used for western blotting. Sponge and paper were soaked in transfer buffer, and Immobilon-P Transfer Membrane was activated after washing 30 sec in MeOH. The cassette was assembled Sponge/Paper/Gel/Membrane/Paper/Sponge from the black to the red side; bubbles were carefully squeezed out by rolling a cylinder over the sandwich before closing the cassette. Transfer was performed 75 min at 95 V with a cooling block in the chamber, to keep a low temperature.

iii) After blotting, the membrane was washed again in MeOH 30 sec and let dry for 30 min onto a paper towel, to allow several immunoblotting and stripping cycles. Then, the membrane was activated again in MeOH, shortly washed in PBST and incubated 5 min in Ponceau S solution, to visually evaluate the protein loading. Then membrane was briefly washed in PBST and blocked 45 min in PBST/5%Milk or 3%BSA, according to the antibody manual. Primary antibodies were diluted in blocking solution and incubated O/N at 4ºC. After 3 x 10 min washes in PBST, secondary antibodies was diluted 1:5000 and incubated 1 h at R/T. Then membrane was washed 3 x 10 min in PBST and signal was acquired using ECL reagents, either by film exposure or digitalized using ChemiDoc™ XRS+ System. Stripping was performed incubating the membrane 30 min to 1 h in stripping buffer, washing 5 times 1 min in PBST and blocking again. After all antibodies have been used, loading control was performed using anti-Vinculin and anti-mouse secondary antibody, both 1:10000 for 30 min at R/T.

2.2.3 Primary cell culture

2.2.3.1 Neural stem cells derived from adult SVZ

The culture of neural stem cells was performed as previously described (Reynolds & Weiss 1992; Reynolds et al. 1992). Briefly, mice from 6 to 8 weeks old were sacrificed and the brains were removed in ice-cold PBS. Two or three coronal

sections containing the medial zone of the lateral ventricles were made with a scalpel, and in a petri dish the SVZs were dissected with 20G needles used as micro scalpels. The tissue was mechanically dissociated with the needles and the smaller pieces were digested in papain containing enzymatic solution, 30 min at 37ºC.

The tissue was centrifuged 5 min at 1000 rpm, enzymatic solution aspirated, and cells were mechanically dissociated and plated in 10 cm dishes, one brain per plate, in Complete Adult NeuroCult™ Proliferation Medium, containing 20 ng/ml EFG, 20 ng/ml bFGF and 0.7 U/ml heparin. After 4-5 days the neurosphere formation was observed, and cells were passed after a 3 min trypsin digestion and mechanical dissociation, and seeded at 50000 cells/ml density. Experiments were performed at passages 2 to 5, to ensure uniformity.

2.2.3.2 Ependymal cell culture from newborn forebrain

Ependymal primary culture was performed as previously y described (Guirao et al. 2010; Paez-Gonzalez et al. 2011). Prior dissection, 25cm^2 flasks were coated with Poly-L-Lysine (PLL 40 µg/ml) at least 1 h at 37ºC, then washed three times with MilliQ water and let dry 1 h in sterile conditions. P0 to P2 brains were isolated in ice-cold PBS, and dissected, discarding meninges, olfactory bulb and hippocampal formation. The rest of brain tissue was mechanically dissected in small pieces using p1000 pipette, and digested in 1 ml ependymal enzymatic solution per brain, 45 min at 37ºC. Reaction was stopped with 1 ml stop solution and followed by three rounds of centrifugation at 1000 rpm and mechanical dissociation in Leibovitz's L-15 medium. Cells were plated in previously PLL coated 25cm^2 flasks (one brain per flask), incubated during 3-5 days in 37ºC, 5% CO_2, 95% humidity until the culture reached confluence. When confluent, flasks were shaken O/N at 250 rpm, at R/T and next day cells are de-attached after 5 min trypsin incubation, and plated in 15mm glass coverslips in p24 well plates, 1.5x10^5-2x10^5 cells in a 20 µl drop, to ensure confluent attachment. After one hour incubation in 37ºC, 5% CO_2, 95% humidity, 1 ml medium was added. Next day, medium was changed to differentiation medium DMEM/1%P/S, and cells were incubated for 10-15 days.

Alternatively, cell suspension from newborn mice was plated directly in flask or glass coverslips at 450,000–500,000 cells/ml in proliferative medium. After 3-4 days cells reached 90-100% confluence, medium was changed to 2% containing

serum, and not changed during 10-15 days, to promote differentiation (Paez-Gonzalez et al. 2011).

2.2.3.3 Embryonic stem (mES) cells from blastocyst inner cell mass

Dr. Geert Michel's group (Transgene Technologies FEM, Charité Berlin) isolated embryonic stem cells from blastocysts derived from mating of *Lin41*$^{+/gt}$ mice. They isolated the blastocysts at embryonic day 3.5, seeded them in the presence of MEFs and cultured them for 4 to 5 days. Then, they extracted the outgrowths of the inner cell mass, discarding those from the trophoblast, and initiate a culture of the ES cells in the presence of MEFs and medium containing LIF 1000U/ml.

18 lines were genotyped using the Gene Trap genotyping primers. At least 3 clones of each genotype were karyotyped to ensure a regular number of chromosomes, and they were cultured in plates coated with gelatin 0.2% PBS solution in presence of a feeder layer of mouse embryonic fibroblasts (MEFs). All experiments were carried between passage 20 and 50.

2.2.3.4 Mouse Embryonic Fibroblasts (MEFs) as feeder cells for mES cells

Mouse embryonic fibroblasts MEFs cells were derived from skin of mouse E12.5 or E13.5 embryos from the strain Tg(DR4)1Jae/J. We were provided with passage 2 active MEFs (1^10^6 cells per vial) and expanded them until passage 5, following a 1:3-5 expanding ratio. Then, cells were inactivated by incubation 3-5 h in presence of Mitomicyn C at 10 µg/ml, and frozen at 1^10^6 cells per vial in the presence of 10% DMSO. Each vial was used to coat 120 cm^2 of cell culture dish surface as feeder cells, at approx. 20000/cm^2.

2.2.4 Embryonic stem cells karyotype

Mouse ES cells were plated for one or two passages in gelatin coated p60 dishes, to minimize the presence of MEFs. The day before they were split at a 1:3 ratio, to ensure a big number of cells in proliferative state. Cells were washed twice with PBS and incubated 2 to 4 h in ES cells proliferative medium supplemented with 20 µl /mL Colcemid™ KaryoMAX®. A change in shape to a round appearance was monitored under the microscope. Then cells were washed with PBS, treated with trypsin 3 min at 37ºC to detach them from the plate, transferred to a conical 15ml tube and centrifuged at 1000rpm for 10 min. Supernatant was aspirated, leaving approximately 1ml in the tube. Then around 8 drops of hypotonic solution (0,4%NaCl/0,4%Na-Citrat in H_2O, warmed at 37°C water bath) were carefully

added to the supernatant with a glass pipette, stirred slowly to mix, followed by the addition of more hypotonic solution and a very vigorous resuspension of the pellet. Cell suspension was incubated at 37ºC in the water bath for 30 min, to complete the cell lysis. Then, cell lysates were pelleted 1000 rpm 10 min and fixed in fixative solution: Methanol-Glacial acetic: 3:1, kept at -20ºC, following the previous protocol: supernatant aspirated except for the last ml, few drops of solution added, stir to mix and vigorous mixing with glass pipette, for a total of 3 rounds. Fixed nuclei were mounted in glass slides by pipetting 5-6 drops of lysate solution from 50 cm over the slides, to ensure the spreading of the nuclei and facilitate the count. Mounting was performed with DAPI and Fluor protective mounting medium, and pictures were acquired with the 100x objective of Olympus microscope, to count the chromosomes.

2.2.5 Cell transfection

Astrocyte primary cultures derived from P0-P4 mouse brain were kindly provided by Lehnardt's group, from the Institute for Cell and Neurobiology. Cells were plated in p6 well plates at 80% confluence, and transfected using Lipofectamine® 2000 reagent, according to manufacture's instructions, with different plasmids containing GFP. FACS assay was performed 48h after transfection.

2.2.6 Overview of the conditional knockout vector generation

To overcome the limitations of the gene trap mouse embryonic lethality, and study in more detail and with precision the role of Lin-41 in mouse, we designed and constructed a vector for the generation of a conditional knock out (cKO) mouse. The most common system is the Cre-LoxP recombination based, were part or the complete gene of interest is flanked by two loxP sites, 34 bp palindromic sequences that are recognized by the enzyme recombinase Cre (Causes recombination), resulting in a single loxP sequence plus the segment between them circularized and finally degraded. Using this method, deletion of desired and precise DNA segments can be easily achieved by exposure to Cre (Hoess et al. 1982).

We aimed to eliminate the exon number 4 of the gene, as well as part of the 3' UTR region containing the binding sites for the microRNA let-7, upon Cre recombination. We expect, as in the gene trap model, that a protein lacking the C-terminus will be not functional due to the loss of interaction domains, as well as

the miRNA let-7 binding sites, despite the presence of the RING domain. For that, one loxP (5') site sequence must be inserted in the intron number 3, and a second one (3') in the 3' UTR of the gene (Figure 13).

For the construction of a vector with these modifications, we took advantage of the recombination-based system widely use to generate cKO mice models. This is based on the recombination of homologous DNA in long regions (around 5-10 kbp) using the activity of phage lambda virus *Red* genes, and allowing to integrate the mutant construct, with the desired modifications (loxP sites and selection genes) in the original genome with high efficiency (D. Yu et al. 2000; Liu et al. 2003). The *Red* genes required for recombination are three: first, *exo*, that encodes for a 5'-3' exonuclease; this enzyme targets the 5' side of the dsDNA, and leaves a 3' overhang. The second gene is *bet*, which recognizes the 3' overhangs and pairs them with the complementary sequences created in the complementary DNA. The third gene, coding for Gam protein, blocks *E.coli* RecBCD endogenous activity, an exonuclease that degrades linear dsDNA. In the defective prophage, these genes are under the control of the promoter $P_{L,}$ itself repressed by cI857, active at 32ºC. When temperature is raised to 42ºC for 15 min, the repression is loss and P_L works expressing the *Red* genes with high efficiency (Poteete 2001; Zhang et al. 1998). Thus, lambda-containing strains were regularly grew at 32°C, when the recombination machinery is inhibited. When recombination was required, the cells containing the fragment of interest were activated at 42°C for 15 min, inducing transformation, and obtaining combinatory products that were selected with the appropriate antibiotics.

Cre-induction was achieved by adding 10% Arabinose solution 1:100 to an O/N grown bacterial culture *E. coli* EL350 for one hour before proceeding to midi-prep.

2.2.7 Southern blot analysis

2.2.7.1 Genomic DNA enzymatic digestion, electrophoresis, and gel treatment.

Genomic DNA (gDNA) was provided by Dr. Boris Jerchow (MDC, Berlin) in lyophilized condition in p96 well plates. Those were centrifuged prior to the addition of 35 µl enzymatic digestion mix, and afterwards, to ensure the resuspension of all the material.

Enzymatic digestion mix:

Reagent	Final amount	Volume (µl)
Enzyme	20 U	x
BSA (100 µg/ml)	1 µg /ml	0.35
Buffer 10x	1x	3.5
MilliQ		Up to 35

gDNA was digested O/N at 37ºC, spined down to collect steam from the lid and added 4 µl loading buffer. Samples were loaded in 0.4 to 0.6% agarose gels (26 x 26cm, 2x51 well combs) made in TBE 1x guanosine (to protect DNA integrity from UV) 1mM buffer and containing 0.1 µg/ml EtBr. Samples were run at 50V O/N (16h) and band size separation monitored with a picture under a UV table.

The agarose gel was treated for blotting by submerging it in 500 ml of the following solutions, in three washing steps:

- Depurination: HCl 0.2N solution, 10 min. Necessary for transfer of <10Kb fragments. Short rinse in MilliQ.
- Denaturation: 1.5M NaCl/0.5M NaOH. 45 min.
- Neutralization: 1M Tris-HCl pH 7.4/1.5M NaCl. 45 min.
- Equilibrate in 20xSSC

2.2.7.2 Blotting transfer of DNA

Treated gels were assembled to transfer the DNA to a nylon membrane. A support platform was placed in a deep tray that contains the buffer, 20xSSC, and covered with a large piece of Whatman paper that overhangs to contact the buffer and transfer it constantly. The gels were carefully flipped and placed upside down (wells opens facing down) and on top of them a piece of nylon membrane positively charged (Hybond-N+, RPN303B, GE Healthcare) of the same dimensions than the gel. It was important to prevent the membrane from overhanging, to avoid direct contact with the Whatman paper. Over the membrane, three Whatman papers of same size were placed, and then a thick stack of paper towels, covered with a glass plate and approx. 500 g weight. The paper towels absorbed the buffer that transferred the DNA by capillarity (Figure 10).

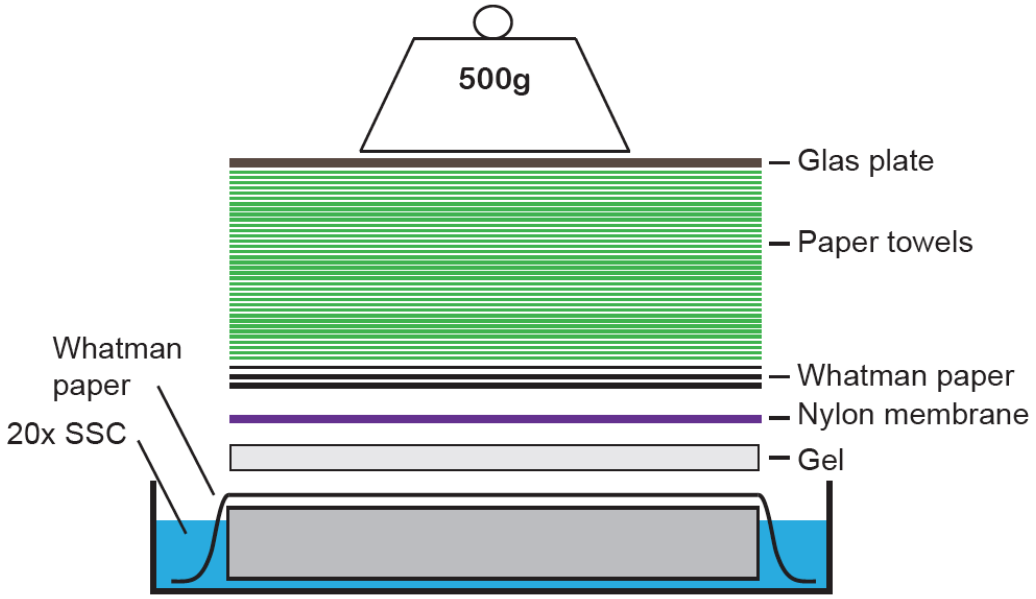

Figure 10. Scheme of Southern blot. DNA is transferred from the agarose gel to a nylon membrane by capillarity, using 20xSSC buffer.

The transfer was performed O/N with 2 l of 20xSSC, and refilled next morning when necessary. The DNA was then cross-linked to the membrane using the GS Gene Linker® UV Chamber from Bio-Rad, in the program C3 (150 mJ).

2.2.7.3 Radioactive probes label

To label the DNA probes for Southern blot hybridization the Prime-It II Random Primer Labeling Kit was used, following manufacturer's instructions. 25 µg of DNA were labeled using 5 µl labeled alpha-P^{32} dCPT at 2970 Ci/mmol per reaction, and then 1 µl of the 50 µl reaction was measured in a scintillation reaction.

The radiolabeled probes were purified using Qiagen Kit, following the manual, and after elution 1 µl is measured again in scintillation reaction, to estimate the specific radioactivity incorporated in the probe.

2.2.7.4 Filter hybridization

The nylon membrane was pre-hybridized in 15 ml hybridization buffer for at least 30 min at 68ºC. The labeled probe was denatured by boiling in water for 5 min, and immediately dissolved in 5 ml hybridization buffer pre-warmed at 68ºC, that was applied to the tube with the nylon membrane and incubated in a rotor oven O/N at 68ºC.

Unspecific bindings ware washed off by a series of astringent washes:

- Two times 2xSSC, 0.1%SDS R/T 10 min.

- Two times 2xSSC, 0.1%SDS at 50ºC, 5 min.
- Once or twice 1xSSC, 0.1%SDS, at 60ºC 10 min.

The filter radioactivity was monitored with the radioactivity counter/contamination monitor and the washes stopped when the counting was around 0,5-0,7.

2.2.7.5 X-Ray film exposure

The membrane was then transferred into a plastic foil and expose to an X-Ray film with in a film cassette at -80ºC in between 5 and 30 days. When necessary, membrane was stripped with boiling 0.1xSSC, 0.1% SDS for 10 min or until the measure count was (0.00), and resumed the protocol at the pre-hybridization step.

3. Results

3.1 *Lin41* gene trap mouse generation

Gene Trapping is a widely used method to randomly cause gene loss of function and reportable mutations in the mammalian genome through the insertion of a so-called ¨trap cassette¨ in the intron of a given gene. The classical gene trap vector is formed by a splice acceptor (SA) sequence followed by the "trap" cassette, which contains the reporter and/or selectable gene (usually *LacZ* and/or neomycin resistance - Neo^R) and ending in a polyadenylation (polyA) signal. As a result, the translated messenger will generate a chimeric protein containing the original endogenous initial fragment, but truncated, with the exons located downstream of the insertion site substituted for the reporter protein (Figure 11).

This construct lacks its own promoter; therefore it is expressed under the endogenous promoter activity. There are additional types of Trap vectors that have their own promoters, like the enhancer or promoter-trap. The classical gene trap approach has the advantage of reporting the endogenous expression of the targeted gene, even though it presents several limitations, like a restriction to genes active in mouse embryonic stem cells (mES cells), due to the need for expression of the selectable marker (Stanford et al. 2001). To investigate the consequences of *Lin41* disruption in mammals, while characterizing its expression in detail, a *Lin41* gene trap mouse line was generated in our laboratory. The standard gene trap vector used is composed by a splice acceptor sequence, followed by the reporter/selection gene (a fusion of ß-Galactosidase (ß-Gal) and Neo^R genes, named *ß-Geo*), and the polyA signal to terminate transcription. This cassette is inserted after the second exon of *Lin41*. As a result, the transcription will contain the beginning of the LIN41 sequence, fused to the ß-GEO reporter in the end. Specifically, the translation product from the mRNA will result in a fusion protein containing an N-terminal sequence of 327 aa from the original *Lin41* sequence, with the C-terminus replaced by ß-GEO protein. The estimated total size of the chimeric protein is 2577 aa, corresponding to an approximate molecular weight of 280 kDa. In comparison, the wild type LIN41 protein is 855 aa, and approximately 95 kDa (Figure 11).

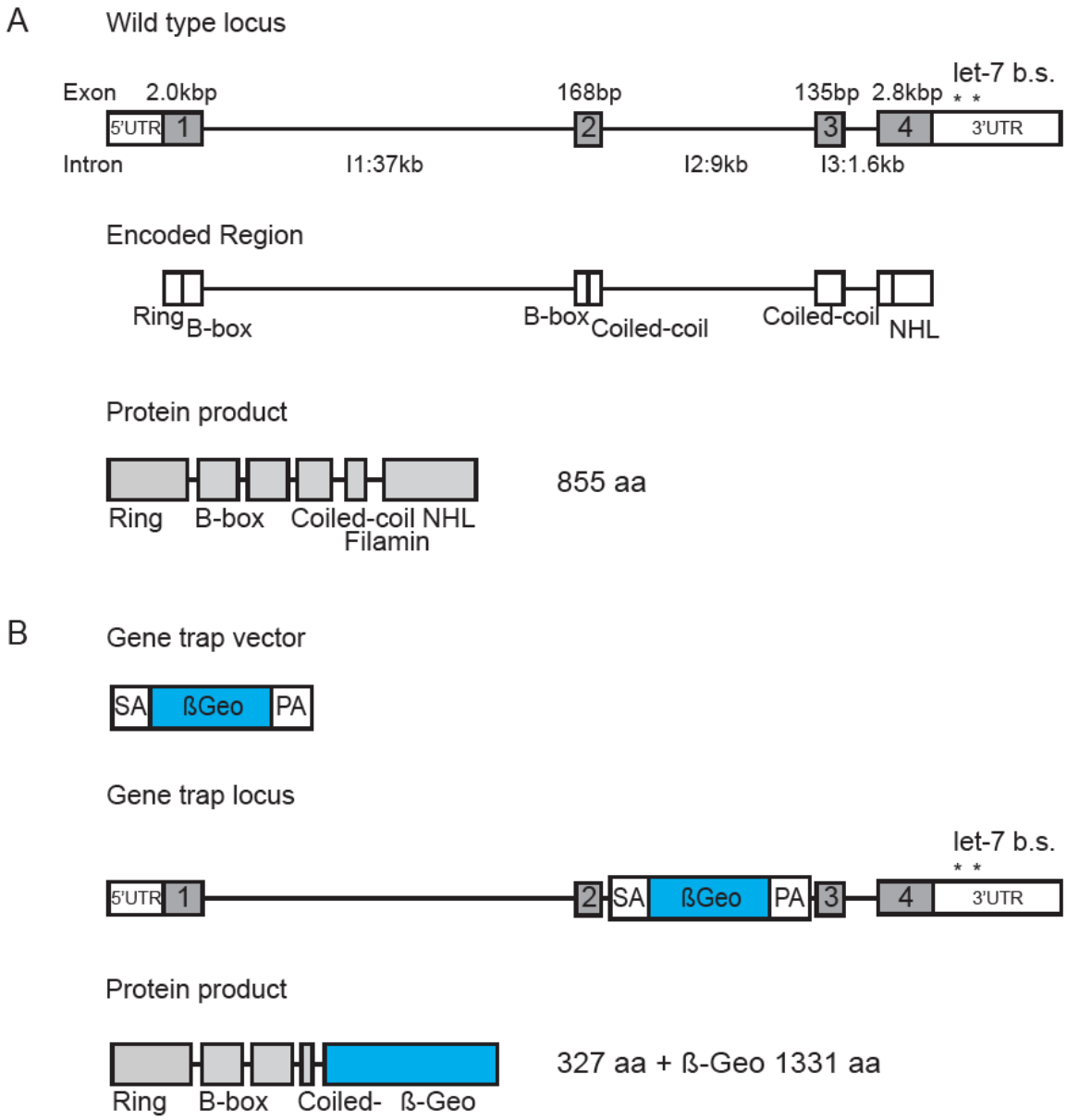

Figure 11. Schematic of Lin-41$^{Gt(lacZ\text{-}Neo)fgw}$ (Lin41^{gt}) gene trap insertion in mouse *Lin41* locus. A. Scheme of *Lin41* wild type mouse allele, composed of 5' untranslated region (UTR), four exons depicted in grey boxes and 3'UTR containing two let-7 miRNA binding sites (asterisks). The encoded domains of the wild type are represented below as white boxes, corresponding to each exon. The protein product with its domains is represented in light grey boxes. B. Simplified gene trap cassette scheme, containing a splice acceptor (SA) sequence to avoid alternative splicing, a selectable gene combination of ß-Galactosidase and neomycin resistance gene (*ß-Geo*), and polyA (PA) to induce termination of transcription. Scheme of gene trap cassette inserted in the second intron of *Lin41* gene and the resulting protein product, with truncated Coiled coil domain fused to ß-GEO protein.

RING, B-boxes and part of Coiled-coil domains from *Lin41* are conserved, whilst the final part of Coiled-coil and the NHL repeats are absent, replaced by *ß-Geo*. Based on known *Lin41* loss of function mutations in *C. elegans* the resulting fusion protein is predicted to be non-functional, and is not detected by available Lin41

antibodies, which target the NHL repeats. Nevertheless, transcription is governed by the endogenous *Lin41* promoter, so that promoter activity can be traced by ß-Gal enzymatic activity via X-Gal staining, or detected by immunostaining using anti-ß-Gal antibodies. This model allowed us to study *Lin41* expression and function in mouse.

We obtained a line of mES cells carrying the *Lin41* gene trap vector from the German Gene Trap consortium:
(http://www.informatics.jax.org/javawi2/servlet/WIFetch?page=alleleDetail&key=91390). In collaboration, Boris Jerchow's group (MDC, Berlin-Buch) injected the cells into C57BL/6J blastocysts generating seven chimeric mice that reached sexual maturity, of which number three was a female. All animals were mated with wild type partners and the progeny (F1 generation) were analyzed by PCR to identify germline transmission of the vector.

For genotype analysis, I used one common forward primer specific for the sequence upstream of the vector insertion, and one reverse primer specific for the vector or the wild type gene, respectively (Figure 12A). From the total of seven chimeras, numbers 1, 5 and 7 were fertile, and produced pups carrying one copy of the insertion (Figure 12B).

Mice obtained from this first generation of chimeras were inbred, generating the Lin41 gene trap *Lin41*$^{Gt(lacZ\text{-}NeoR)fgw}$ (referred to hereafter as *Lin41*^{gt}) mouse colony. Since the parental mES cells were derived from 129 mouse strain, the colony was backcrossed to C57/BL6J mice for five generations to ensure a uniform genetic background before performing further experiments.

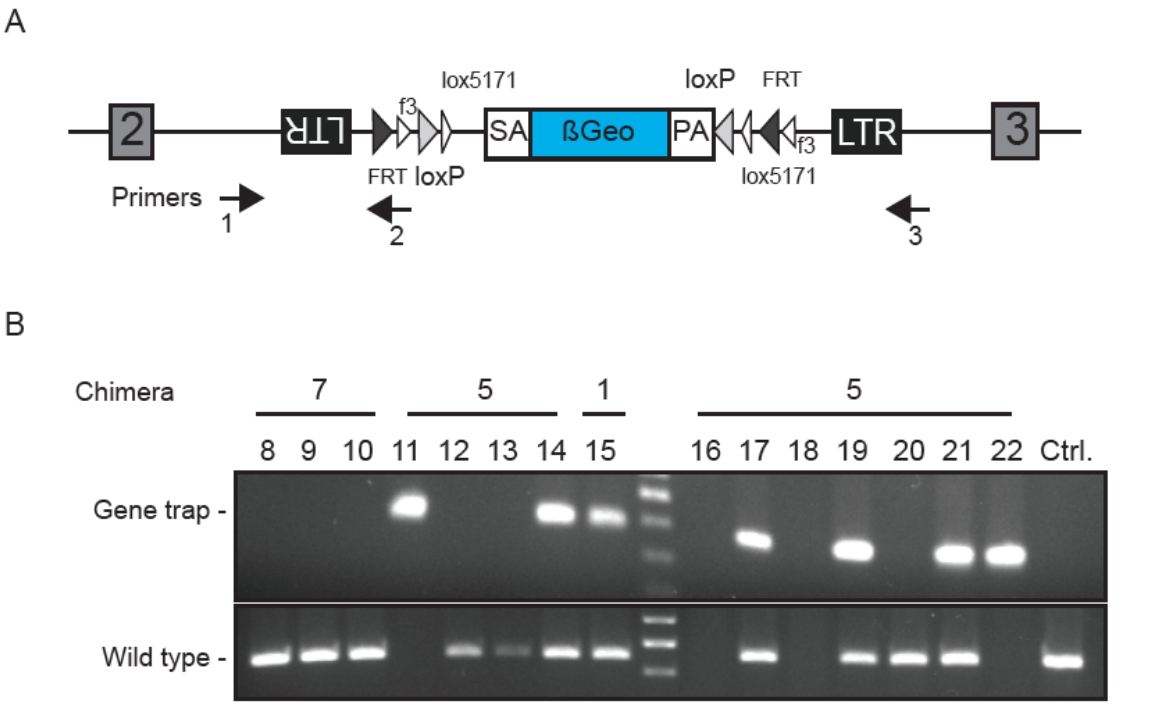

Figure 12. Scheme of the gene trap cassette insertion in the *Lin41* locus and PCR strategy to genotype F1 generation born from the chimeric mice. A. Complete scheme of the gene trap cassette integrated in the second intron of Lin41. LTR: long terminal repeat. FRT, f3, loxP and lox5171: recombination sites not used in the genetic model. Arrows indicate the primers: 1. Common forward primer (Intron2 Fw). 2. Reverse primer for gene trap insertion (Gene Trap Rev). 3. Reverse primer for wild type allele (Intron2 Rev). B. PCR genotype of the F1 generation. The number of the chimeric parents is displayed above the number of the F1 pups. Top gel shows the result using primers 1 and 2, to detect cassette integration (Gene trap). Bottom gel shows results from primers 1 and 3 to detect wild type sequence. In the control (Ctrl.) in the last lane genomic DNA from BL6/C57J mouse was used as template.

3.2 Lin41 Conditional Knockout mouse generation

3.2.1 Vector generation

One limitation of the gene trap mouse line is the fact that it generates a full null mutation. *Lin41* is universally disrupted, complicating the differential study of specific tissues and developmental stages. A conditional knockout mouse permits to bypass this limitation, allowing controlled mutation under combination with promoters active in the spatiotemporal frame of interest for *Lin41* deletion. The strategy to generate a mouse with a conditional mutation in gene *Lin41* is summarized in Figure 13.

The wild type Lin41 gene is located in chromosome 9 of the mouse genome. It comprises four exons, followed by a 3'UTR that contains two binding sites for let-7 miRNA (Figure 13A). We chose to target the exon number 4 and the beginning of

the 3'UTR containing the regulatory sequences; therefore, it is necessary to insert two loxP sites on the flanks of this region of interest, so it is removed upon Cre-induced recombination. Once the vector is generated, it is electroporated into mES cells and recombination between homologous regions (homology arms) is induced to replace the wild type sequence with the vector one. In addition to the loxP sites, a *Neo*^{R} gene is inserted, to allow the selection of cells containing the insertion (Figure 13B and 13C).

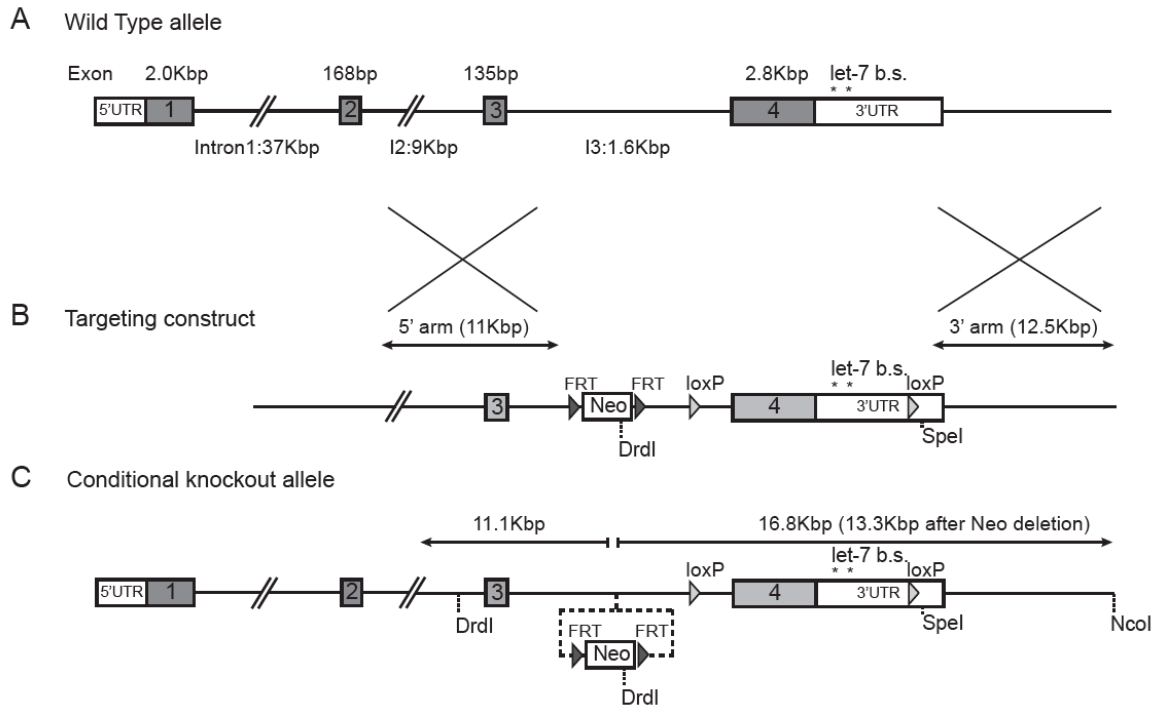

Figure 13. *Lin41* conditional knockout generation overview. A. Scheme of *Lin41* wild type mouse allele, composed of 5' untranslated region (UTR), four exons depicted in dark grey boxes separated by three introns, and 3'UTR containing two let-7 miRNA binding sites (asterisks). The length of each section is displayed in base pairs (bp) or kilo base pairs (kbp). B. Scheme of the conditional knockout vector, with a *Neo*^{R} as selection gene, flanked by FRP sites, and the exon number 4 flanked by loxP sites. Exons are depicted in light grey. The crosses between the wild type allele and the conditional vector represent homologous recombination between the homology arms (10 kbp long). C. Scheme of the conditional knockout allele integrated in the *Lin41* locus, indicating the restriction sites artificially introduced.

The precise steps necessary for the construction of the conditional knockout vector are depicted in Figure 14: Firstly, a partial segment of the gene *Lin41* was cloned into a plasmid (pDTA, derived from pBluescript), for easier manipulation. I used a BAC containing *Lin41* genomic sequence obtained from the mouse BAC

library RPCI-23, made from female C57BL/6J mouse kidney and brain genomic DNA.

For this, two small homology arms ~320 bp (A-B and Y-Z) flanking the region of interest in the BAC are amplified by PCR using primers that include restriction sites to allow insertion in the circular plasmid by cloning with HindIII and SpeI (A-B) and XhoI and HindIII (Y-Z) in pDTA; this construct is denominated retrieval vector (Figure 14A). The retrieval vector is then used to transfer the entire *Lin41* sequence between the A-B and X-Y segments from the BAC through homologous recombination via GAP repair, mediated by the lambda prophage *Red* genes (see Methods 2.2.6). For this, the BAC is retransformed from the strain DH10B to EL350, which contains a defective lambda prophage in which the *Red* genes can be expressed from a temperature sensitive promoter. The homology regions in the retrieval vector guide homologous recombination with *Lin41* sequences on the BAC upon co-electroporation of vector and BAC followed by temperature induction of homologous recombination. The product of recombination is referred to as a retrieved vector, comprising the plasmid backbone with the gene for selection with ampicillin (amp^R) along with the desired genomic region of *Lin41* (Figure 14A and 14C – step1).

In parallel to the retrieved vector, two mini-retrieval vectors are generated from the plasmid pNeo. This plasmid contains the Neo^R gene, flanked by one pair of FRT sites (sequences recognized by the recombinase Flp, in a similar system to loxP-Cre) and one pair of loxP sites. The restriction sites between these features allow the insertion of new homology arms maintaining or suppressing the FLT and loxP sites at convenience (Figure 14B). Each of these two mini targeting vectors will be inserted following a determined order at the 3' and 5' sides of *Lin41* exon 4, to achieve the final conditional vector.

First, is necessary to assemble the insertions at the 3' side: it will contain the complete "Neo^R cassette", consisting of two loxP sites flanking two FRT sites with the Neo^R gene in the center. Two homology regions (G-H and I-J) were amplified by PCR and cloned into the pNeo plasmid using the enzymes XhoI and HindIII (G-H) and NotI and SacI (I-J). After insertion and selection using neomycin, Cre

recombination is induced, resulting in a unique loxP site downstream of exon 4 (see 2.2.6 and Figure 14C – step 1 and 2). Then, the second mini-targeting vector is inserted in the 5' side of exon 4. This time the first loxP site of pNeo has been replaced by cloning the homology region C-D with XhoI and EcoRI, and the region E-F is cloned with NotI and SacI, like in I-J arm in the first mini vector. The resulting cassette will have the *Neo*^{R} selection gene flanked by two FRT sequences, followed by a unique loxP site (Figure 14C – step 3). Hence, *Neo*^{R} can be used for selection of the positive clones, prior to deletion by Flp recombinase activity. When integrated in the genome, the two resulting loxP sites will be at the 3' and the 5' sides of the targeted region (Figure 14C – step 4). The DNA analysis by enzymatic digestions to monitor every step in the vector generation is shown in Figure 14D.

Summarizing, the final product generated is a vector, inserted in the pDTA backbone, that contains the end of the *Lin41* gene, with a *Neo*^{R} sequence that can be deleted by Flp recombination. In addition, two loxP sites flank the exon 4 and the let-7 binding sites of the 3'UTR at the end of the gene. This vector was linearized and subsequently electroporated in mES cells for integration in the genome.

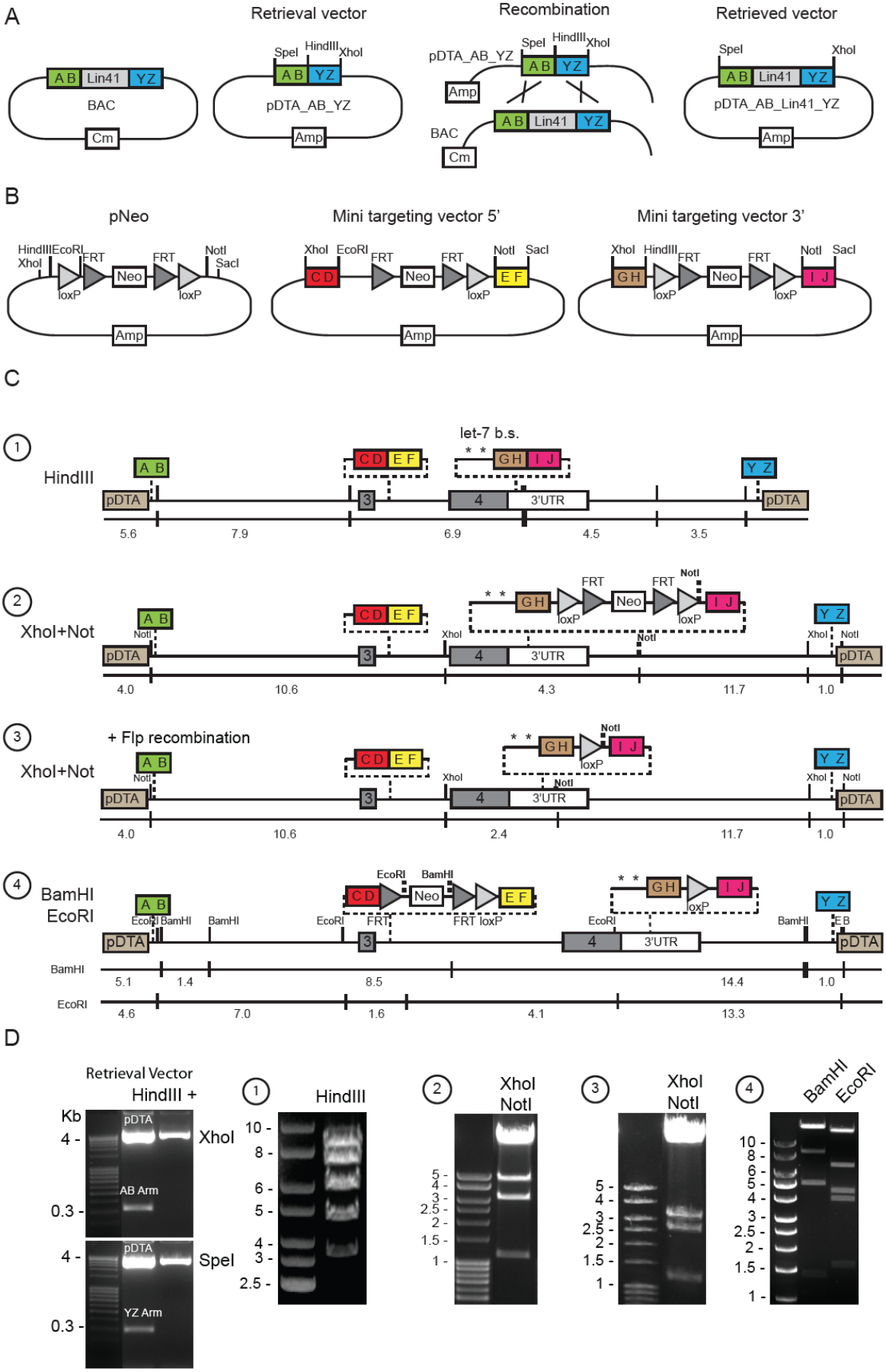
A
Retrieval vector
Recombination
Retrieved vector
A B Lin41 Y Z
BAC
Cm
SpeI HindIII XhoI
A B Y Z
pDTA_AB_YZ
Amp
pDTA_AB_YZ
Amp
BAC
Cm
A B Lin41 Y Z
SpeI XhoI
A B Lin41 Y Z
pDTA_AB_Lin41_YZ
Amp
B
pNeo
Mini targeting vector 5'
Mini targeting vector 3'
HindIII EcoRI XhoI FRT Neo FRT NotI SacI
loxP loxP
Amp
XhoI EcoRI FRT C D Neo FRT NotI SacI E F
loxP
Amp
XhoI HindIII FRT G H Neo FRT NotI SacI I J
loxP loxP
Amp
C
1
HindIII
let-7 b.s.
A B
C D E F
G H I J
Y Z
pDTA
3
4
3'UTR
pDTA
5.6
7.9
6.9
4.5
3.5
2
XhoI+Not
NotI
XhoI
FRT
loxP
4.0
10.6
4.3
11.7
1.0
3
XhoI+Not
+ Flp recombination
4.0
10.6
2.4
11.7
1.0
4
BamHI
EcoRI
BamHI
EcoRI
5.1
1.4
8.5
14.4
1.0
4.6
7.0
1.6
4.1
13.3
D
Retrieval Vector
HindIII +
Kb
4 -
0.3 -
pDTA
AB Arm
XhoI
SpeI
YZ Arm
1
HindIII
10 -
8 -
6 -
5 -
4 -
3 -
2.5 -
2
XhoI
NotI
5 -
4 -
3 -
2.5 -
2 -
1.5 -
1 -
3
XhoI
NotI
4
BamHI
EcoRI
10 -
8 -
6 -
5 -
4 -
3 -
2.5 -
2 -
1.5 -
1 -

Figure 14. Strategy to construct the conditional knockout vector. A. Simplified scheme of the bacterial artificial chromosome (Bac) containing *Lin41* gene, and the retrieval vector used to subclone a fragment of *Lin41* in pDTA vector, using homologous recombination between homology regions AB and YZ. The resulting construct is pDTA plasmid containing a fragment of *Lin41*, is called retrieved vector. B. pNeo plasmid and mini targeting vectors generated from pNeo by cloning small homology regions of *Lin41* sequence. C. Steps in the generation of the vector, indicating the restriction sites used to monitor proper sequences. 1) Retrieval vector containing *Lin41* partial sequence. 2) Insertion of the first mini targeting vector. The entire sequence was introduced at the 3' side of the exon by homologous recombination. 3) After Cre recombination, one loxP remained in the vector, right to the fourth exon. 4) The second mini targeting vector introduced a Neo^R selectable gene flanked by FRT sites and one loxP site, at the 5' side of exon 4. D. Agarose gels of DNA digestion from every step of the construction, to monitor proper integrations.

3.2.2 Test of miRNA activity on *Lin41* 3'UTR

After the proper generation of the vector for a *Lin41* conditional knockout (cKO), and prior to electroporation into mES cells, we wanted to confirm that the second loxP site, in the 3'UTR, did not interfere with the regulatory activity of microRNA let-7 (see Figure 13C). There are two let-7 miRNA binding sites in the 3'UTR sequence of *Lin41*, predicted by TargetScan and experimentally confirmed (Rybak et al. 2009), located 165 and 261 bp after the end of the fourth exon. The second loxP site is located 813 bp after the end of the coding sequence, and we wanted to corroborate that this sequence addition does not interfere with the normal miRNA regulatory activity.

I cloned the first 1282 bp of the wild type 3'UTR, and 1383 bp of the cKO vector sequence containing one loxP site, into a modified version of the eGFP plasmid pEGFP-C1, called pWu. As a positive control I used a synthetic let-7 sensor construct, with two perfectly complementary let-7 binding sites located in the 3'UTR of eGFP, also cloned in the reporter plasmid pWu. In the absence of let-7 miRNA, this construct constantly produces GFP, and the signal can be detected either by microscopy and FACS analysis. If the transfected cells express let-7, the miRNA binds its specific sites in the construct, inhibiting the production of the protein.

I transfected these vectors into a primary culture of astrocytes, which express let-7 (Smirnova et al. 2005), to observe if the modification in the 3'UTR in the conditional allele resulted in any difference in activity compared to the wild type.

The results are shown in Figure 15: intensity of GFP fluorescence of pWu construct was taken as reference, and compared to it, the let-7 sensor was clearly

downregulated due to the let-7 repression. Wild type and cKO vector 3'UTR fluorescence signals were slightly repressed due to the regulation through the two let-7 binding sites. This repression occurs in both constructs to the same extent, indicating that the insertion of the loxP site downstream of the let-7 binding sites does not interfere significantly in the regulation of the mRNA by miRNA activity. This experiment validates the integrity of the *Lin41* conditional knockout vector, which is not expected to alter endogenous *Lin41* production and regulation before Cre recombination is induced.

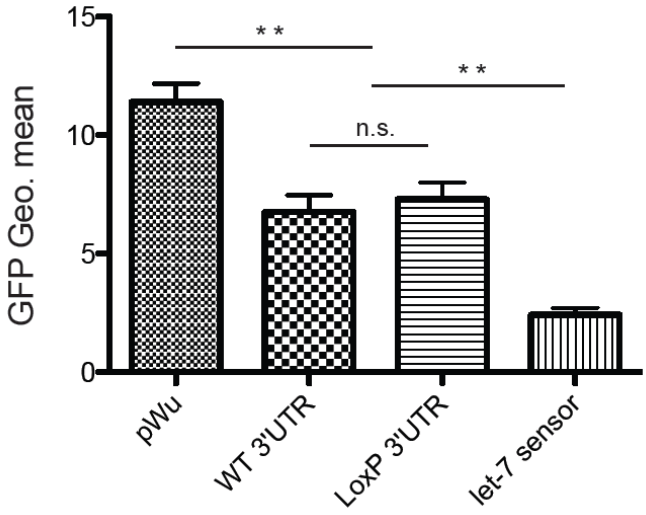

Figure 15. FACS analysis of *Lin41* 3'UTR regulation by let-7 activity in the wild type and vector sequence. Comparison of 3'UTR of wild type *Lin41* allele and conditional knockout vector containing one loxP site, in relation to miRNA *let-7* regulatory activity. Astrocytes were transfected with pWu plasmid, containing GFP (pWu) or with cloned 3'UTR from wild type (W.T. 3'UTR) or vector (LoxP 3'UTR); sponge vector with four perfect binding sites for let-7 after GFP was used as negative control. X axis represents Geometric mean of GFP intensity analyzed by FACS. Statistical analysis one-way ANOVA Bonferroni adjustment: **: $p<0.005$, ***: $p<0.0005$, n.s.: not significative.

3.2.3 Vector injection and analysis of clones by Southern blot and PCR

Following generation of the targeting vector, the construct was linearized using the single-cutter PspXI site (outside the 5' homology arm A-B) prior to introduction into mouse embryonic stem cells by electroporation, performed in collaboration with Dr. Boris Jerchow. We provided 5 µg of linearized DNA for electroporation into mES cell lines derived from strains 129 and C57/BL6J. The Jerchow laboratory performed electroporation, selection, colony isolation and culture. Ultimately, we received genomic DNA (gDNA) lysates obtained from colonies for analysis. Southern blotting was performed to confirm that the desired homologous recombination event has resulted in exchange of the targeted wild type sequence with the modified sequence from the targeting vector. gDNA was digested with a

restriction enzyme that cuts at a site outside the construct region, and at a site that is unique to the inserted sequence. Digested DNA was run in an agarose gel for size resolution, and then capillary blotted to a positively charged nylon membrane and cross-linked, as described in Methods section 2.2.7. The membrane was hybridized with a ^{32}P labeled DNA probe complementary to a unique sequence present either in the wild type sequence or in the vector, and exposed to a film. Comparison of observed band size with that predicted in the properly targeted allele confirms that the vector is present and integrated at the expected locus.

I designed a series of probes and digestion enzyme patterns to identify proper integration of the vector at both the 5' and the 3' sides (Table 1 and Figure 16A). I took advantage of a restriction site for SpeI enzyme that was added for this purpose to the I-J region of the vector, used in combination with PspXI. Restriction sites for PspXI are located upstream and downstream of the region of interest, but are absent in the vector. I digested the gDNA obtained from a series of positive clones from 129 background mES cells with these two enzymes, and probed the blotted membrane initially with an internal probe for the *Neo*^{R} gene, that is only present in the vector. Using these enzymes, digestion of the wild type allele should result in a ~38 kbp PspXI fragment spanning the region of interest, which lacks *Neo*^{R} sequence. After vector integration, the *Neo*^{R} sequence should be contained on an ~18 kbp PspXI-SpeI fragment. Results are shown in Figure 16B. Five clones appear to display a *Neo*^{R} positive band of the expected size. The filter was then stripped and hybridized a second time with a probe (wild type 1) against *Lin41* sequence present in the same fragments. The same five clones appeared to contain both a ~38 kbp wild type fragment and a ~18 kbp targeted fragment, as expected. Unfortunately, I was not able to re-probe the same membrane afterwards, and further confirm these clones as positive events.

The main disadvantage of this strategy was the size of the fragments that have to be analyzed. The expected size of the 5' arm with this enzymatic combination is around 18 kbp, very big for conventional Southern blot. This requires a very low percentage of agarose in the gels for size resolution, down to 0.4%, which results in extremely fragile gels, considering their size (20 x 15 cm for 96 probes) and the manipulation during multiple treatment steps required for Southern blotting.

As an alternative to avoid the high size of expected bands, we decided on a second strategy with different enzymes and probes. The second set of employed enzymes for analysis of the 5' integration of the vector was the combination DrdI and SpeI. DrdI cuts immediately upstream of the homology region A-B, outside the vector, and additionally inside the *Neo*^{R} sequence. Although the location of the sites is optimal, a potential problem was that the DrdI site in *Neo*^{R} is potentially subject to inhibitory methylation and might result in inefficient digestion. We therefore co-digested with SpeI, making use of the site introduced in the I-J fragment described above, to have a back-up vector-specific restriction site in the event of incomplete DrdI digestion. The expected fragments after digestion are 11 kbp for the integrated vector and 18 kbp for the wild type sequence, notably shorter than with the previous enzymatic combination.

We used this approach to repeat the test for the first five candidate clones that appeared positive for *Neo*^{R}, and two of them (numbers 4 and 5) gave a clear signal of the expected size for *Neo*^{R} as well as for the wild type external probe. Number 3 was negative for the vector band, and number 1 and 2 seemed to be positive, although the intensity of the band was not strong enough for full confidence. Moreover, we observed that the second DrdI digestion site in Neo^R cassette was not blocked by methylation, as the probe also recognized an additional fragment of 4 kbp, that corresponds to the sequence between the DrdI in *Neo*^{R} and the SpeI site (Figure 16C). Despite the presence of positive bands at the expected sizes for the conditional vector, the fact that the lower band (for 5' External WT2) has a higher intensity, in particular in clone number 5, may be a sign of aberrant integration. We would expect a similar intensity in wild type and *Neo*^{R} bands, reflecting the same amount of DNA for both alleles.

After confirming the presence of *Neo*^{R} gene, and the correct 5' integration of the vector, it was still necessary to corroborate the structure of the 3' integration downstream of the Neo^R cassette. I used a new strategy in terms of enzymatic digestion and probe selection, using SpeI once again from I-J region, and NcoI outside the vector, downstream the Y-Z homology arm. The sizes resulting from this digestion should be ~12 kbp for the integrated vector, and ~15 kbp for the wild type, due to the presence of an NcoI site right next to the region E-F. Because the fragments of interest do not contain the *Neo*^{R} sequence, I designed two wild type

probes, one internal to the vector and one external, to confirm the correct 3' integration of the vector (Figure 16C).

Only the 3' internal probe produced the two bands of expected size (15 and 12 kbp) in clones number 4 and 5. Of particular concern, however, are two additional bands (one higher than the highest expected, one lower than the lowest) of unknown origin. In addition, I was unable to detect the integrated vector band using a wild type probe external to the vector in either clone 4 or 5, expected at 12 kbp, even though the wild type band is visible at 15 kbp. Although we cannot explain which possible integration phenomenon can produce such result in the Southern blot analysis, it led us to conclude that aberrant multiple integration in the 3' side of the vector had occurred. Therefore, we considered it would be risky to proceed with either of these clones for blastocyst injection.

Probe	Location	Position	Length	Enzymes
Neo	Vector	10030bp	795	PspXI + SpeI
5' Internal WT1	Vector	11505bp	954	PspXI + SpeI
5' External WT2	Upstream vector	(-) 781bp	781	PspXI + SpeI
3' Internal	Vector	24396bp	987	NcoI + SpeI
3' External	Downstream vector	27079bp	406	NcoI + SpeI

Table1. Southern blot probes. Location, position (taking as reference the beginning of the vector sequence), length and restriction enzymes used for detection.

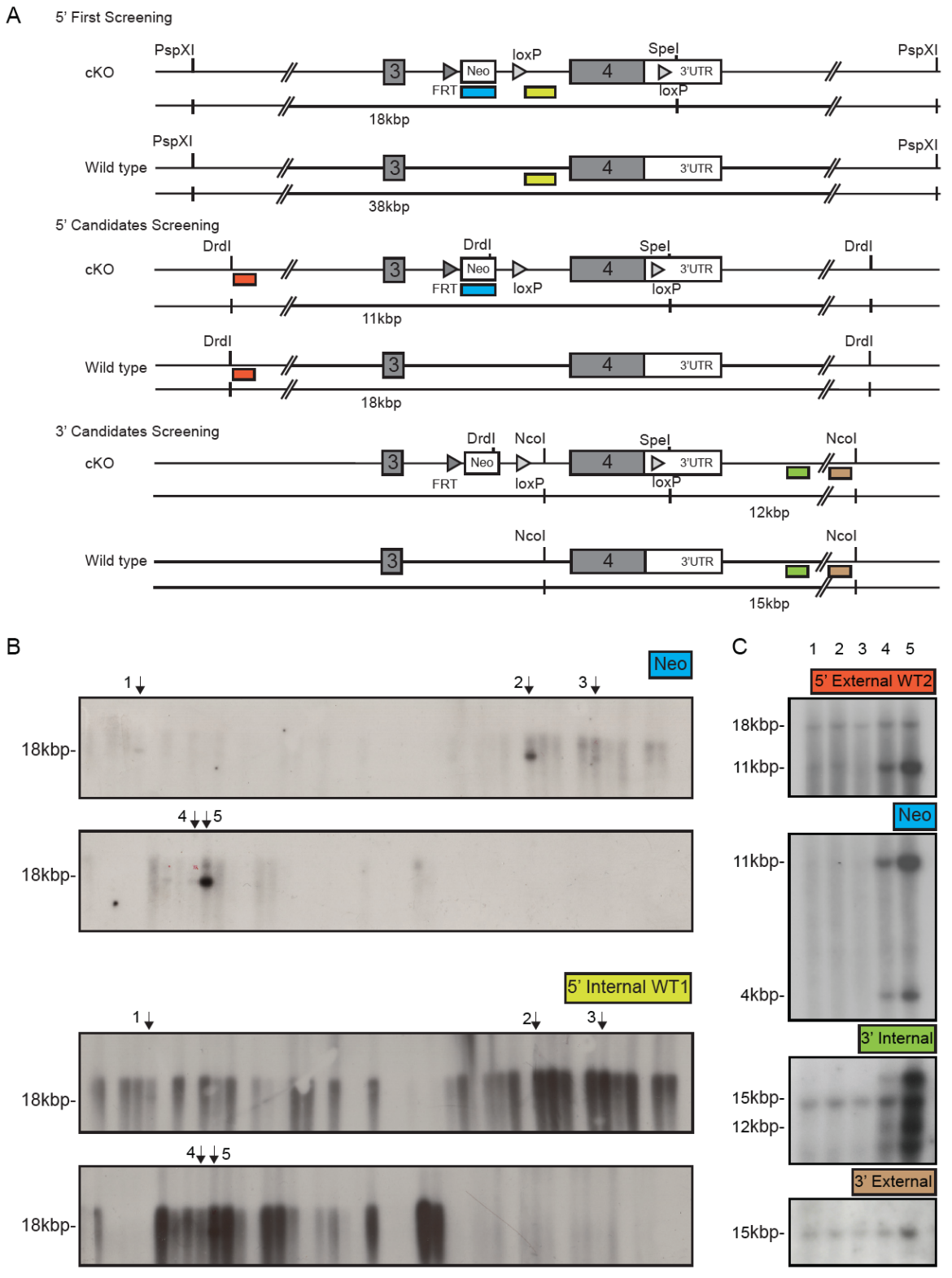

Figure 16. Southern blot to identify integration of the cKO vector in the mES cells genome. A. Restriction sites used to digest the gDNA, comparing the vector integrated sequence with the wild type allele, and expected bands size in kpb. Probes used are represented in colored boxes. B. Southern blot film used to screen for candidates of the first electroporation, using a probe against *Neo* and a wild type sequence (5' Internal WT1). Arrows point the identified positive candidates. C. Southern blot analysis of the candidates identified in the first analysis, using a specific 5' External WT2 probe and a probe against *Neo* sequence (top panels). Bottom panels show the result of 3' External and Internal probes. Specific bands of expected size are indicated.

As a complementary assay to study the vector integrity, I also performed PCR on the region surrounding the loxP sequences in candidate clones (Figure 17). Clone number 3 was used as negative control, and clones 4 and 5 as probes. The primers correspond to the ones used for the generation of the two mini-targeting vectors: C and G as forward, and F and J as reverse primers, respectively (see Figure 14B). The insertion of *Neo*^{R} and a loxP site will cause a shift in the band size, as indicated in Figure 17A. As expected, in the product of C-F primers, all three clones produce a wild type band of 549 bp; in addition, clones 4 and 5 display a band of 2532 bp that indicates the presence of the Neo^{R} cassette insertion. Moreover, in clones 4 and 5, but not in control 3, there is a second band using primers G-J of 629 bp, in addition to the wild type sequence 544 bp, due to the inserted loxP site. Nevertheless, the larger band (containing the loxP site) present in clones 4 and 5 is surprisingly intense compared to the wild type one. These results added evidence to the theory of aberrant multiple integration events at the 3' arm of the vector, consistent with the results of Southern blotting. We therefore came to the conclusion that none of the candidate clones obtained from the first round of electroporation were suitable for blastocyst injection.

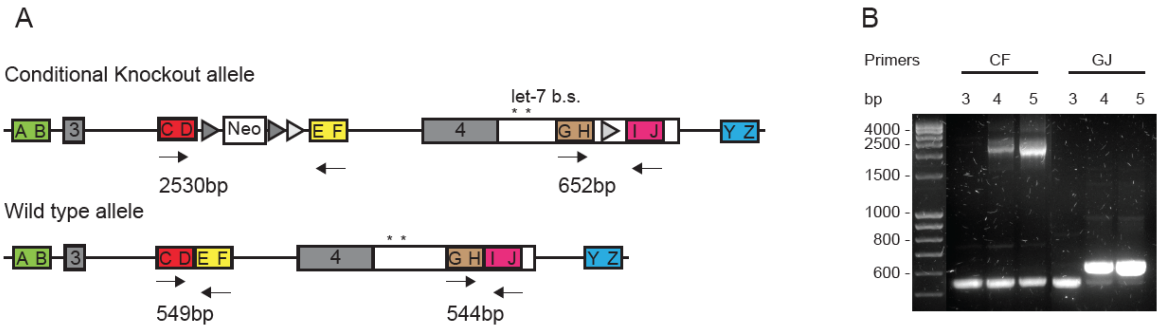

Figure 17. PCR analysis of the conditional knockout vector clones. A. Scheme of the *Lin41* conditional knockout and wild type allele. Arrows indicate the primer pairs used to amplify the sequence integrated in each mini targeting vector, and expected band size is displayed below. B. PCR obtained with the two pairs of primers. The 3' analysis reveals a band corresponding to the vector integration of greater intensity compared to the wild type.

A total of three independent electroporation rounds of the conditional knockout vector in 129 and C57BL6/J mES cells lines, resulting in 522 clones, were performed and screened by Southern blotting using a combination of Neo^{R} and 5' external probes. I was unable to identify further potential candidates, a result that may be due to insufficient DNA quality for Southern blot analysis (Figure 18). To

overcome this problem I tried a systematic PCR analysis of DNA plates from the clones, as an initial screen for the presence of the Neo^R cassette, prior to more exhaustive Southern blot-based analysis of expanded clones. This PCR analysis demonstrated conclusively that none of the 522 clones were positive for vector insertion, regardless of the integration site (data not shown). Since clones should have been the product of selection based on neomycin resistance, the absence of *Neo*^{R} sequence suggests there was a severe problem in the cell culture and/or clone selection procedures. Thus, after a total of 714 clones analyzed by Southern blot and/or PCR, we elected to forego further attempts with our targeting vector, particularly since in the meantime targeted mouse ES cells generated by the International Knockout Consortium had become available.

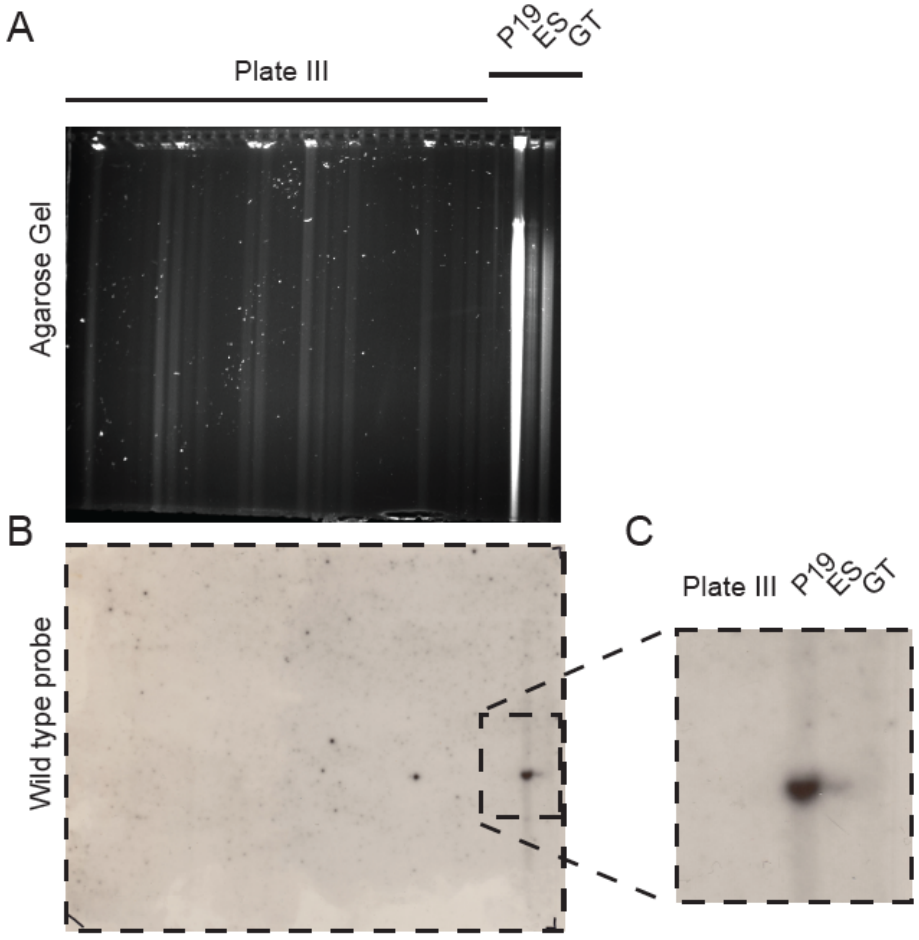

Figure 18. Southern blot troubleshooting. A. Agarose gel with DNA samples from electroporated ES cells from Dr. Jerchow (PlateIII), and control samples: 10 µg gDNA from EC (P19), 5 µg gDNA from mES (ES) cells and 5 µg gene trap mouse tail biopsy (GT). B. Film exposed to wild type probe. PlateIII clones for analysis display low DNA intensity and no signal from the probe. C. Magnification of the detected signal in controls. P19 and mES cells reveal a signal corresponding to the amount of loaded DNA. Biopsy DNA from mouse tail was extracted with a DirectPCR® lysis reagent, that yields low DNA quality and does not allow detection despite the quantity of material.

3.2.4 *Lin41* conditional knockout mouse generation using EUCOMM mES cells

The European Conditional Mouse Mutagenesis (EUCOMM) Program is part of the International Knockout Mouse Consortium (IKMC), which aims to generate conditional knockout mutations of protein-coding genes in C57/BL6 background mES cells. By the time we detected the anomaly in the 3' integration of our conditional knockout vector, it became possible to purchase mES cells already containing a vector either with or without conditional potential for *Lin41* from EUCOMM (http://www.knockoutmouse.org/martsearch/project/71825). The parental cell line is JM8A3.N1, derived from C57/BL6 but with agouti fur color. This provides a double advantage, because it allows easy identification of chimeric animal by coat color, but in the C57/BL6 background. It is therefore not necessary to backcross several generations to obtain a genetically uniform mouse line.

EUCOMM uses an *in silico* "critical exon" approach that selected *Lin41* exon 4 for targeting, so the deletion strategy is similar to our initial scheme (Figure 19A). The EUCOMM project combines the Gene Targeting approach with a so-called "first Gene Trap" cassette, meaning that the final vector is not merely a selection cassette and the fourth exon flanked by loxP sites: its first part is a splice acceptor, followed by the reporter gene *LacZ* under the control of an IRES sequence, ending in a polyA signal. Next, after the first loxP site, there is another transcript unit, formed by the constitutive human beta-actin promoter, driving a Neo^R selection gene. Two FRT sites flank *LacZ* and Neo^R units, and afterwards the fourth exon is flanked by two loxP sites. Thus, cells containing this construct without further processing will express a gene trap form of *Lin41* after the third exon, reportable using *LacZ*. After the integration has successfully taken place, it is necessary to eliminate the sequence between the FRT sites by crossing the mice with a constitutive Flp-expressing line. This will give rise to a pure conditional knockout inducible by Cre activity and to avoid the recombination between the first and second loxP sites (between the two reporter cassettes and before the 4^{th} exon, respectively) that would not result in protein truncation (Figure 19A).

We purchased three different clones containing the conditional cassette (Trim71_A03, Trim71_C01 and Trim71_D03). Prior to injection, clones were

subjected to a cytogenetic analysis by the company ChromBios (ChromBios GmbH, www.chrombios.com). This comprises a “quick test” for polyploidy of chromosomes 8, 11, X, and Y, as well as chromosome counting, using Fluorescent *In Situ* Hybridization (FISH). All the three clones presented a Y chromosome, but only one (Trim71_A03) had a normal chromosome count. Both Trim71_C01 and Trim71_D03 presented a trisomy in chromosome number 8, one of the most common aneuploidies that prevents successful generation of transgenic mice from mES cells (Sugawara et al. 2006).

We therefore proceeded to use clone Trim71_A03 due to its normal chromosome profile. The blastocyst injection and transfer were performed in collaboration with Dr. Geert Michel’s group (FEM, Berlin), who also expanded the clone for further analysis. Out of a total of two blastocyst transfers we obtained six chimeras (five males and one female) that reached sexual maturity. Four of them presented a high degree of chimerism, close to 100%, while two of them (number 3 and 4) had a lower degree, close to 20%, based on fur color estimation. All six chimeras were mated to C57/BL6/J mice, and the progeny was analyzed by PCR for the presence of the *LacZ* gene.

The PCR strategy is described in Figure 19A: two pairs of primers were designed to identify the presence of the vector in the pups born from the chimeras, which will indicate the contribution of the cells to the germline. The first pair of primers (wild type) is formed by a forward primer before the cassette, in the 3’ homology arm sequence, and a reverse primer after the cassette, in the 5’ region. In the wild type allele the absence of vector will produce a product of 180 bp, but if the vector is present and correctly integrated it will increase the product to 7.4 kbp. The main disadvantage of this method is that amplifying such a big sequence might require adjustments, and the lack of the product could indicate either the absence of the vector, or a failure in the PCR reaction. To overcome this problem we designed a second pair of primers (LacZ), to amplify a 218 bp fragment of the *LacZ* gene present in the construct. This would allow us to use other genomic DNA to adjust the PCR conditions as a positive control, such as samples from *Lin41* gene trap mice previously described. We therefore used the first pair of primers to detect the wild type allele, and the second pair to identify any animal carrying the *LacZ* gene.

Positive candidates obtained from this screen would then be analyzed in detail for the proper integration of the vector. We confirmed the effectiveness of our PCR approach using as positive control gDNA extracted either from the cell clone used for the injection and from ear clip biopsies obtained from the chimeras. All samples analyzed for *LacZ* resulted in a band at the expected size (with exception of the mouse number three, with only 20% chimerism), supporting the design of the experiment (Figure 19B).

More than 170 mice born from the chimeras were analyzed, but none of them tested positive for the *LacZ* fragment. We are therefore forced to conclude that germline transmission was not obtained for any of the fertile chimeras. The details of the number of litters from each chimera are shown in Table 2. Information from EUCOMM estimates 60% germline integration of their mES cells clones, due to the C57/BL6 background of the cells, and therefore recommends the use of at least three independent clones. Therefore, we purchased two new clones from EUCOMM (Trim71_B04 and Trim71_E02) that underwent long range PCR analysis to assure the correct insertion of the vector, in addition to the karyotype and chromosomal count, and we proceeded to a new round of blastocyst injection. The outcome consisted in five males and eight females presenting high degree of chimerism. Such a large number of females derived from a XY mES cell line is an uncommon outcome. It is more likely that F1 pups derived from the males would carry the vector, although all the animals were mated and offspring tested.

We identified several positive candidates, all descending from one of the males with 100% chimerism (m17, obtained from clone Trim71_E02) (Figure 19C and Table 2). As of this writing, eight pups descendant from male number 17 were identified by PCR as positive candidates that will be used to establish a colony of, to our knowledge, the first *Lin41* conditional knockout mouse line. The gDNA from these animals is currently being analyzed by Southern blot, to confirm the proper integration of the cassette.

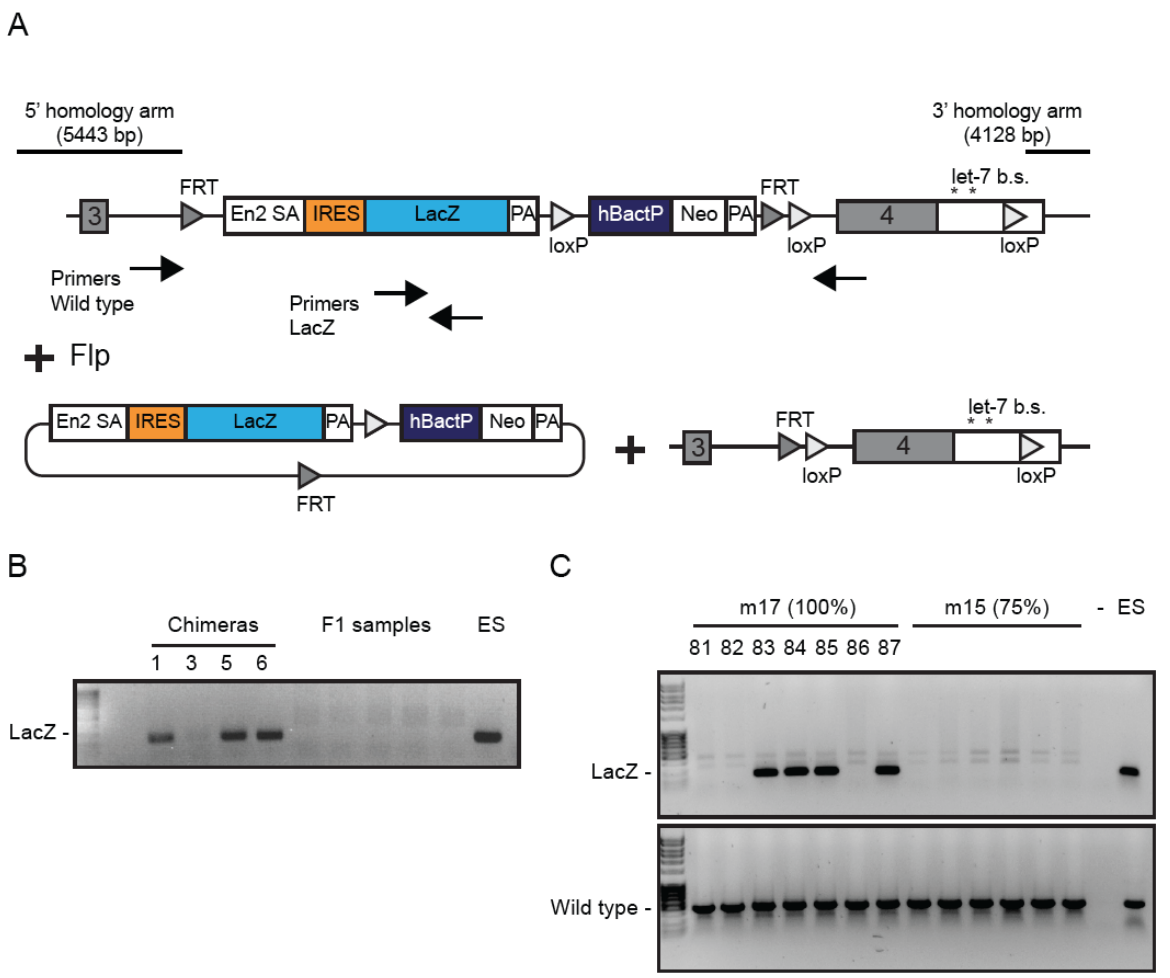

Figure 19. EUCOMM mES cells containing *Lin41* conditional vector. A. Scheme of EUCOMM first gene trap conditional knockout allele for *Lin41*, with two independent transcriptional units and floxed exon number 4 Arrows indicate the primer pairs used for the vector detection. Pair 1: wild type sequence (5'Arm Fw2 and 3'Arm Rev). Pair 2: *LacZ* sequence in the first gene trap cassette (LacZ Fw and LacZ Rev). Flp treatment leads to the excision of the first gene trap cassette, resulting in exon 4 flanked by two loxP sites (light grey triangles) and a residual FRT site (dark grey triangles) in the 3' side of the intron 3. B. PCR of the pups from the first injection using pair 2 primers. Biopsies from chimeras were used as controls (see Table 2). F1 samples resulted negative for all pups analyzed. mES cells from EUCOMM were used as positive control. C. PCR of the pups derived from the second round of injection using primer pairs 1 and 2. F1 Pups derived from indicated chimeric mouse on top (chimersim%). mES were cells as positive control.

First injection

Ear clip	%Chimerism	Gender	Litters	Positive/Total Pups
1	100	m	4	35
2	100	m	0	0
3	20	m	9	79
4	20	f	0	0
5	100	m	1	10
6	100	m	8	50
			Total:	174

Second injection				
Ear clip	**%Chimerism**	**Gender**	**Litters**	**Positive/Total Pups**
7	80	f	0	0
8	15	m	0	0
9	95	f	1	10
10	90	f	1	5
11	85	f	1	9
12	10	f	0	0
13	100	m	0	0
14	85	f	0	0
15	75	m	4	38
16	75	f	1	4
17	100	m	2	8/14
18	95	m	0	0
19	85	m	0	0
20	80	f	1	3
			Total:	8/83

Table 2. Summary of the blastocysts injection with clones from EUCOMM. Six chimeric animals resulted from the first injection, although none of them produced positive descendants. 14 animals resulted from the second round, from which male 17 produced F1 pups containing the *LacZ* sequence.

3.3 Generation and characterization of *Lin41* gene trap mES cells

Mouse embryonic stem cells (mES cells) are isolated from the inner cell mass of the E3.5 mouse blastocyst and can be cultured in the presence of the differentiation-inhibiting cytokine leukemia inhibitory factor (LIF). mES cells have the ability to differentiate into cells of the three germ layers (ectoderm, mesoderm and endoderm) under appropriate culture conditions. They provide an excellent tool to study the role of *Lin41* in a variety of developmental processes while avoiding the organism lethality that occurs after E9.5 in gene trap mutants.

In collaboration with Dr. Geert Michel's group we mated 28 female and 35 male heterozygotes for the *Lin41* gene trap allele ($Lin41^{+/gt}$), which are healthy, fertile, and do not present any detectable phenotype compared to the wild type mice (the gene trap phenotype will be discussed more in detail in section 3.4). Michel's team isolated the blastocysts at day E3.5 of embryonic development. To establish a culture of mES cells, the blastocysts are plated in gelatin-coated p24 well in presence of a layer of feeder cells derived from mouse embryonic fibroblasts (MEFs). Cells from the trophoblast and the inner cell mass are allowed to proliferate for five to six days; then, the inner cell mass outgrowths are picked, dispersed by enzymatic digestion with trypsin and plated again in gelatin-coated

wells and in the presence of MEFs and LIF. Under these conditions, mES cells will continue to divide while maintaining pluripotency and self-renewal ability (Conner 2001).

A total of 18 independent clones were generated by Michel's team, and were genotyped using the same primers as for our gene trap mice (see Figure 12). Eight of them were homozygote knockouts (*Lin41*$^{gt/gt}$), seven were heterozygotes (*Lin41*$^{+/gt}$), and only one was wild type (*Lin41*$^{+/+}$) (Figure 20). It is difficult to conclude from this sample if the skewed recovery means that *Lin41* deficiency provides a selective advantage, but it provided a first indication that *Lin41* is not required for maintenance of the pluripotent state.

A

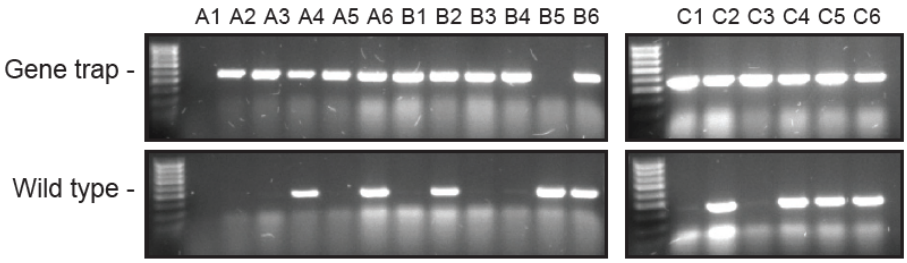

B

	1	2	3	4	5	6
A		K.O.	K.O.	Het	K.O.	Het
B	K.O.	Het	K.O.	K.O.	W.T.	Het
C	K.O.	Het	K.O.	Het	Het	Het
D						

Wild Type (W.T.)	*Lin41*$^{+/+}$
Heteroczygote (Het)	*Lin41*$^{+/gt}$
KnockOut (K.O.)	*Lin41*$^{gt/tg}$

Figure 20. Genotype of gene trap mES cell clones. A. PCR of the clones isolated by Dr. Michel's team, using the same primer pairs as for gene trap mice. B. Scheme of clones' nomenclature. Cells samples were provided lyophilized in a p24 plate, and clones were named after the number and letter corresponding to the well position. Nomenclature for genotype: two wild type copies of Lin41 (wild type, *Lin41*$^{+/+}$), one copy of the gene trap allele (heterozygote, *Lin41*$^{+/gt}$), or two copies of the gene trap allele (knockout, *Lin41*$^{gt/gt}$).

Clones were further expanded in the presence of LIF and MEFs, and stocks were cryo-stored to ensure material for future experiments. To identify changes in the chromosome number they were karyotyped as described in Methods section 2.2.4. A representative sample of three knockout, three heterozygote and the single wild

type clones were used for karyotyping, and no abnormalities were found (data not shown).

X-Gal staining was performed in samples of the wild type (B5) and one knockout (A2) clone, to assess ß-Gal activity. As expected, the knockout clone showed a very intense, deep blue staining, due to the two copies of *LacZ*, while the wild type cells remained colorless (Figure 21A). This confirmed the activity of *Lin41* promoter in proliferative mES cells for the knockout clone. In this case the wild type clone serves as negative control to show specificity of the technique. To investigate if the promoter activity corresponds with LIN41 protein generation, western blot of lysates from one clone of each genotype was performed. As depicted in Figure 21B, LIN41 is expressed in wild type cells, while heterozygote mES cells display approximately half the amount of protein, and knockout cells completely lack LIN41.

I used immunocytochemistry to confirm the expression of LIN41 or ß-GAL protein, and first address the presence of the standard mouse pluripotency markers *Oct4* and *Sox2*. The pluripotency of mES cells is usually addressed by the expression of a panel of transcription factors, among which *Oct4*, *Sox2* and *Nanog* are key components of preimplantation ICM maintenance, and thus widely used to determine the quality of mES cells (Loh et al. 2006). No significant differences were perceived among the different genotypes. In all clones examined nuclear signal was obtained for these markers, as expected for pluripotent mES cells (Figure 21C). Nanog antibody available to us was not suitable for use in immunostaining, therefore *Nanog* expression was addressed only in western blot assays.

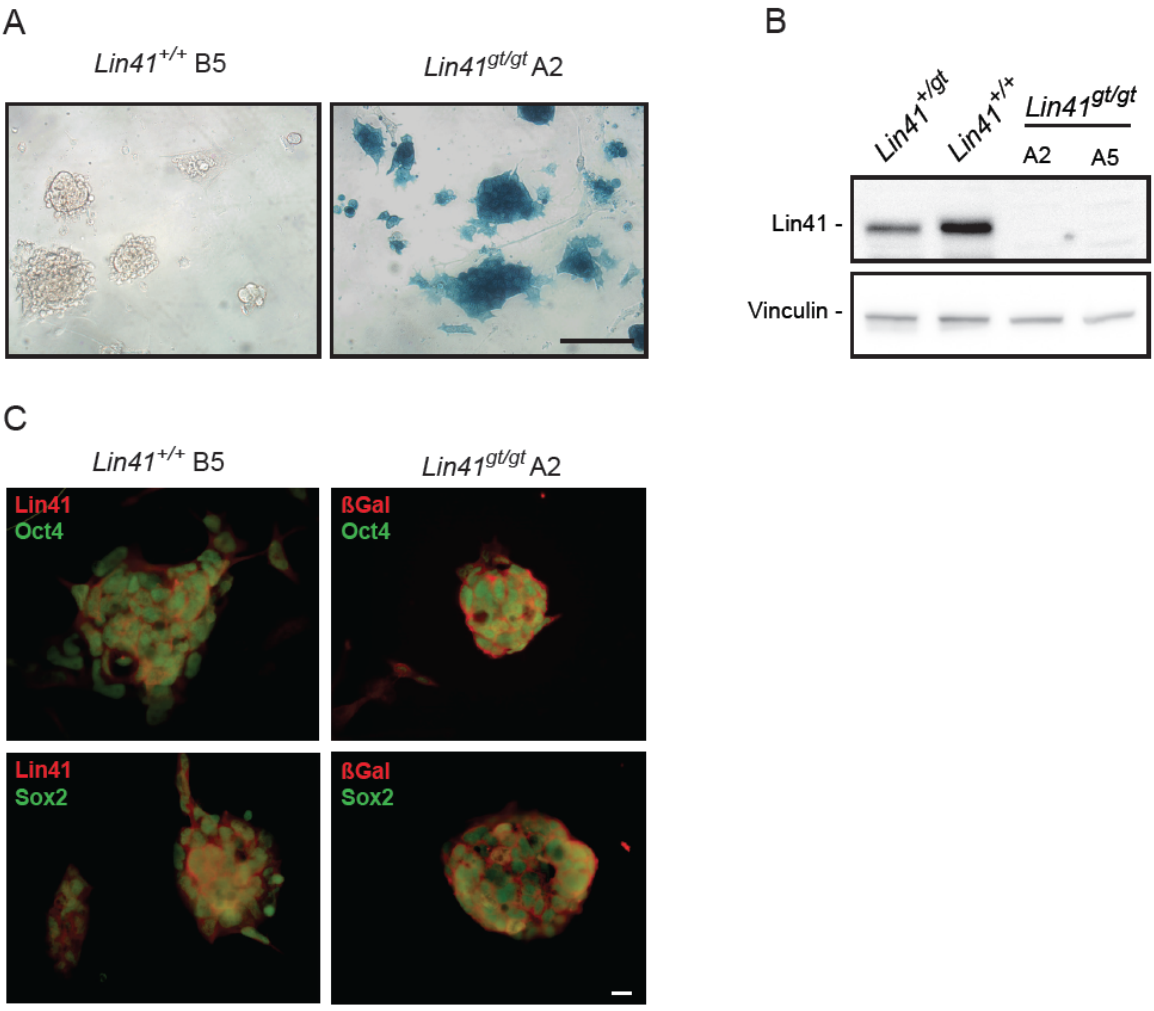

Figure 21. Gene trap mES cells characterization. A. X-Gal staining of B5 *Lin41*$^{+/+}$ and A2 *Lin41*$^{gt/gt}$ clones. Scale bar 100 µm. B. Western bolt of LIN41 protein expression in mES cells. Vinculin was used as loading control. C. Immunocytochemistry of Lin41 or ß-Gal with pluripotency markers Oct4 and Sox2. Scale bar 10 µm.

In addition to immunostaining, I performed western blot analysis to monitor the levels of OCT4, SOX2 and NANOG in comparison to LIN41. A preliminary assay revealed a marked upregulation of OCT4 and SOX2 in the knockout samples (Figure 22A'). When I tried to reproduce these results, the levels of the pluripotency markers changed without correlation to the genotype. After analyzing the culture conditions I realized that the time in culture and medium refreshment are critical parameters with a strong effect on pluripotency marker expression (Figure 22A" and 22A"').

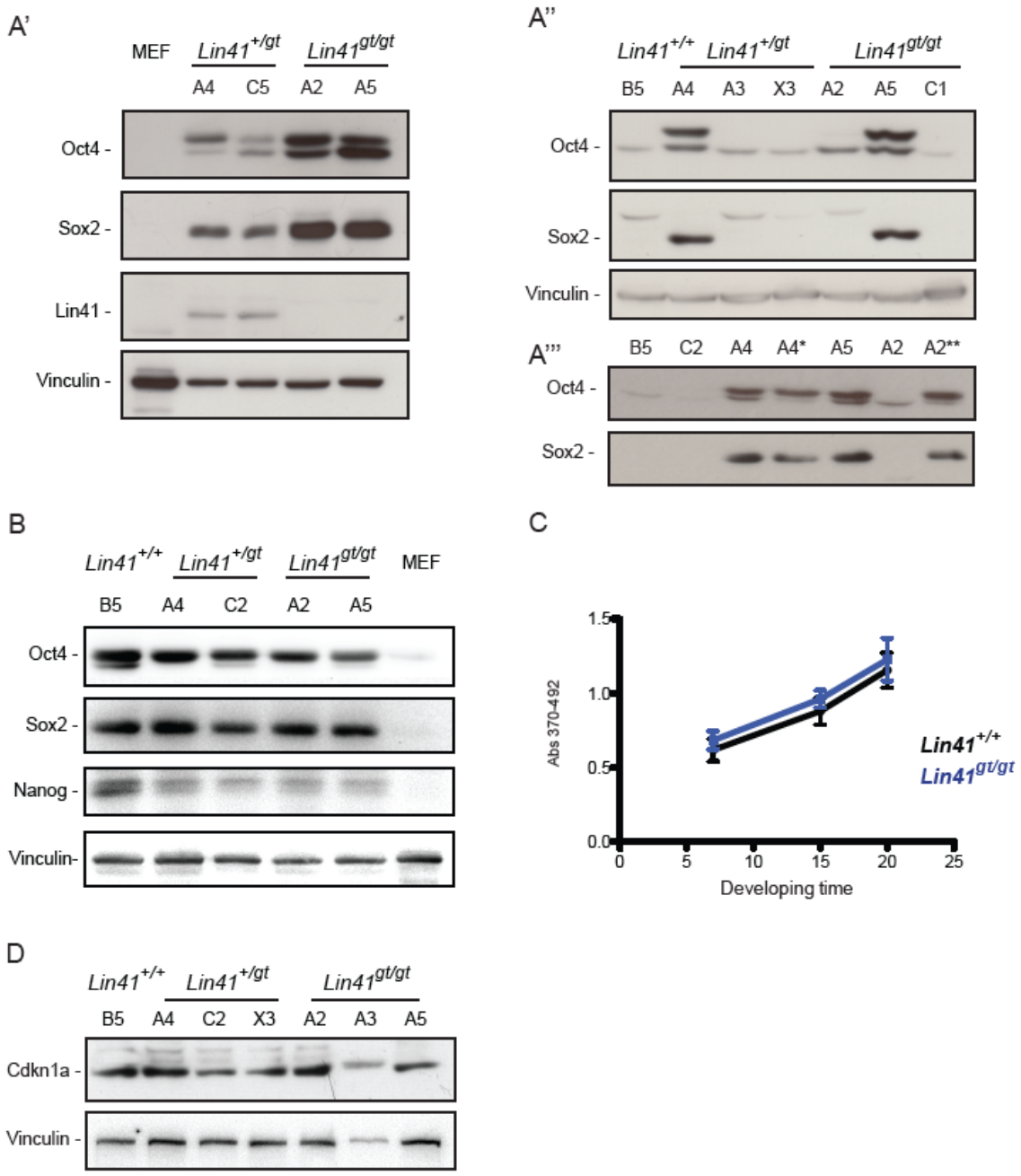

Figure 22. Gene trap mES cells pluripotency markers and proliferation. A'. Western blot of *Lin41*$^{+/gt}$ and *Lin41*$^{+/+}$ clones, in comparison to mouse embryonic fibroblasts (MEFs) used as feeder cells in culture. A". Western blot performed with independent lysates, showing no correlation of protein levels with genotype. A"'. Under controlled culture conditions, pluripotency markers levels depend on medium refreshment: * Starved clone, no medium change.** Clone with medium change 2h prior to sample collection. B. Homogeneous pluripotency marker levels in samples collected 2 h after medium change. C. Representative BrdU incorporation assay of wild type and knockout clones, read by colorimetric development over time. Bars represent S.D. D. Western blot of the cell-cycle dependent kinase Cdkn1a in gene trap mES cells.

Thus, to ensure consistency among the samples, all of them are collected under subconfluence, and after 2 to 3 hours of medium refreshment. Under these conditions, all clones expressed similar levels of pluripotency markers, regardless of their genotype (Figure 22B). In addition, I analyzed whether the lack of *Lin41* affected the proliferative ability of mES cells. Performing BrdU incorporation assay, no significant differences in cell proliferation were found, which confirmed the previous *de visu* impressions observed in cell culture passages (Figure 22C). Complementary, western blot of the cyclin-dependent kinase inhibitor Cdkn1a did not show significant changes among genotypes. In summary, the absence of *Lin41* in mES cells does not seem to affect either the expression of the core pluripotency markers or the self-renewal ability of these cells.

3.4 Characterization of the *Lin41* gene trap mouse

3.4.1 Embryonic lethal phenotype of *Lin41*^{GT} knockout mice

We mated heterozygote animals (*Lin41*$^{+/gt}$) to study the phenotype of both heterozygote and homozygote knockout (*Lin41*$^{gt/gt}$) embryos during development. All genotyped adult mice obtained were either wild type or heterozygotes: the absence of homozygous knockout adult mice was the first evidence of an embryonic lethal phenotype of the animals lacking *Lin41*. *Lin41* expression was previously reported from mES cells and embryonic day 7.5 (E7.5) embryos (Rybak 2009). To further analyze the consequences of *Lin41* absence, and narrow the time points of interest in accordance to the results, we screened different embryonic stages from E8.5 on. We observed that, while the *Lin41*$^{+/gt}$ embryos develop normally, without presenting any difference in size or morphological defect compared to the wild type ones, their knockout littermates stop developing at around E9.5, and die shortly after. Moreover, this lethality is accompanied by a highly penetrant failure of neural tube closure, in the anterior craniofacial region. In mouse three major events define the neural tube closure process (reviewed in (Copp et al. 2003)): the spinal cord (closure 1), and the rostral extremity of the forebrain (closure 3), are events temporally uniform among different mice backgrounds, and are not affected in *Lin41* deficient embryos. In contrast, closure 2 comprises events at the forebrain/midbrain boundary, and can fluctuate from caudal to rostral positions in different mouse strains. It is in this region where we observe a defect in knockout embryos. Moreover, both the neural tube folding

defect and lethality are 100% penetrant in our mouse colony, for we have never found any knockout specimen surviving later than day E11.5, or with normal neurulation before that stage (Figure 23A).

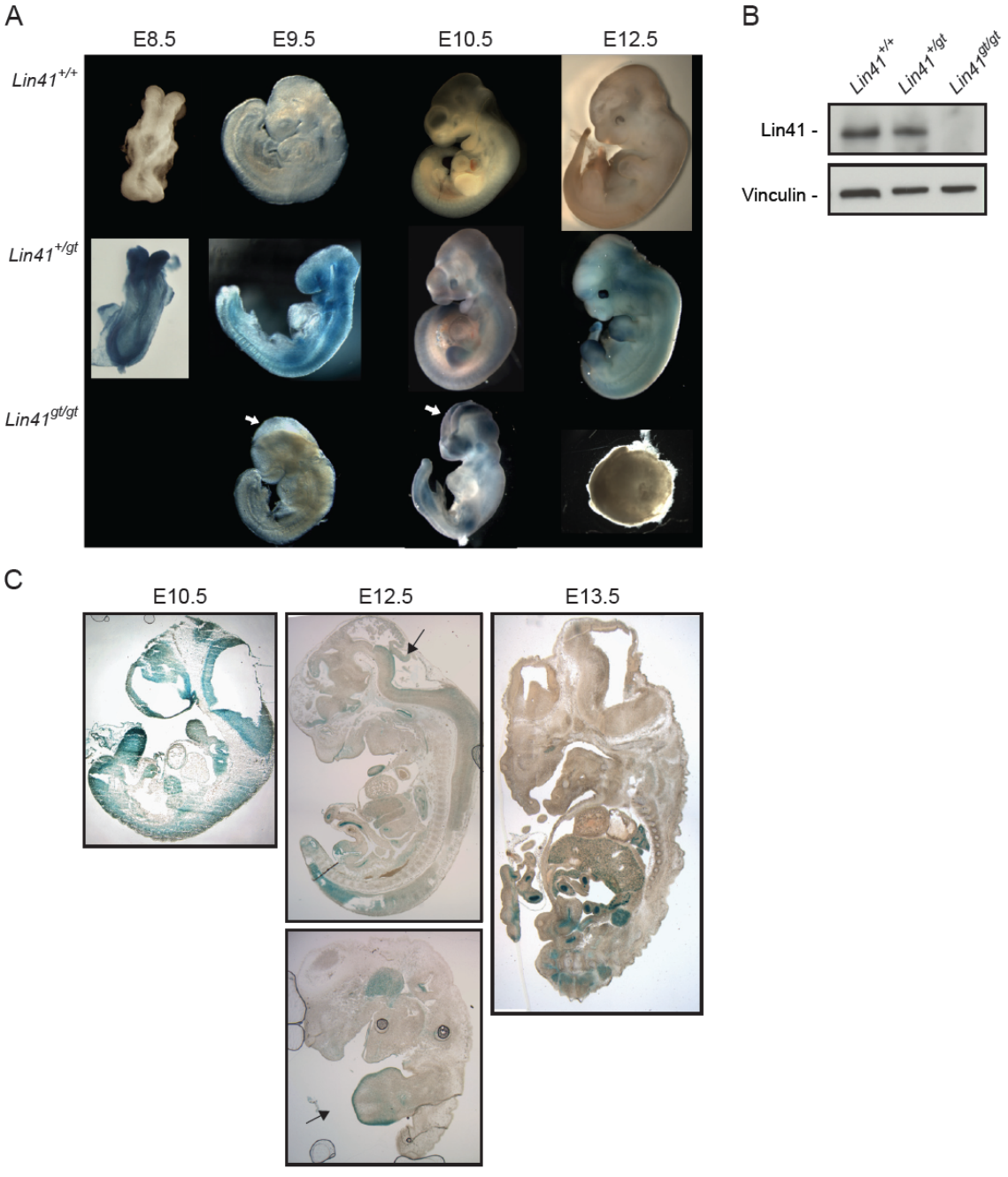

Figure 23. *Lin41* gene trap mouse embryonic development. A. X-Gal staining of wild type, heterozygote, and homozygote knockout embryos, from E8.5 to E12.5. Knockout animals display a failure in neural tube closure (white arrows) and die after E9.5 (E9.5 embryo not stained), encapsulating and reabsorbing after E11.5. Embryos not to scale. B. Western blot from whole E9.5 embryo lysates. C. X-Gal staining of sagittal sections of representative heterozygote embryos. Arrows point to neuroepithelial and limb bud positive tissue.

Previously, other groups observed similar phenotypes in independently generated gene trap lines. Schulman *et al*. obtained the line *MLin41*^{XA144} gene trap from BayGenomics, and determined that the cassette insertion occurred between the first and the second exons, and truncates the protein after 271 aa at the N-terminus. They observed a similar lethal phenotype, accompanied by failure of neural tube closure around E9.5. Although the number of homozygotes after E8.5 rapidly decreases below the mendelian ratio segregation, they were able to recover a few embryos surviving until E13.5 (Maller Schulman et al. 2008).

Using our mouse line, when embryos were observed at later stages, up to E13.5, knockout animals were degrading, often encapsulated and already undergoing a process of reabsorption, indicating a higher penetrance compared to other gene trap lines. Taken together, our results demonstrate and augment the previous evidence that *Lin41* is essential for mouse embryonic development.

3.4.2 Early-medium embryonic expression of *Lin41*

The heterozygote animals, carrying only one copy of the cassette insertion, seem to develop normally. No visible phenotype, like size change or other abnormalities were observed during embryonic or postnatal development. Nevertheless, when I analyzed the genomic segregation, it did not match the expected mendelian ratio. From a total of 124 embryos (E9.5 – E13.5) of 16 litters, 45 were wild type, 51 heterozygotes and 28 knockout homozygotes, rendering 36.2, 41.1 and 22.5% respectively (Table 3). The value of square Chi for the expected mendelian distribution 1:2:1 results in 8.1. This value is higher than 5.99, the reference for 0.05 at two liberty degrees, indicating statistical significance of one deviation from the expected percentage. This means that there is, statistically, a lower number of heterozygote animals than expected. Although we do not have an explanation for this phenomenon, it may be that LIN41 protein levels are critical for viability at the preimplantational stage, and one copy of the wild type gene might not produce sufficient protein. Levels of LIN41 protein are reduced in heterozygote embryos and in mES cells derived from heterozygote blastocysts, compare to wild type (Figure 23B and 21B). If this is the cause, however, this phenomenon would occur with a low penetrance.

	Lin41$^{+/+}$	*Lin41*$^{+/gt}$	*Lin41*$^{gt/gt}$	Total
Number	45	51	28	124
%	36,2	41,1	22,5	100

Chi = 8.5645 > 5.99 for p=0.05

Table 3. Gene trap embryos Mendelian distribution of 16 litters between E9.5 and E13.5.

Despite the slight shift in the number of heterozygote animals, they are normal and healthy during both development and adult life, and therefore we used the reporter gene in the gene trap vector to track the activity of the *Lin41* promoter during development, starting at embryonic developmental day 8.5 (E8.5). We isolated, fixed and stained the embryos following the X-Gal reaction protocol, and the yolk sacs were used to genotype each animal. We observed a ubiquitous expression of *Lin41* at embryonic day E8.5, displaying X-Gal staining in all visible structures. At day E9.5 the expression is still very prominent in the entire embryo, with the exception of the primordial cardiac sac (Figure 23A). The expression of *Lin41* decreases rapidly after this point. At day E10.5 it is still present in the neuroepithelium, branchial arches, spinal cord, somites, limb and tail buds. By E11.5, the expression is maintained in the same structures, but restricted to a smaller area: the neuroepithelium displays a thin inner layer of positive cells, distributed unequally along the surface; the somite expression disappears, and the limb buds, that have grown bigger and expanded, present *Lin41* positive cells only in their most distal segment. This reduction in expression continues through E12.5, and at E13.5 it is not possible to identify *Lin41* positive cells in either the developing nervous system, or in the limb or tail buds (Figure 23C).

Previous work that analyzed *Lin41* mRNA expression using whole embryo *in situ* hybridization (ISH) showed a similar pattern; in mice from CD-1 strain, Schulman and colleagues detected expression in craniofacial structures, and nervous tissue, although they focused on the expression in dorsal posterior forelimb buds between E9.5 and E10.5 in relationship with let-7 regulation (Schulman et al. 2005). These results confirmed a second publication in the same issue, which reported *Lin41* expression during chick limb development. Again, using ISH for mRNA detection, they describe expression in the same structures of the early embryo: pharyngeal arches, somites, frontal-nasal mass, mesonephros, liver and vasculature. This

expression undergoes spatial-temporal changes, indicating a possible fundamental role in development. In our study, we have confirmed the restriction of *Lin41* promoter activity from the total limb bud to the most distal part between E10.5 and E12.5 stages, and the promoter activity is detected in the entire limb region, without polarization. In contrast, Lancman and colleagues reported a polarization of *Lin41* mRNA in the posterior side of limb buds, a matter that will be analyzed in detailed in the discussion section 4.4 (Lancman et al. 2005).

The rapid decrease in *Lin41* expression culminates around E13.5, when expression in no longer detectable in any of these organs. Positive staining was detected in the intestine, but this is due to endogenous ß-Gal activity (Abeliovich et al. 1992), and not to specific *Lin41* promoter activity in this organ, as it was also present in wild type controls (data not shown).

3.4.3 Postnatal expression of *Lin41*

During the medium-late embryonic stages, *Lin41* is no longer detectable in the embryo, with the sole exception of the basal stem cell layer of embryonic skin (Rybak et al. 2009). Focusing my attention on the study of the postnatal central nervous system (CNS), I detected *Lin41* promoter activity in the cells lining the four ventricles of the postnatal brain starting from day P7 on. This staining was maintained thought adulthood, even in animals older than one year. *Lin41* promoter activity was found along the entire ventricle walls: in the lateral, medial and superior walls of the lateral ventricles. Also, the third and the fourth ventricles appeared to be lined by a continuous layer of *Lin41* positive cells (Figure 24A). Other than in these locations, I failed to detect *Lin41* positive cells in the rest of the brain. In the analysis by X-Gal staining, the choroid plexus and the hippocampus were stained as well, but this was due to endogenous ß-Gal activity and not the *Lin41* promoter (Abeliovich et al. 1992).

I then tried to reproduce these results by immunostaining, using an antibody against LIN41 that recognizes a peptide sequence located in the NHL-repeat region. I confirmed the expression of LIN41 at the protein level by immunostaining with this anti-Lin41 antibody. LIN41 protein is detectable in the cells layering all walls of the lateral ventricles, homogenously distributed throughout the cytoplasm (Figure 24B).

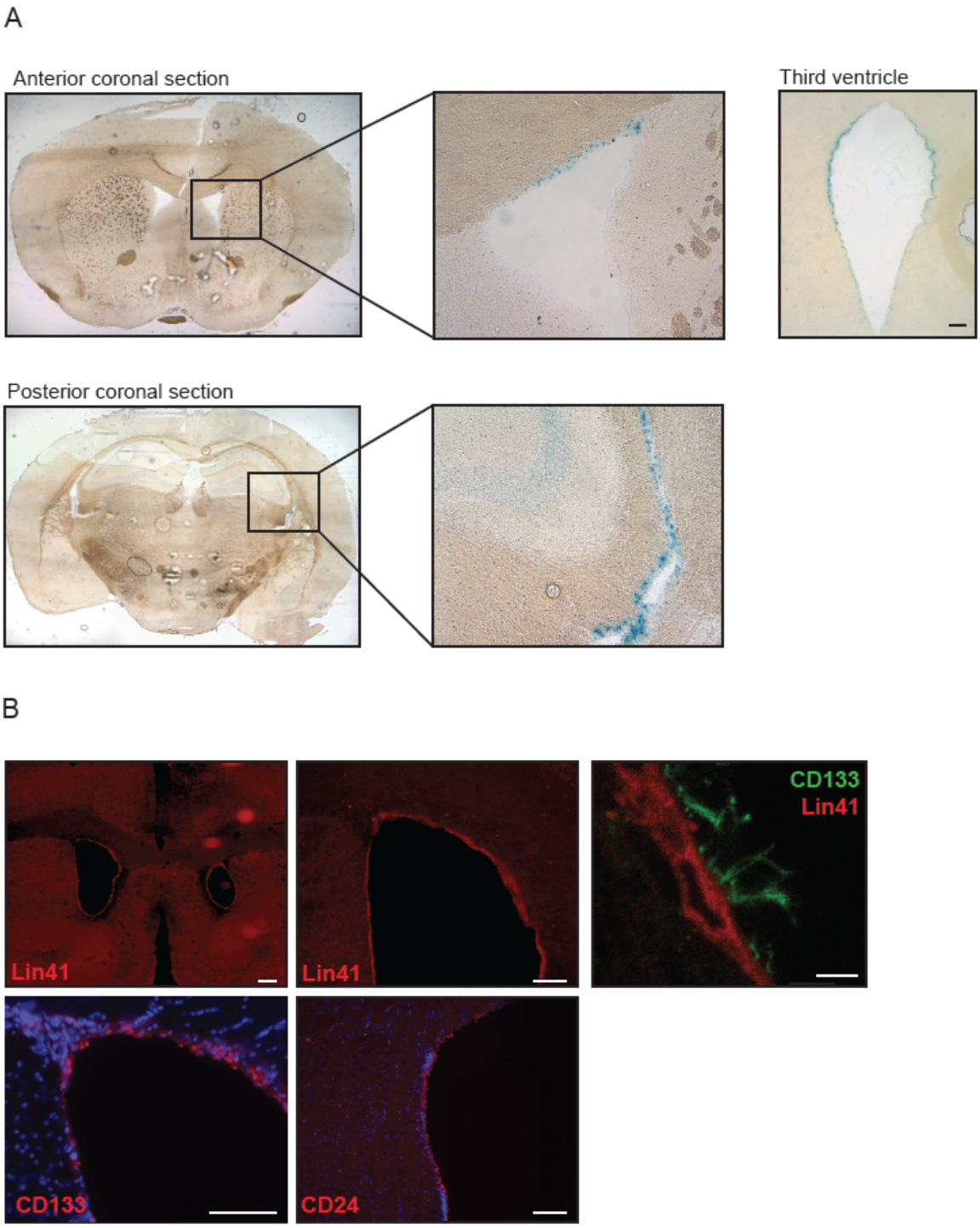

Figure 24. *Lin41* expression in postnatal CNS. A. X-Gal staining of coronal sections of adult heterozygote brain, displaying anterior and posterior areas, and detail on the anterior, posterior lateral, and the third ventricle (scale bar 100 µm). B. Immunostaining of adult wild type brain coronal sections, with antibodies for Lin41 and / or ependymal markers Prominin-1 (CD133) and CD24. Scale bars 100um except for right picture, 5 µm.

To ensure the specificity of the results, negative controls were performed, as described in Methods section 2.2.2.13: for the X-Gal staining, wild type brains were used, to allow the identification of staining derived from *Lin41* promoter activity versus endogenous ß-Gal. In case of the immunofluorescence assays the

use of primary antibody was omitted, which allows evaluation of the background signal derived from secondary antibodies. Our data demonstrated that *Lin41* expression in postnatal CNS is restricted to the walls of all four ventricles in the brain, suggesting a role for this protein in neurogenesis or ependymal homeostasis.

3.5 Adult neural stem cells *in vivo* and *in vitro* are *Lin41*-negative

There are two major stem cells niches identified so far in the adult mammal brain: the dentate gyrus of the hippocampus and the subventricular zone (SVZ) beneath the lateral walls of the lateral ventricles (Reynolds et al. 1992; Richards et al. 1992; Gage et al. 1995).

The presence of *Lin41* in the lateral ventricle walls and the previous work reporting its regulation during stem cell neural differentiation suggested that *Lin41* might play a role in maintenance of the adult neural stem cell niche. I addressed this question using a primary culture of neural stem cells derived from the postnatal subventricular zone, known as neurosphere assay (Reynolds et al. 1992; Reynolds & Weiss 1996). When the tissue obtained from the adult mouse SVZ is dissociated and cultured in serum-free conditions in the presence of FGF and EGF, cells proliferate in floating aggregates called neurospheres (NSPs). Neurospheres contain a heterogeneous mixture of neural stem cells and neural progenitors. This medium is selective, meaning that the postmitotic cells without proliferative ability die and are eliminated with time in culture. Neurospheres can be maintained under these proliferative conditions for a large number of passages; furthermore, they can be differentiated to the three neuronal lineages (neurons, astrocytes and oligodendrocytes) upon withdrawal of the growth factors and in the presence of a low percentage of serum. This system presents a widely used model to study stem cell characteristics (proliferation and differentiation) and the pathways that control these genetic programs *in vitro*.

I isolated SVZ tissue from 4 to 6 weeks old wild type and heterozygote littermates from the *Lin41* gene trap line and maintained them in culture to purify the stem cell population. Experiments were performed between passages 2 and 5, to ensure purity of the culture and homogeneity of the spheres.

The cells did not show changes in proliferation rate based on their genotype, and they were subsequently differentiated towards the three neural cell lineages upon FGF and EGF deprivation, without notable differences (data not shown). I assessed *Lin41* expression in adult neurospheres by immunostaining, X-Gal staining, RT-PCR and western blot (Figure 25). Fluorescent staining using anti-Lin41 and anti-ß-Gal antibodies showed an apparent expression of the gene, as depicted in Figure 25A, together with the classical NSPs markers GFAP and Nestin. In addition, the X-Gal reaction is positive in the heterozygote cultures, displaying blue precipitate staining in comparison to the wild type preparation (Figure 25B). Nevertheless, the RT-PCR resulted in a very faint band of *Lin41* mRNA amplification in the samples from wild type or heterozygote, compared to the positive control P19, suggesting low transcriptional activity, or post-transcriptional regulation events (Figure 25C). Moreover, I failed to detect any band at the corresponding size in western blot analysis with anti-Lin41 antibody. P19 lysates were used as positive control for LIN41 protein, and GFAP to confirm neural stem cell identity of the culture (Figure 25D).

SVZ derived neural stem cells cultured as neurospheres or monolayer express low levels of let-7 miRNA and even lower, almost undetectable levels of *Lin41* mRNA (F. Rehfeld, personal communication). We assume X-Gal staining seen in Figure 25B reflects low promoter activity, which is immediately post-transcriptionally downregulated by the let-7 miRNA, impairing effective translation into protein (Figure 25C and D). This would as well explain the immunofluorescence detection with anti-ß-Gal antibody, due to the lack of let-7 binding sites in the mRNA of the gene trap allele, and therefore the loss of downregulation of the chimeric protein.
Adult mouse neurosphere cultures do not seem to express *Lin41* at biologically relevant levels. With this evidence, we hypothesize that *Lin41* expression is more prominent in other cell populations of the adult brain, rather than in the B cells of the SVZ that proliferate in response to FGF and EGF, and therefore we focused in the ependymal cells of the ventricles, and primary culture of those cells.

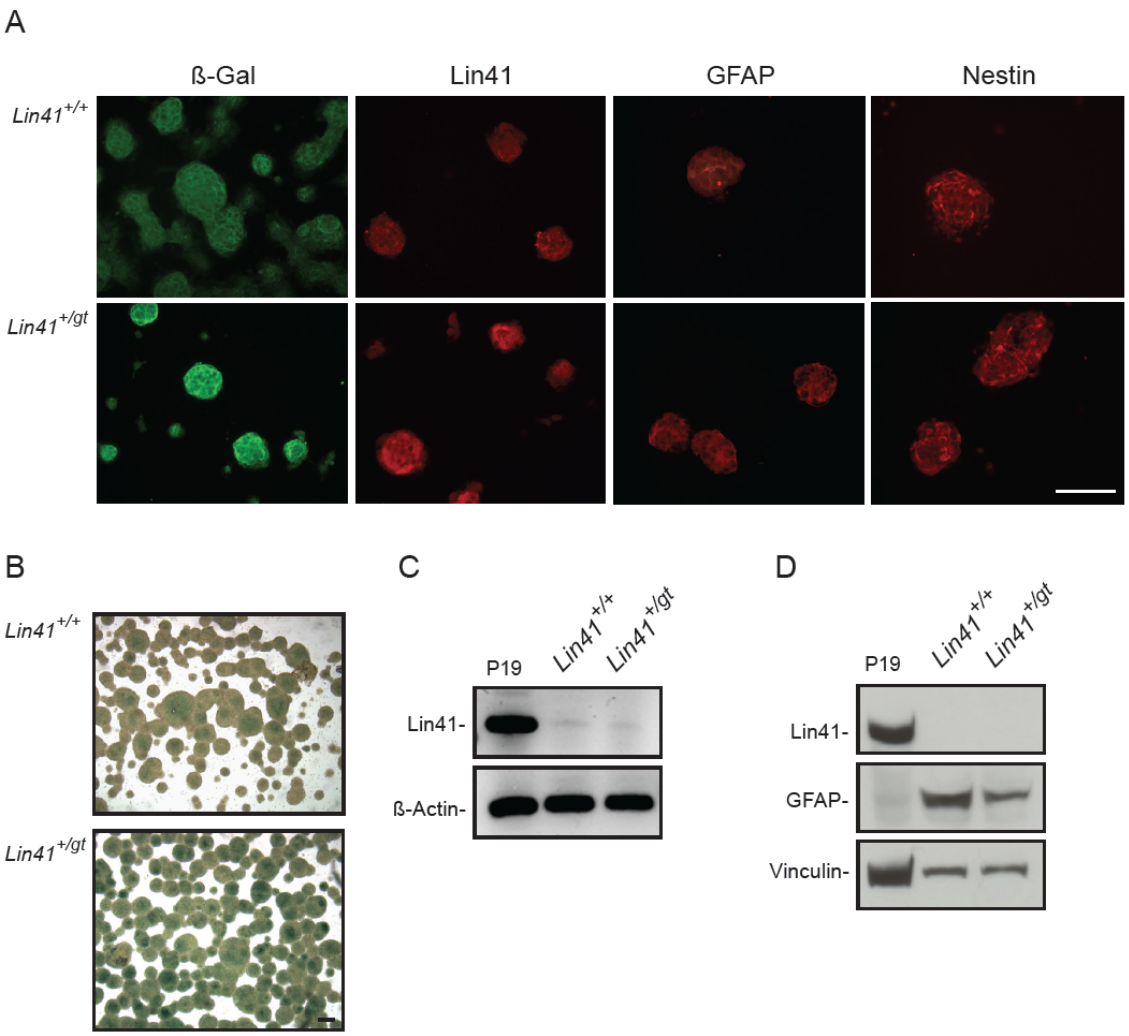

Figure 25. Analysis of neurosphere (NSP) culture derived from SVZ of wild type and heterozygote mice. A. Immunostaining of Lin41, ß-Gal, and NSP markers GFAP and Nestin. Scale bar 100 µm. A. X-Gal staining. Scale bar 100 µm. B. RT-PCR from cDNA of NSP and positive control P19; ß-Actin was used as control. C. Western blot of NSPs lysates, and P19 as positive control; Vinculin was used as loading control.

3.6 *Lin41* is expressed in ependymal cells

3.6.1 *Lin41* is expressed in ependymal cells *in vivo*

After finding that postnatal neural stem cells cultivated as neurospheres were *Lin41* negative, we analyzed *Lin41* positive cells in the postnatal brain in more detail by immunostaining.

Lin41 is expressed all along the four ventricles in the adult brain, in the first layer of cells that contact the lumen, where the ependymal cells are located (Figure 26). Moreover, it is known that the pattern of differentiation in ependymal cells occurs during the second postnatal week, which coincides with the upregulation of *Lin41*

expression in the ventricular walls. To confirm that *Lin41* positive cells represent multiciliated ependymal cells I used classic ependymal markers: Prominin-1 (also known as CD133) is a glycoprotein expressed in many different cell types in the adult organism, including neuroepithelial progenitors and ependymal cells (Pfenninger et al. 2011). Prominin-1 was co-expressed with LIN41 in the lateral ventricles, labeling the cilia of the cells. A second specific marker, the adhesion molecule CD24 is also expressed in the same cells of the ventricles (Figure 24B). Co-staining with these markers confirmed the ependymal identity of *Lin41* positive cells (Calaora et al. 1996).

To address in more detail the expression of *Lin41* along the lateral wall of the lateral ventricles, I took advantage of the recently developed whole mount procedure. With this histological preparation, the entire lateral wall of the lateral ventricle can be visualized at once, exposing the ependymal cells from the apical aspect. Using this method, the three-dimensional architecture of the stem cell niche has been described: ependymal cells are distributed in the ventricle wall as so-called pinwheel structures. A GFAP positive neural stem cell lies at the center of the pinwheel with direct contact to the ventricle through its basal primary cilia. Each stem cell is completely surrounded by at least one row of multiciliated ependymal cells (Mirzadeh et al. 2008)(Figure 8).

We used this technique to better describe *Lin41* expression along the lateral walls of the lateral ventricles, and therefore unravel its possible roles. A general overview employing X-Gal staining shows that a large number of cells in the lateral wall express *Lin41* (Figure 26A). Immunostaining with anti-Lin41 antibody confirms the expression, and reveals that the protein is located in the cytoplasm, equally distributed through the whole cell, and does not aggregate exclusively in p-body like structures, as seen in other cell types (Rybak et al. 2009)(Figure 26B).

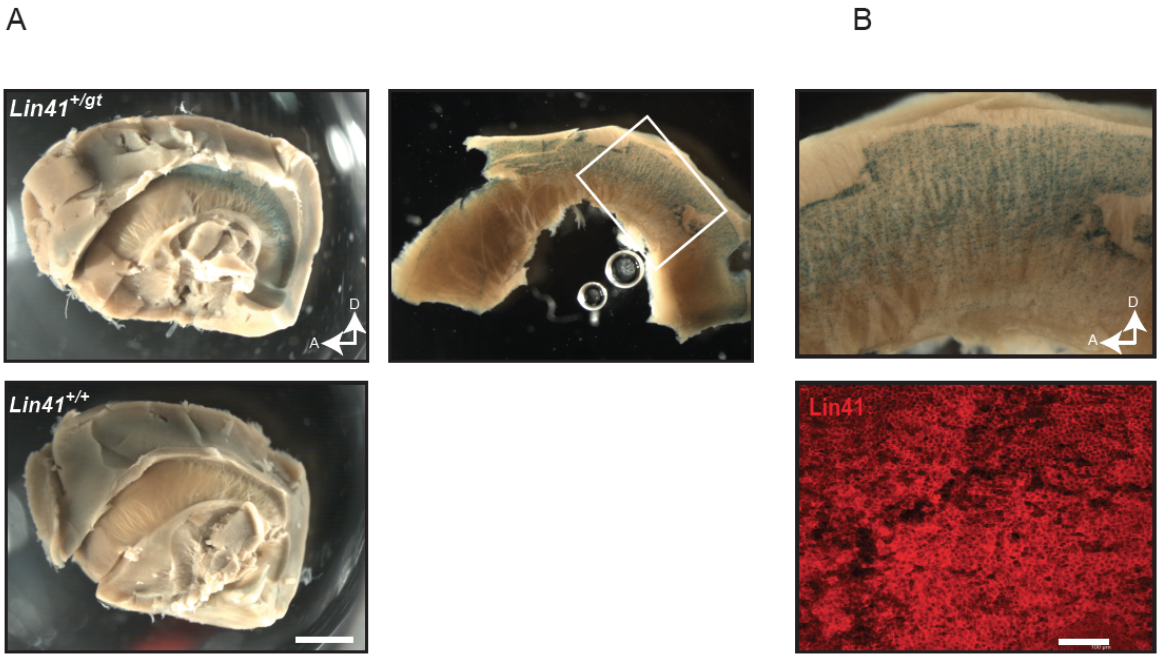

Figure 26. Brain Whole mount preparation. A. Whole mount of adult brain from heterozygote mouse (bottom, wild type as negative control). Arrows point dorsal and anterior sides. Scale bar 1 mm. Right panel shows the detailed section of the tissue. B. Detail of the lateral wall of the lateral ventricle displaying X-Gal staining (top panel) in comparison to immunostaining of Lin41 in the same area (bottom panel) Scale bar 100 µm.

Comparison of the X-Gal and immunofluorescence result also revealed an inconsistency in the expression pattern: X-Gal staining reflects the activity of *Lin41* promoter with a blue precipitate: using this technique I found *Lin41*-positive cells all throughout the ventricle surface in the lateral whole mount. Nevertheless, there is a concentration of positive cells in the superior and dorsal side of the lateral wall, while the central and ventral sections of the lateral wall contain fewer blue cells. On the other hand, immunohistochemistry analysis that identifies protein, showed a uniform layer of LIN41 positive cells covering the totality of the ventricles, including the medial wall. It is not easy to speculate on post-transcriptional regulatory mechanisms in this case, because the observation of promoter activity is more restricted than the final translated product. We understand that the nature of the procedure, an enzymatic reaction in case of X-Gal versus antibody immune reaction in the fluorescence staining, might account for the difference in the intensity and pattern.

More detailed description of Lin41 in whole mount preparations compared to ependymal culture cells is provided in the following section.

3.6.2 *Lin41* is expressed in ependymal cells *in vitro*, and co-localizes with ependymal markers

To further study the expression and role of *Lin41* in ependymal cells, I established a primary culture model, based on a recently described method (Guirao et al. 2010; Paez-Gonzalez et al. 2011). This model has been proven useful for the study of ciliogenesis and the cilia orientation program, because it is based on a proliferative and a differentiation phase, when ciliogenesis occurs, thus partially resembling physiological conditions. Astroglial cells from newborn mouse brain are plated in the presence of serum and allowed to divide for several days until they reach confluence. Then, the growth medium is replaced with serum-free medium, inducing a differentiation phase during the next 10 to 15 days in which the genesis and maturation of cilia occurs.

We used this technique to study how *Lin41* expression was modulated in relationship to the change in ependymal characteristics. Initially, I established an ependymal primary culture (EpC) from wild type and gene trap heterozygote animals. X-Gal staining was performed at different time points to monitor promoter activity. *Lin41* transcription is induced upon ependymal differentiation, and the heterozygote culture starts to show X-Gal positive cells after five days of differentiation. The wild type culture, used as control, remains negative throughout differentiation. The blue cells observed on the first day in both cultures likely correspond to choroid plexus contamination, because it has endogenous ß-Gal activity. These residual cells disappear with time in culture, as observed in the day 5 specimen, prior to specific *Lin41* activity in heterozygote culture. The number of positive cells increases with time in culture, until reaching approximately 70% of the total number of cells after 15 days in culture (Figure 27).

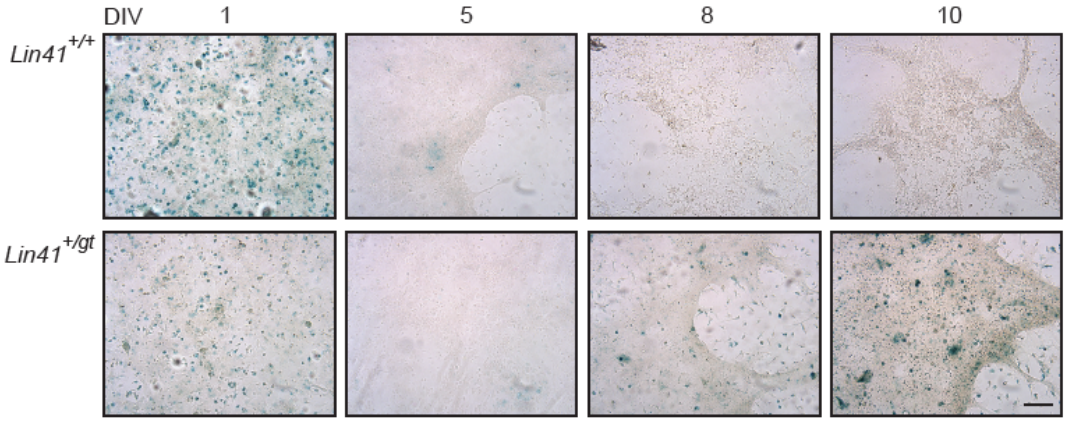

Figure 27. X-Gal staining of ependymal primary culture. Cultures derived from wild type and heterozygote P0 brain tissue. Differentiation time is expressed in days *in vitro* (DIV). Scale bar 100 µm.

Afterwards, I confirmed the ependymal identity of the EpC cells *in vitro* preforming immunostaining analysis with a panel of specific antibodies in comparison to whole mount preparations from the lateral ventricle (Figure 28). Firstly, both the lateral wall tissue and ependymal culture preparation show co-expression of Lin41 and S100ß, a classic ependymal marker (Didier et al. 1986), in addition to others like CD133 or CD24 previously showed for brain coronal sections (Figure 24). The position of *Lin41* positive cells within the pinwheel structure corresponds to large, flattened, ß-Catenin-positive cells with multicilia projecting from the center of the surface, in whole mount and culture cells. The long, motile cilia project from the apical surface of cells can be observed in the acetylated α-tubulin staining, that labels the cytoskeletal structure (axoneme) of the cilia (Mirzadeh, Coates, et al. 2010a). Cilia seem to be anchored to the apical surface in the center of the cell (approximately above the nuclei), and this can be better appreciated with the γ-tubulin staining of the basal bodies (Muresan et al. 1993). In case of the primary culture, the basal bodies are highly concentrated in one point of the relatively large cell surface, whereas the whole mount cells show a more dispersed, distributed pattern. More importantly, I confirmed the presence of the transcription factor FoxJ1, responsible for the ciliogenesis program (X. Yu et al. 2008), to be highly expressed in *Lin41*-positive cells in the ventricle and culture a result that reinforces the idea of *Lin41* intimate relationship with this specialization of ependymal cells.

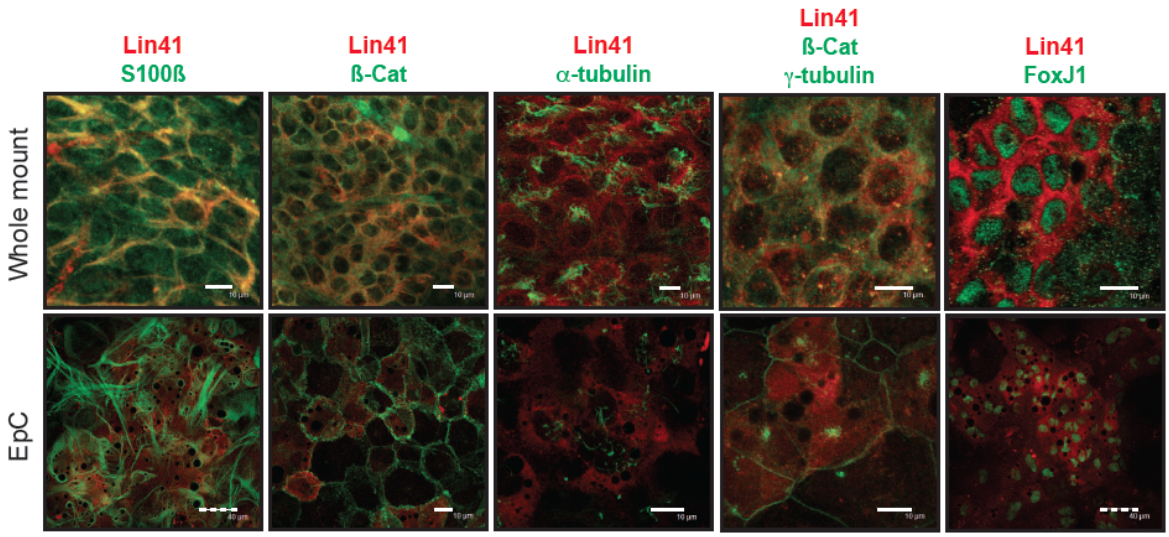

Figure 28. Immunostaining of lateral wall whole mount from adult wild type mouse brain and EpC derived from P0 brain tissue after 15 days of differentiation. S100ß is an ependymal marker, ß-Catenin is used to label the cell-cell contacts, α-tubulin the cilia and γ-tubulin the basal bodies of the cilia. FoxJ1 is a transcription factor responsible for the multicilia differentiation program. Scale bar 10 µm, dashed line 40 µm.

3.6.3 *Lin41* positive cells are motile multiciliated cells *in vitro*.

One aspect that reinforces the ependymal identity of *Lin41*-positive cells derived from primary culture is the presence of motile cilia arranged in high number within the cells. After around 10 days in culture, multiciliated cells exhibit a clear and strong beating of these cilia. The beating is not established in a particular direction, as each cell shows a random orientation of the movement. This is expected, due to the lack of fluid movement necessary to coordinate the cilia beating (Guirao et al. 2010). In physiological circumstances of brain development, the cerebrospinal fluid flows from the rostral pole of the brain in the direction of the aqueduct, and this stream determines the orientation of the basal bodies in ependymal cells of the ventricle to achieve a coordinated and aligned beating of the cilia, and actively cooperates in the fluid movement (Guirao et al. 2010). In the absence of directed flow, cilia beat in randomized directions. The demonstration that upregulation of *Lin41* temporally coincides with the appearance of cells with functional motile cilia is an important confirmation that the ependymal differentiation program is faithfully modeled in this cell culture system and at the same time suggests a role for *Lin41* in the establishment of this lineage (Video).

Taken together, our results show the expression of *Lin41* in ependymal cells both *in vitro* preparations and *in vivo* tissue of the lateral wall of the ventricles, co-

localizing with ependymal markers and developing motility of the cilia in the primary culture model.

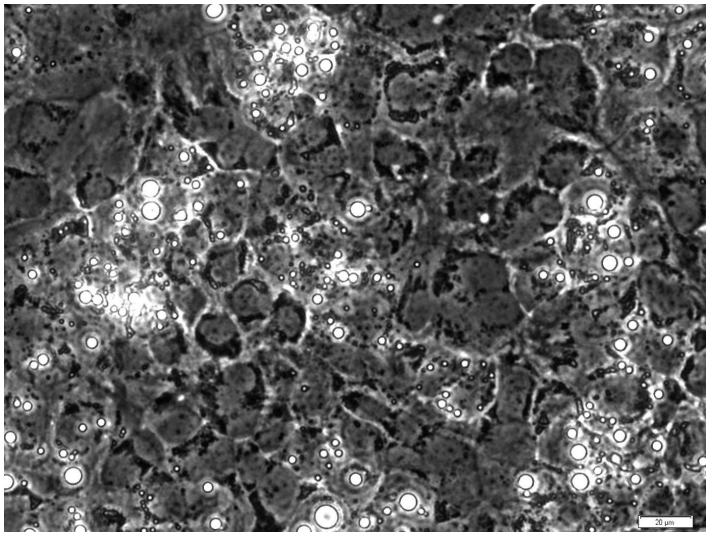

Video. Recording of EpC cells after 15 days of differentiation, displaying beating cilia.
(http://www.youtube.com/watch?v=3mcWpBHMLgs)

4 Discussion

4.1 *Lin41* is essential for mouse embryonic viability.

Lin41 is a gene highly conserved during animal evolution, from *C. elegans* to humans, and plays a major role in the development of these organisms. The importance of its activity can be addressed by studying the consequences of its disruption. *Lin41* was originally discovered in *C. elegans*, in a screen of heterochronic mutations, as part of a group of genes that regulate the timing of stem cell decisions during larval and adult developmental transitions. *Lin41* was shown to be epistatic to a second novel heterochronic gene, the *let-7* miRNA, that is responsible for inducing the differentiation program at the larval to adult transition. *Lin41* loss of function leads to a precocious terminal differentiation of seam cells, causing execution to adult phase from L3 stage. Contrarily, in *let-7* null animals seam cells fail to execute the differentiation program to final stage, resulting in death by the bursting of the vulva. Moreover, *Lin41* overexpression resembled the *let-7* deficiency phenotype, resulting in some cases in lethal vulva bursting, and strongly suggesting that *let-7* acts via regulation of *Lin41* to direct proper molecular timing (Slack et al. 2000).

D. melanogaster also served as a model for the study of the sub-family of Trim-NHL proteins, to which Lin41 belongs. The homologous gene *Wech* was independently identified and called *Dappled*. This gene is similar to *Brat* (paralog of *Lin41*), as both were identified as proto-oncogenes and lack the N-terminal Ring domain characteristic of the Trim-NHL sub-family. Study of mutants expressing low WECH protein levels displayed muscle detachment from the body wall and embryonic lethality. Lethality can be partially rescued until the third instar (arthropod developmental stage) by expressing WECH protein specifically in muscle and tendon cells (Löer et al. 2008). An independent *Wech* loss of function study focused on description of a melanotic tumor formation with a characteristic appearance (Rodriguez et al. 1996). Overexpression results in eye malformation, which reflects an alternative effect of the developmental programming ruled by this family of proteins (O'farrell et al. 2008).

The essential role of *Lin41* in development has also been confirmed in vertebrates: in zebrafish (*Danio rerio*), the repression of *Lin41* by morpholino or siRNA injection at one cell stage embryos causes severe defects in the animals, including a shortened trunk and deformed yolk sac and tail, followed by death after 48 to 60 hours. Like in *C. elegans* this phenotype is similar to those displayed by embryos overexpressing let-7a via oligo injection, reinforcing the evidence of the regulatory influence of let-7 over *Lin41* (Lin et al. 2007).

Finally, assorted mouse models have confirmed *Lin41* relevance in mammal development. Three independent mouse lines containing gene trap mutations (after the first or the second exon) in *Lin41* showed embryonic lethal phenotypes from day E9.5 on, always accompanied by a characteristic failure in the neural tube closure (Maller Schulman et al. 2008; J. Chen et al. 2012). As part of this thesis work a novel gene trap mouse line was generated with insertion of a ß-Geo gene trap cassette after the third exon (Figure 29). By the time Schulman and colleagues published the embryonic lethality of *Lin41* null mice, we were obtaining comparable results using our mutant line. In our gene trap model embryos lacking *Lin41* did not survive after day E9.5 or E10.5, and in all cases analyzed they displayed an open neural tube phenotype (Figure 23). The penetrance of the phenotype was different among the mouse lines, as we failed to retrieve embryos later than E11.5, whereas Maller Schulman and Chen reported embryos up to E14.5, although at a very low Mendelian rate.

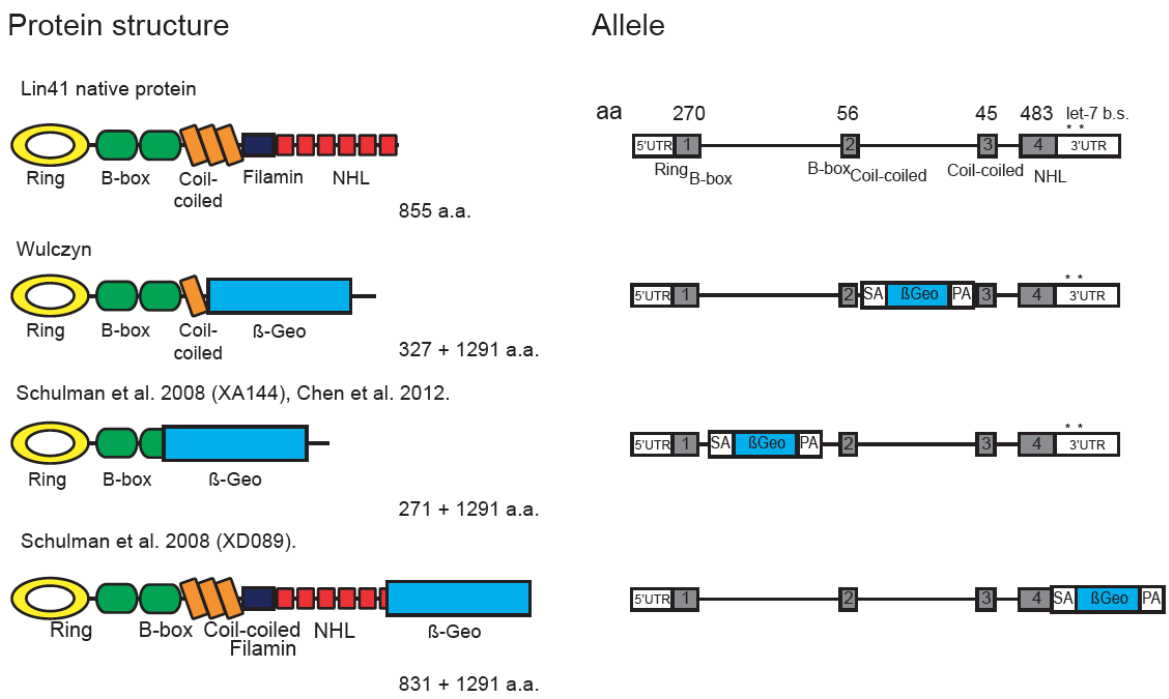

Figure 29. Lin41 gene trap mouse lines. The left panel shows the wild type protein in comparison to the chimeric proteins, labeled with each author's name. Right panel displays Lin41 locus and different locations of gene trap cassette.

These results reinforce the evidence of a characteristic role of *Lin41* in the neuroepithelial fusion events of neurulation, in addition to the viability of the organism. On the other hand, observations in all three gene trap lines agreed on characterizing the heterozygote animals as viable, fertile and morphologically indistinguishable from their wild type littermates, suggesting that mutation in one *Lin41* allele does not affect development, although they express half the amount of protein (Figure 23B).

Only one study reported so far a mechanistic explanation for the *Lin41* mutant phenotype. Using the neuroepithelial tissue obtained from one gene trap mouse line, Chen and colleagues screened diverse signaling pathways involved in neural tube specification, identifying a failure in FGF response as a result of *Lin41* mutation. Furthermore, in two-hybrid screen, the FGF signaling cascade effector SHCBP1 was found to interact with, and be ubiquitinated by *Lin41* in a non-degradative fashion that stabilizes SHCBP1. They hypothesize that *SHCBP1* expression in proliferative cells points to a role in the maintenance of self-renewal in progenitor cells. Thus, in the absence of *Lin41*, SHCBP1 is not stabilized and cells stop self-renewal, undergoing premature differentiation, which leads to a

cranial growth and fusion defect in the neuroepithelium (J. Chen et al. 2012). This gene trap mouse model suggests a parallelism with the phenotype described for *C. elegans*, where *Lin41* is necessary to maintain proliferative cells and avoid premature differentiation, as discussed above (Slack et al. 2000). The reduced number of homozygous knockout embryos and the limiting amount of neuroepithelial tissue that can be isolated from them represented technical limitations for us to reproduce the results from the Chen publication regarding FGF signaling. mES cells represent a versatile source of abundant material to induce FGF effectors and observe if *Lin41* deficiency alters this signaling pathway, as well as screen for its role in other circuits.

Despite these data, the molecular mechanism underlying mouse lethality has not yet been elucidated. Although neural tube defect phenotypes are often observed in different *Lin41* gene trap mouse models, they are not the sole cause of embryonic lethality either at mid-gestation, late development or even postnatal stages (Copp et al. 2003). The main causes for embryonic lethality at mid-development are encompassed by circulatory deficiencies; these could occur due to a failure in the embryonic formation of the heart, or to alterations in the extraembryonic structures and the accompanying placental insufficiency. *Lin41* is not expressed in the primordial heart of the embryos: therefore, it is feasible that the cause of death has an underlying nature related to placental insufficiency, due to the misdevelopment of the extra embryonic structures (yolk sac, allantoides or chorion), or defective trophoblast (Papaioannou & Behringer 2011). It is unknown whether Lin41 is expressed in one or more of these extraembryonic structures. Addressing the promoter activity and protein expression would be the first step to elucidate whether the disruption of *Lin41* expression endangers the environment necessary for the survival of the embryo. The embryonic death of mouse knockout embryos at mid-gestational stages, in addition to the absence of phenotype features in the heterozygous animals represents a limitation to define the exact position of *Lin41* in molecular pathways such as FGF signaling. To elucidate the role of *Lin41* at a tissue-specific level, and in particular to study the neurogenic defect independently from the lethality phenotype at day E9.5, it will be necessary to abrogate Lin41 expression in a more precise manner. This can be achieved with the use of a *Lin41* conditional knockout mouse.

4.2 *Lin41* conditional knockout mouse generation

To approach the study of *Lin41* in the mouse and avoid the limitations of the gene trap strain, the generation of a conditional knockout is the most accurate and complete tool. The combination of the floxed allele with Cre-expressing promoters, specific in time and tissue expression, allows an array of deletions under controlled parameters. This is a convenient feature for the study of genes that undergo spatiotemporal regulation, such as *Lin41*.

We initiated the strategy to generate the conditional knockout simultaneously with the characterization of the gene trap mouse for *Lin41*, and therefore the first evidences of embryonic lethality upon *Lin41* loss. Considerable time and effort was invested in the project, from the design and generation of the vector to the screening of the electroporated cells using Southern blot and PCR techniques.

Homologous recombination is a broadly used method to introduce specific modifications in the mouse genome, and has been optimized to achieve efficient conditional knockout mutations (Liu et al. 2003; Bradley et al. 1984; Thomas et al. 1992; Smithies et al. 1985). We aimed to construct a targeting vector containing two loxP sites flanking last exon (exon 4) and the beginning of the 3'UTR of the *Lin41* gene. Targeting the last exon would prevent loss of the mutation in the event of alternative splicing; furthermore, we had previous evidence from the gene trap that a protein lacking the C-terminus results in loss of function.
In the vector, flanking the targeted area of *Lin41*, the original sequence of the gene extends for 10 kbp, designated as the homology arms. After the electroporation of the vector in mouse ES cells, the induction of homologous recombination between homologous sequences facilitates the specific incorporation of the gene sequence containing modifications into the genome, replacing the wild type allele (Liu et al. 2003).
Our collaborators performed the electroporation into mES cells and the subsequent colony selection and cell culture. I received the cell lysates for Southern blot analysis, and was able to identify five candidates based on a signal of the expected band size when probed for integration of the neomycin resistance gene. Out of these five, two clones showed the expected integration pattern in the 5' side. However, the pattern observed in the 3' side included unaccountable

bands, indicating that an aberrant integration most likely occurred in or near the homology arm (Figure 16C). Subsequent PCR analysis revealed that even though the amplified region resulted in a band of the expected size, the intensity of the bands corresponding to the vector was markedly more intense (Figure 17B). The integration of the vector in one locus of *Lin41* should result in one mutated and one wild type allele per genome, providing equal amount of template for the PCR. For that reason, the abnormally intense bands might indicate multiple integrations of the 3' arm either at the *Lin41* locus or somewhere else in the genome.

After the inability to identify a correct integration event in the first round of electroporation our collaborators performed a second round using both BL6/C57J and 129 mES cells. The DNA analysis by Southern blot was arduous, and I was unable to identify any integration event. Moreover, I could not detect any wild type sequence, which is expected for every clone. The troubleshooting analysis and control experiments provided evidence that insufficient quantity and quality of the supplied DNA was the cause of the technical difficulties (Figure 18). We therefore performed an initial screen of each one of the potential clones using PCR. The PCR can be used as an alternative method that provides reliable results without demanding large amounts or high quality DNA. Nonetheless, I was unable to identify a single integration event amidst more than 200 independent clones analyzed. It is unclear why integration, although defective, was achieved in the first round but not a single event was detected in subsequent experiments. Without the ability to determine whether the failure was due to a biological problem with our targeting vector or to difficulties in the selection and culture of neomycin resistant colonies, we chose to circumvent both steps by purchasing targeted mES cells after they became available from the EUCOMM gene-targeting consortium. Similarly to the vector we designed, in these the knockout strategy targeted exon 4. One advantage of the EUCOMM vector employed is the so-called "first gene trap" design, a combination of traceable *LacZ* and selectable *Neo* resistance genes, flanked by FRT sites, followed by the fourth exon flanked by two loxP sites. The gene trap cassette precedes and is independent of the loxP sites designed for deletion of the fourth exon (Figure 19).

We undertook this project in collaboration with the group of Dr. Geert Michel in FEM, who performed a first round of injections of these cells (previously characterized for aneuploidies and Y chromosome presence by the company ChromBios), resulting in seven medium-to-high chimeric males. We therefore expected germline integration of the cells in at least one of the chimeras. After more than six generations descending from the chimeras (F1 generation), comprising a total of 174 mice genotyped by PCR, I failed to detect the vector in any of the analyzed mice. We attempted the same strategy using a second independent clone of cells that resulted in five males and eight females presenting high degree of chimerism. A high number of female chimeras derived from a XY line injection is an indicative of problems with germline integration. Generally, F1 pups derived from male chimera have a higher probability of carrying the vector, although all the animals were mated and offspring tested. I identified eight positive candidates, all descendants from one of the males with 100% chimerism (m17) (Figure 19C). The other male chimeric mice presented a degree of chimerism varying from 75 to 95%, however they did not produce offspring positive for the vector. We speculate that the cells containing the vector might be reluctant to integrate in the germline, which would explain the negative results from the injection of the first clone and only one of several male 100% chimeric transmitting the vector to its offspring.

Southern blot analysis of the gDNA from these candidates is still necessary to confirm the proper vector integration in the genome. In case of corroborating the expected *Lin41* conditional knockout mouse line, we will proceed to increase the colony size. Afterwards, we will design a series of experiments derived from the mating of these animals with specific Cre-lines to obtain as much information as possible about the consequences of *Lin41* loss in mouse.

First, we will use a mouse expressing Flp in a ubiquitous and efficient way, Tg(CAG-Flpe)2Arte, in the BL6/C57J background (Y. Wu et al. 2009). This will allow us to delete the gene trap cassette containing both *LacZ* and Neo^R genes, and therefore investigate if such an insertion interferes with the normal expression of the *Lin41* gene (Figure 19A). We will maintain a subset of the colony with the original target insertion (i.e. without Flp-induced deletion) to allow comparison of this and other gene trap mouse lines (Maller Schulman et al. 2008; J. Chen et al.

2012).

With the animals derived from Flp-Cre mating, and therefore containing a pure conditional knockout mutation, we will begin to approach the specifics of the *Lin41* phenotype in the null mice embryos. For this, we will use lines expressing Cre in the central nervous system between E9.5 and E13.5, when *Lin41* is specifically expressed in this tissue, and the homozygous mutation displays a phenotype (Figure 23A). The abrogation of *Lin41* in particular cell types of the neurogenic tissue will allow us to study the consequences for the CNS morphogenesis, while avoiding embryonic lethality. The following list contains several options for this purpose:

- Notch1tm3(cre)Rko/J, expressing Cre under the control of Notch (active in embryonic neural tube by day E9.5).
- B6.129S2-Emx1tm1(cre)Krj/J, expressing Cre from the Emx1 locus, will drive ablation of Lin41 from developing day E9.5 in telencephalon, and more thoroughly in the ventricular zone from E12.5 *(Cecchi & Boncinelli 2000)*.
- B6.Cg-Tg(Nes-cre)1Kln/J, also known as Nestin-Cre. Expressed at first at E10.5 in mesenchyme and nervous system precursor structures.

These mouse lines should help elucidate the consequences of deleting *Lin41* specifically in neural tissue. Moreover, it would be interesting to clarify if avoiding the deletion in extraembryonic structures results in viable embryos, which would provide the first evidence to explain the lethal phenotype of *Lin41* gene trap embryos independently from the neural tube defect. To study Lin41 during limb bud development the best option would be a mouse carrying Cre under the control of a Prxl enhancer, with high expression in the limb bud mesenchyme and a subset of the craniofacial mesenchyme *(Logan et al. 2002)*. The effect of Lin41 deletion in limb will help elucidate its role within the FGF signaling pathway, and identify putative downstream effectors of Lin41 *(Lancman et al. 2005)*.

Research in the postnatal stages will focus on the ependymal lineage, due to the restricted expression of *Lin41* in these cells of the CNS. We will study the role of *Lin41* during ependymal cell differentiation, beginning between postnatal days 7 to 15, as this is concurrent to *Lin41* upregulation. From that age onwards, the main scope is the influence of *Lin41* on the homeostasis of the SVZ neurogenic niche. The present study reveals for the first time that *Lin41* is expressed in multiciliated

ependymal cells of the brain ventricles. The importance of these cells and their disposition surrounding the stem cells in maintaining the adult neurogenic ability in the rostral migratory stream has been previously reported (Paez-Gonzalez et al. 2011). Unraveling the influence of *Lin41* in this compartment of the brain might also help to elucidate the genetic program of multicilia specialization, to which effectors *Lin41* is intimately related. Proposed strategies for experiments to be performed in postnatal stages are discussed in the ependymal section 4.6.

4.3 *Lin41* in stem cells

One of the first studies addressing the function of Lin41 in mammals at the molecular level reported *Lin41* expression in mES cells, as well as in the embryocarcinoma line P19. The work focused on its regulatory pathway, coupled with miRNA let-7 in stem cells. *Lin41* expression was restricted to a proliferative, pluripotent state, and when cells were induced to neural differentiation, the expression faded in contraposition to upregulation of the miRNA let-7 (Rybak 2009). This correlates to the pattern observed in *C. elegans*, when *Lin41* is expressed in immature stages, and *let-7* is a marker of differentiated tissues (Slack et al. 2000). Moreover, in the pluripotent cell lines analyzed it was found that *Lin41* also affects let-7 expression, thus establishing a negative auto-regulatory loop that tunes the balance between undifferentiated and neural committed molecular stages of the cells (Rybak 2009). During neuronal lineage differentiation of embryocarcinoma and embryonic stem cells *Lin41* levels decrease concomitantly to the upregulation of miRNA let-7. The molecular switch governing this transition was described as a double negative autoregulatory loop between the two players. Neuronal differentiated cells express let-7 miRNA, which targets the 3'UTR of *Lin41* mRNA and prevents its translation into protein. On the other hand, the pluripotent cells maintain low levels of several miRNAs, such as let-7, via a cooperative mechanism between *Lin41* and other regulators, in particular *Lin28,* which targets let-7 maturation. Mechanistically, the E3 ubiquitin ligase *Lin41* promotes proteasomal degradation of the essential microRNA-induced silencing complex (miRISC) protein AGO2, therefore decreasing the overall activity of miRNAs pathway in pluripotent cells (Figure 5) (Rybak et al. 2008; Rybak 2009).

In addition, disparate studies have approached *Lin41* mechanisms to control and maintain pluripotency in stem cells. Recently, Chang and colleagues reported a

function of *Lin41* in mouse ES cells related to cell proliferation control. In their work, *Lin41* associates with miRNAs expressed in mES cells, like miR-302, and represses the expression of *Cdkn1a*, a cycling-dependent kinase inhibitor that negatively regulates the G1-S transition. They show that reducing levels of *Lin41* by siRNA results in a increase in CDKN1A expression, and slows the proliferation rate (Chang et al. 2012). We performed western blot analysis of *Lin41* gene trap mES cells, and observed that knockout clones did not display an increase of CDKN1A protein compared to the heterozygous or wild type lines (Figure 22D). In addition, the $Lin41^{+/+}$, $Lin41^{+/gt}$ or $Lin41^{gt/gt}$ gene trap mES cell lines did not present changes in cell division (Figure 22C). Chang and colleagues obtained their results by transient knockdown of *Lin41*, while we performed our experiments using *Lin41* null cells. This methodological difference might account for the dissimilar results, if our gene trap cells developed compensatory mechanisms to maintain CDKN1A protein levels, an important regulator of mES cell proliferation and cell cycle control.

In 2012, a publication of Loedige and colleagues focused on the influence that *Lin41* has at the level of mRNA regulation. They identified the NHL domain of *Lin41* to be essential and specific in the recognition and repression of target mRNAs, through a mechanism highly similar to that of *Brat*, a *Lin41* gene paralog in *D. melanogaster*. Moreover, they identified retinoblastoma-like protein 1 and 2 (*Rbl1* and *Rbl2*) as targets of *Lin41*. These two transcription factors negatively regulate the expression of genes implicated in cell cycle control in embryonic stem cells, and are also the targets of stem cell specific miRNAs (Loedige et al. 2012). Taken together, these data suggest a promoting role for *Lin41* in cell cycle and self-renewal control of mES cells. Nevertheless, it is possible that *Lin41* is member of a robust network controlling these mechanisms, and upon its loss some other player can take over and compensate *Lin41* function. This strategy would be limited to proliferative mES cells and early developing embryos, as the absence of *Lin41* in mid-development is not compatible with life.

4.4 *Lin41* expression in development

Lin41 is expressed in mouse embryonic stem cells isolated from the inner cell mass of E3.5 blastocysts (Figure 21). The earliest evidence of *Lin41* expression in living embryos is by immunohistochemistry at E7.5, revealing that LIN41 and

OCT4 are co-expressed in the ectoplacental cone (Rybak et al. 2009). In the present study, experiments performed with gene trap mice revealed that E8.5 embryos present ubiquitous *Lin41* promoter activity (Figure 23A). Therefore, it is reasonable to assume that *Lin41* is expressed throughout gastrulation, although so far no data are available for the period E4.5 – E6.5. From the stage E9.5 on, *Lin41* expression is restricted to specific tissues, and progressively confined within these organs until day E13.5, when its expression is no longer detectable. At E10.5, X-Gal activity can be observed in the branchial arches, limb buds (including the tail bud), and especially in the neuroepithelium. The signal remains in the following stages: E11.5 and E12.5, albeit the number of positive cells is notably reduced. The activity is restricted to the distal fraction the limb buds and the tip of the tail bud, and certain areas of the telencephalic neuroepithelium (Figure 23C).

The expression of *Lin41* in limb bud was previously studied in chicken and mouse embryos. Avian *Lin41* is ubiquitously detected by *in situ* hybridization in the mesoderm of wing and leg, by Hamilton and Hamburger stages 22 and 23. The expression undergoes temporal changes and by stage 24 is restricted to the distal section, and marginally biased to the posterior pole of the limb, with a more defined gradient in the leg compared to the wing (Lancman et al. 2005; Schulman et al. 2005). Interestingly, this pattern is inverted to that of let-7 miRNA, more prominent on the anterior side of the forelimbs, as observed in E11.0 mouse embryos (Mansfield et al. 2004). This provides evidence for the conservation, not only of *Lin41* and *let-7* genes during evolution, but of their reciprocal regulation. Let-7 binding sites are present and regulatory functional in the 3'UTR of all studied homologs of *Lin41* from *C. elegans* to *Homo sapiens* (Vella et al. 2004; Lin et al. 2007; O'farrell et al. 2008; Maller Schulman et al. 2008).

For the present study, I performed experiments aiming to detect *Lin41* promoter activity by X-Gal staining in *Lin41*$^{+/gt}$ mice. I observed a pattern of *Lin41* expression in developmental limb buds to some extent similar to the results published by Lancman and Schulman. At E10.5 stage, X-Gal staining in whole embryos or sections reveals a uniform staining in the forelimb buds. At later stages, the signal is restricted to the distal area in the limb, in the primordial of the digits, but no polarization along the anterior-posterior axis could be detected (Figure 23C). My work was mainly based on an enzymatic reaction, X-Gal, which reports the

promoter activity, therefore reflecting transcriptional activity. On the other hand, the publications mentioned above determined *Lin41* mRNA expression by *in situ* hybridization. The differences in *Lin41* intensity can be explained by the post-transcriptional regulatory activity of miRNA let-7, which would reduce the levels of *Lin41* mRNA in the anterior aspect of the bud, but do not affect the gene promoter activity. Moreover, a second article published by Schulman and colleagues, studying one *Lin41* gene trap mouse line, shows a lack of polarization in the limb buds in X-Gal staining samples of E10.5 to E12.5, similarly to our observations (Maller Schulman et al. 2008), reinforcing the idea of posttranscriptional regulation of *Lin41* mRNA as the polarizing element in limb buds. Despite the diverse data describing *Lin41* expression in the limbs during embryonic development, little is known about the regulatory pathways that govern this process. *Lin41* expression is lost upon disruption of Sonic Hedgehog signaling, and expression is recovered around the tissue with implanted beads containing the protein SHH, although a direct interaction and mechanism have not yet been described (Lancman et al. 2005). The overall dichotomy between *Lin41* and let-7 functions suggests an orchestrated series of events: first, a proliferative stage, characterized by *Lin41* expression and dependent on the *Shh* regulatory center, located in the posterior pole of the limb (Sanz-Ezquerro & Tickle 2000). This is followed by a terminative differentiation stage governed by let-7 modulation, beginning in the anterior region. These events are accompanied by a decrease in promoter activity in a proximal to distal progression.

During development, neural stem cells divide and give rise to the vast majority of cells in the brain. The rudimentary neural tube of mid-gestational embryos is a pseudostratified epithelium composed of neuroepithelial cells that divide symmetrically to enlarge the tissue in size. Before the onset of neurogenesis, the neuroepithelium undergoes changes in its molecular profile and the cells become radial glia cells. Radial glia divide asymmetrically, producing one daughter cell that maintains the population of stem cells in the ventricular zone of the fetal brain (basal progenitors), and another that might produce an intermediate progenitor for neurons or glia. The neural progenitor generates neurons that migrate (using the very same radial glia cells as scaffold) in temporally coordinated waves to form the neuronal layers of the cortex. The glia progenitor is the cell of origin for the glia

populations of the brain: macroglia, oligodendrocytes, parenchymal astrocytes and ependymal cells (Merkle & Alvarez-Buylla 2006; Götz & Huttner 2005). Radial glia cells remain after birth as postnatal stem cells in species like birds and amphibians. In mammals they are absent from the adult brain, although it is known that the B cells, neural stem cells that persist in the adult SVZ, are a subset of particular astrocytes derived directly from embryonic radial glia (Merkle et al. 2004; Malatesta & Gotz 2013; Kriegstein & Alvarez-Buylla 2009; Anthony et al. 2004). The reciprocal relationship between *Lin41* and let-7 was also evaluated in a model of neural stem cells derived from E12 forebrain that closely resemble the radial glia of the *in vivo* tissue. When the let-7 miRNA was subjected to competitive inhibition using so-called sponge vectors, the levels of LIN41 protein increase, indicating that the transcription is presumably active in these cells, but mRNA is silenced by let-7, preventing translation (Rybak et al. 2008).

Overall, *Lin41* has been described as a dual effector: it acts in the promotion of cell proliferation and also preventing differentiation, counteracting the activity of highly specialized molecules such as let-7. In developing tissues like limb bud or neuroepithelium, this balance between cell division and initiation of cell fate determination is spatiotemporal regulated, and requires a tight molecular program. The suppression of *Lin41* activity probably occurs due to a combination of mRNA modulation by let-7 miRNA (and maybe others, such as miR-125), in parallel to the decline in promoter activity between E12 and E13.5 (Figure 23C).

As mentioned above, it has been speculated that *Lin41* might play a role in the FGF pathway in the neuroepithelium, stabilizing SHCBP1 and thus further promoting FGF signaling. In embryonic limb buds of *Fgf4/6* null mice, *Lin41* is first expressed but rapidly lost, pointing to a dependence on signaling to maintain *Lin41* expression. Available evidence in development and mES cells suggests an ambivalent role of *Lin41* within the FGF pathway, acting on one hand as a stabilizing enhancer of FGF signaling in the developing neural tube (J. Chen et al. 2012), and on the other hand as a downstream responsive element in the limb buds (Lancman et al. 2005). More studies are necessary to unravel whether *Lin41* has a pivotal position in FGF regulation, and the dependence of that role on spatiotemporal context.

In the present work I have observed *Lin41* activity in general contexts of cellular proliferation: mES cells and embryonic tissues undergoing rapid growth. *Lin41* seems to be dispensable for the maintenance of an undifferentiated state, but results in death of the organism during mid-gestation, pointing to an exclusive, non-compensable role for an as yet unidentified differentiation program. Nevertheless, the CNS postnatal expression of *Lin41* is surprisingly restricted to a highly specialized epithelial cell type, the ependymal covering the ventricular surface. With exception of limb buds mesenchyme, the other *Lin41* positive cells harbor epithelial identity: mES cells, neuroepithelium and ependymal cells. To investigate whether Lin41 plays a role in the features of these cells could help unravel its role in such disparate cellular types.

4.5 Role of *Lin41* in SVZ niche

The present work has mainly focused on the characterization of *Lin41* expression using a mouse gene trap model. To our knowledge, it is the first time that *Lin41* postnatal activity is reported in the CNS. I observed that its expression is confined to the walls of the ventricles, beginning with the second week of postnatal development and remaining throughout adulthood (Figure 24). The SVZ of the lateral walls, located in the lateral ventricles is the largest adult neurogenic niche in mammals. The neural stem cells, also called B cells, are intimately tangled within the brain parenchyma, below the ependymal cells that cover the ventricle. As a consequence of this complex distribution, the histologically distinction of each cell type in the niche is challenging. Previous experiments reported *Lin41* expression changes during neural differentiation of mouse embryonic stem cells, and in radial glia culture from E12.5 neuroepithelium (Rybak et al. 2008; Rybak 2009). Therefore, we first addressed the question of *Lin41* expression in adult neural stem cells. Neural stem cells can be cultured *in vitro* using the neurosphere assay, in which cells grow and form spheres composed of a heterogeneous mixture of stem cells and committed mitotic progenitors (Reynolds et al. 1992). The analysis of these cultures revealed low but detectable expression of *Lin41* promoter activity. Despite this, LIN41 protein could not be detected in NSPs, most likely due to repression of *Lin41* mRNA by let-7, as neurospheres express moderate amounts of let-7 miRNA. Moreover, NSPs from heterozygote brains expressed ß-Gal detectable by immunostaining. Because the mutant mRNA lacks let-7 binding sites, this results is consistent with the theory of low transcription and subsequent

posttranscriptional repression of the native mRNA in NSPs (Figure 25). These results argue against B cells as *Lin41*-positive cells in the ventricular wall, as they give rise to most of the multipotent NSCs in NSPs culture (Doetsch et al. 1999). We therefore focused on the description of *Lin41* in ependymal cells, located apically from B cells in the SVZ. Ependymal cells are derived from radial glia in the last days of embryonic development, but they do not differentiate and acquire their characteristic features until the second postnatal week (Spassky et al. 2005), precisely the time point when *Lin41* promoter activity is observed in these cells. We characterized ependymal cells by co-immunohistochemistry of *Lin41* and ependymal markers (Figure 24 and 28).

As previously described, the structure of the SVZ niche has a complex three-dimensional architecture, harboring several distinct cell types (Figure 8). Only the astrocytic type B cells are unanimously accepted as bona fide stem cells, although they rely on the environment to maintain their proliferative and neurogenic ability, as demonstrated by the intimate communication with the vascular niche (Shen et al. 2008). The role of the ependymal marker CD133 in the SVZ neurogenic niche was subject of some debate: a series of papers either supported or rejected CD133 as a marker of neural stem cell subpopulations in the rodent brain. Currently, the widely accepted theory maintains that some of these CD133 positive cells divide and generate neurons upon insult to the neighboring tissue, but they do not proliferate in regular conditions. Therefore, they are not considered bona fide stem cells (Corti et al. 2007; Coskun et al. 2008; Pfenninger et al. 2007; Chojnacki et al. 2009). Ankyrin 3 (*Ank3* or *AnkG*) is an adapter molecule that organizes membrane domains. It is expressed after birth in radial glia progenitors that will exclusively become ependymal cells in the SVZ niche of the lateral walls, but not in the stem cells (B cells). *AnkG* expression is directly controlled by the transcription factor FoxJ1, which operates the molecular program responsible for multicilia differentiation. If *AnkG* expression is prevented by the conditional abrogation of *FoxJ1*, ependymal cell maturation and assembly is affected and adult neurogenesis is impaired *in vivo* (Paez-Gonzalez et al. 2011). It would be of interest to analyze if *Lin41* is a target of *FoxJ1*, and if deletion of *Lin41* in the ependymal lineage results in a deficient production of new neurons. These experiments could establish a functional role for *Lin41* in the multicilia molecular

program. To answer this question, we will take advantage of the mouse line Tg(Foxj1-cre/ERT2)1Blh, expressing Cre under control of the *FoxJ1* promoter, to specifically delete *Lin41* from ependymal cells in the postnatal brain. If *Lin41* deletion affects the organization of the SVZ, it will be necessary to address the number and identity of progenitors migrating in the rostral migratory stream towards the olfactory bulb, in order to identify alterations in neurogenesis. A complementary strategy would be to design a lentiviral construct to downregulate *Lin41* in ependymal primary cultures. This tool would allow efficient targeting of cells either in proliferative conditions or undergoing differentiation, and would help elucidate if and when *Lin41* is required for the acquisition of multiciliated ependymal identity.

During the last years the interest in the function of mammalian *Lin41* has increased. *Lin41* seems to be a highly polyvalent protein, with specific domains that perform different molecular functions depending on the biological context. Previous work was able to partially replicate the results published in our lab, like ubiquitination of AGO2 by *Lin41*, although they did not observed subsequent degradation (Loedige et al. 2012). In a similar manner, we could not reproduce some results like the positive regulation of *Cdkn1a* in mES cells lacking *Lin41* (Figure 22D). The large number of targets and regulatory mechanisms described by us and other groups probably reflects the versatility of *Lin41* in many pathways related to cell cycle, pluripotency or differentiation control. Further studies are necessary to confirm each one of its molecular mechanisms, to fully understand the role of this protein during mammal development and adulthood (Ecsedi & Grosshans 2013).

The present work describes the generation of the first *Lin41* conditional knockout mouse. This represents a valuable tool to address questions related to development and *Lin41* regulation by FGF signaling, avoiding embryonic lethality. The role of *Lin41* in the proliferative neuroepithelium and limb buds can be studied independently, with the use of Cre-lines under the desired promoter. The research of postnatal and post-mitotic cell types, such as ependymal cells, is particularly challenging in the *Lin41* gene trap mouse model, from the methodological point of

view. Conditional ablation allows reduced side effects and the study of the consequence of mutation in exclusive tissues and time points.

The characterization of *Lin41* expression in postnatal CNS raises new questions about *Lin41* function in that specialized niche, and the generation of a conditional knockout mouse simultaneously provides a valuable tool to undertake their study.

6 Bibliography

Abbott, A.L. et al., 2005. The let-7 MicroRNA family members mir-48, mir-84, and mir-241 function together to regulate developmental timing in Caenorhabditis elegans. *Developmental cell*, 9(3), pp.403–414.

Abeliovich, A. et al., 1992. On somatic recombination in the central nervous system of transgenic mice. *Science*, 257(5068), pp.404–410.

Alvarez-Buylla, A. & Lim, D.A., 2004. For the long run: maintaining germinal niches in the adult brain. *Neuron*, 41(5), pp.683–686.

Ambros, V., 1989. A hierarchy of regulatory genes controls a larva-to-adult developmental switch in C. elegans. *Cell*, 57(1), pp.49–57.

Ambros, V., 2000. Control of developmental timing in Caenorhabditis elegans. *Current Opinion in Genetics & Development*, 10(4), pp.428–433.

Ambros, V., 2004. The functions of animal microRNAs. *Nature*, 431(7006), pp.350–355.

Ambros, V. & Horvitz, H.R., 1984. Heterochronic mutants of the nematode Caenorhabditis elegans. *Science*, 226(4673), pp.409–416.

Anthony, T.E. et al., 2004. Radial glia serve as neuronal progenitors in all regions of the central nervous system. *Neuron*, 41(6), pp.881–890.

Balastik, M. et al., 2008. Deficiency in ubiquitin ligase TRIM2 causes accumulation of neurofilament light chain and neurodegeneration. *Proceedings of the National Academy of Sciences of the United States of America*, 105(33), pp.12016–12021.

Bartel, D.P., 2004. MicroRNAs: genomics, biogenesis, mechanism, and function. *Cell*, 116(2), pp.281–297.

Bartel, D.P., 2009. MicroRNAs: target recognition and regulatory functions. *Cell*, 136(2), pp.215–233.

Betschinger, J., Mechtler, K. & Knoblich, J.A., 2006. Asymmetric segregation of the tumor suppressor brat regulates self-renewal in Drosophila neural stem cells. *Cell*, 124(6), pp.1241–1253.

Borden, K.L., 1998. RING fingers and B-boxes: zinc-binding protein-protein interaction domains. *Biochemistry and cell biology = Biochimie et biologie cellulaire*, 76(2-3), pp.351–358.

Bradley, A. et al., 1984. Formation of germ-line chimaeras from embryo-derived teratocarcinoma cell lines. *Nature*, 309(5965), pp.255–256.

Breunig, J.J. et al., 2008. Primary cilia regulate hippocampal neurogenesis by mediating sonic hedgehog signaling. *Proceedings of the National Academy of Sciences of the United States of America*, 105(35), pp.13127–13132.

Brightman, M.W. & Palay, S.L., 1963. The Fine Structure of Ependyma in the Brain of the Rat. *The Journal of cell biology*, 19, pp.415–439.

Büssing, I., Slack, F.J. & Grosshans, H., 2008. let-7 microRNAs in development, stem cells and cancer. *Trends in molecular medicine*, 14(9), pp.400–409.

Calaora, V. et al., 1996. mCD24 expression in the developing mouse brain and in zones of secondary neurogenesis in the adult. *Neuroscience*, 73(2), pp.581–594.

Caygill, E.E. & Johnston, L.A., 2008. Temporal regulation of metamorphic processes in Drosophila by the let-7 and miR-125 heterochronic microRNAs. *Current biology : CB*, 18(13), pp.943–950.

Cecchi, C. & Boncinelli, E., 2000. Emx homeogenes and mouse brain development. *Trends in neurosciences*, 23(8), pp.347–352.

Chang, H.-M. et al., 2012. Trim71 cooperates with microRNAs to repress Cdkn1a expression and promote embryonic stem cell proliferation. *Nature Communications*, 3, pp.923–10.

Chen, C.-Y.A. et al., 2009. Ago–TNRC6 triggers microRNA-mediated decay by promoting two deadenylation steps. *Nature Structural & Molecular Biology*, 16(11), pp.1160–1166.

Chen, J., Lai, F. & Niswander, L., 2012. The ubiquitin ligase mLin41 temporally promotes neural progenitor cell maintenance through FGF signaling. *Genes & development*, 26(8), pp.803–815.

Chojnacki, A.K., Mak, G.K. & Weiss, S., 2009. Identity crisis for adult periventricular neural stem cells: subventricular zone astrocytes, ependymal cells or both? *Nature reviews Neuroscience*, 10(2), pp.153–163.

Conner, D.A., 2001. Mouse Embryonic Stem (ES) Cell Isolation. *Current protocols in molecular biology / edited by Frederick M Ausubel [et al]*, pp.1–9.

Cook, H.A. et al., 2004. The Drosophila SDE3 homolog armitage is required for oskar mRNA silencing and embryonic axis specification. *Cell*, 116(6), pp.817–829.

Copp, A.J., Greene, N.D.E. & Murdoch, J.N., 2003. The genetic basis of mammalian neurulation. *Nat Rev Genet*, 4(10), pp.784–793.

Corbit, K.C. et al., 2005. Vertebrate Smoothened functions at the primary cilium. *Nature*, 437(7061), pp.1018–1021.

Corti, S. et al., 2007. Isolation and characterization of murine neural stem/progenitor cells based on Prominin-1 expression. *Experimental neurology*, 205(2), pp.547–562.

Coskun, V. et al., 2008. CD133+ neural stem cells in the ependyma of mammalian postnatal forebrain. *Proceedings of the National Academy of Sciences of the United States of America*, 105(3), pp.1026–1031.

Cruz, C. et al., 2010. Foxj1 regulates floor plate cilia architecture and modifies the response of cells to sonic hedgehog signalling. *Development (Cambridge, England)*, 137(24), pp.4271–4282.

del Valle, I. et al., 2010. Characterization of novel monoclonal antibodies able to identify neurogenic niches and arrest neurosphere proliferation and differentiation. *Neuroscience*, 169(3), pp.1473–1485.

Deng, W., Aimone, J.B. & Gage, F.H., 2010. New neurons and new memories: how does adult hippocampal neurogenesis affect learning and memory? *Nature reviews Neuroscience*, 11(5), pp.339–350.

Deshaies, R.J. & Joazeiro, C.A.P., 2009. RING domain E3 ubiquitin ligases. *Annual review of biochemistry*, 78, pp.399–434.

Didier, M. et al., 1986. Differential immunocytochemical staining for glial fibrillary acidic (GFA) protein, S-100 protein and glutamine synthetase in the rat subcommissural organ, nonspecialized ventricular ependyma and adjacent neuropil. *Cell and tissue research*, 245(2), pp.343–351.

Doetsch, F. et al., 1999. Subventricular zone astrocytes are neural stem cells in the adult mammalian brain. *Cell*, 97(6), pp.703–716.

Ecsedi, M. & Grosshans, H., 2013. LIN-41/TRIM71: emancipation of a miRNA target. *Genes & development*, 27(6), pp.581–589.

Eriksson, P.S. et al., 1998. Neurogenesis in the adult human hippocampus. *Nature Medicine*, 4(11), pp.1313–1317.

Esquela-Kerscher, A. & Slack, F.J., 2006. Oncomirs - microRNAs with a role in cancer. *Nature reviews. Cancer*, 6(4), pp.259–269.

Frank, D.J. & Roth, M.B., 1998. ncl-1 is required for the regulation of cell size and ribosomal RNA synthesis in Caenorhabditis elegans. *The Journal of cell biology*, 140(6), pp.1321–1329.

Freemont, P.S., 2000. RING for destruction? *Current biology : CB*, 10(2), pp.R84–7.

Freemont, P.S., 1993. The RING finger. A novel protein sequence motif related to the zinc finger. *Annals of the New York Academy of Sciences*, 684, pp.174–192.

Freemont, P.S., Hanson, I.M. & Trowsdale, J., 1991. A novel cysteine-rich sequence motif. *Cell*, 64(3), pp.483–484.

Fridell, R.A. et al., 1995. Identification of a novel human zinc finger protein that specifically interacts with the activation domain of lentiviral Tat proteins. *Virology*, 209(2), pp.347–357.

Friedman, R.C. et al., 2009. Most mammalian mRNAs are conserved targets of microRNAs. *Genome Res*, 19(1), pp.92–105.

Frosk, P. et al., 2002. Limb-girdle muscular dystrophy type 2H associated with mutation in TRIM32, a putative E3-ubiquitin-ligase gene. *American journal of human genetics*, 70(3), pp.663–672.

Gage, F.H. et al., 1995. Survival and differentiation of adult neuronal progenitor cells transplanted to the adult brain. *Proc Natl Acad Sci U S A*, 92(25), pp.11879–11883.

Garcia, A.D.R. et al., 2004. GFAP-expressing progenitors are the principal source of constitutive neurogenesis in adult mouse forebrain. *Nature Neuroscience*, 7(11), pp.1233–1241.

Gerdes, J.M. et al., 2007. Disruption of the basal body compromises proteasomal function and perturbs intracellular Wnt response. *Nature genetics*, 39(11), pp.1350–1360.

Gilbert, S.F., 2005. *Developmental Biology* 7 ed, Sunderland (MA): Sinauer Associates; 2000.

ISBN-10: 0-87893-243-7.

Götz, M. & Huttner, W.B., 2005. The cell biology of neurogenesis. *Nature reviews Molecular cell biology*, 6(10), pp.777–788.

Gross, C.G., 2000. Neurogenesis in the adult brain: death of a dogma. *Nature reviews Neuroscience*, 1(1), pp.67–73.

Guirao, B. et al., 2010. Coupling between hydrodynamic forces and planar cell polarity orients mammalian motile cilia., 12(4), pp.341–350.

Hammond, S.M. et al., 2001. Argonaute2, a link between genetic and biochemical analyses of RNAi. *Science*, 293(5532), pp.1146–1150.

Han, Y.-G. et al., 2008. Hedgehog signaling and primary cilia are required for the formation of adult neural stem cells. *Nature Neuroscience*, 11(3), pp.277–284.

Hatfield, S. & Ruohola-Baker, H., 2008. microRNA and stem cell function. *Cell and tissue research*, 331(1), pp.57–66.

Herranz, H. et al., 2010. The miRNA machinery targets Mei-P26 and regulates Myc protein levels in the Drosophila wing. *The EMBO journal*, 29(10), pp.1688–1698.

Hicke, L., Schubert, H.L. & Hill, C.P., 2005. Ubiquitin-binding domains. *Nature reviews Molecular cell biology*, 6(8), pp.610–621.

Hoess, R.H., Ziese, M. & Sternberg, N., 1982. P1 site-specific recombination: nucleotide sequence of the recombining sites. *Proc Natl Acad Sci U S A*, 79(11), pp.3398–3402.

Horn, E.J., 2003. RING protein Trim32 associated with skin carcinogenesis has anti-apoptotic and E3-ubiquitin ligase properties. *Carcinogenesis*, 25(2), pp.157–167.

Hung, A.Y. et al., 2010. Degradation of Postsynaptic Scaffold GKAP and Regulation of Dendritic Spine Morphology by the TRIM3 Ubiquitin Ligase in Rat Hippocampal Neurons. *PloS one*, 5(3), p.e9842.

Huntzinger, E. & Izaurralde, E., 2011. Gene silencing by microRNAs: contributions of translational repression and mRNA decay. *Nat Rev Genet*, 12(2), pp.99–110.

Ibañez-Tallon, I. et al., 2004. Dysfunction of axonemal dynein heavy chain Mdnah5 inhibits ependymal flow and reveals a novel mechanism for hydrocephalus formation. *Human Molecular Genetics*, 13(18), pp.2133–2141.

Ibañez-Tallon, I., Heintz, N. & Omran, H., 2003. To beat or not to beat: roles of cilia in development and disease. *Human Molecular Genetics*, 12 Spec No 1, pp.R27–35.

Jacquet, B.V. et al., 2009. FoxJ1-dependent gene expression is required for differentiation of radial glia into ependymal cells and a subset of astrocytes in the postnatal brain. *Development (Cambridge, England)*, 136(23), pp.4021–4031.

Joazeiro, C.A. & Weissman, A.M., 2000. RING finger proteins: mediators of ubiquitin ligase activity. *Cell*, 102(5), pp.549–552.

Johnson, S.M. et al., 2005. RAS is regulated by the let-7 microRNA family. *Cell*, 120(5), pp.635–647.

Khazaei, M.R. et al., 2011. The E3-ubiquitin ligase TRIM2 regulates neuronal polarization. *Journal of neurochemistry*, 117(1), pp.29–37.

Kim, J., Kato, M. & Beachy, P.A., 2009. Gli2 trafficking links Hedgehog-dependent activation of Smoothened in the primary cilium to transcriptional activation in the nucleus. *Proceedings of the National Academy of Sciences of the United States of America*, 106(51), pp.21666–21671.

Kim, V.N., 2005. MicroRNA biogenesis: coordinated cropping and dicing. *Nature reviews Molecular cell biology*, 6(5), pp.376–385.

Kloosterman, W.P. et al., 2004. Substrate requirements for let-7 function in the developing zebrafish embryo. *Nucleic Acids Research*, 32(21), pp.6284–6291.

Kriegstein, A. & Alvarez-Buylla, A., 2009. The glial nature of embryonic and adult neural stem cells. *Annual review of neuroscience*, 32(1), pp.149–184.

Kudryashova, E. et al., 2009. Deficiency of the E3 ubiquitin ligase TRIM32 in mice leads to a myopathy with a neurogenic component. *Human Molecular Genetics*, 18(7), pp.1353–1367.

Kudryashova, E. et al., 2005. Trim32 is a ubiquitin ligase mutated in limb girdle muscular dystrophy type 2H that binds to skeletal muscle myosin and ubiquitinates actin. *Journal of molecular biology*, 354(2), pp.413–424.

Lancman, J.J. et al., 2005. Analysis of the regulation of lin-41during chick and mouse limb

development. *Developmental dynamics : an official publication of the American Association of Anatomists*, 234(4), pp.948–960.

Lee, R., Feinbaum, R. & Ambros, V., 2004. *A short history of a short RNA*,

Lee, R.C., Feinbaum, R.L. & Ambros, V., 1993. The C. elegans heterochronic gene lin-4 encodes small RNAs with antisense complementarity to lin-14. *Cell*, 75(5), pp.843–854.

Lee, Y. et al., 2003. The nuclear RNase III Drosha initiates microRNA processing. *Nature*, 425(6956), pp.415–419.

Lee, Y.S. et al., 2005. Depletion of human micro-RNA miR-125b reveals that it is critical for the proliferation of differentiated cells but not for the down-regulation of putative targets during differentiation. *The Journal of biological chemistry*, 280(17), pp.16635–16641.

Lim, L.P., Glasner, M.E., et al., 2003a. Vertebrate microRNA genes. *Science*, 299(5612), p.1540.

Lim, L.P., Lau, N.C., et al., 2003b. The microRNAs of Caenorhabditis elegans. *Genes & development*, 17(8), pp.991–1008.

Lin, Y.-C. et al., 2007. Human TRIM71 and its nematode homologue are targets of let-7 microRNA and its zebrafish orthologue is essential for development. *Molecular biology and evolution*, 24(11), pp.2525–2534.

Liu, P., Jenkins, N. & Copeland, N., 2003. A highly efficient recombineering-based method for generating conditional knockout mutations. *Genome Res*, 13(3), pp.476–484.

Loedige, I. et al., 2012. The mammalian TRIM-NHL protein TRIM71/LIN-41 is a repressor of mRNA function. *Nucleic Acids Research*.

Logan, M. et al., 2002. Expression of Cre Recombinase in the developing mouse limb bud driven by a Prxl enhancer. *genesis*, 33(2), pp.77–80.

Loh, Y.-H. et al., 2006. The Oct4 and Nanog transcription network regulates pluripotency in mouse embryonic stem cells. *Nature genetics*, 38(4), pp.431–440.

Löer, B. et al., 2008. The NHL-domain protein Wech is crucial for the integrin-cytoskeleton link. *Nature cell biology*, 10(4), pp.422–428.

Lund, E. et al., 2004. Nuclear export of microRNA precursors. *Science*, 303(5654), pp.95–98.

Malatesta, P. & Gotz, M., 2013. Radial glia - from boring cables to stem cell stars. *Development (Cambridge, England)*, 140(3), pp.483–486.

Malatesta, P. et al., 2003. Neuronal or glial progeny: regional differences in radial glia fate. *Neuron*, 37(5), pp.751–764.

Maller Schulman, B.R. et al., 2008. The let-7 microRNA target gene, Mlin41/Trim71 is required for mouse embryonic survival and neural tube closure. *Cell cycle (Georgetown, Tex)*, 7(24), pp.3935–3942.

Mansfield, J.H. et al., 2004. MicroRNA-responsive “sensor” transgenes uncover Hox-like and other developmentally regulated patterns of vertebrate microRNA expression. *Nature genetics*, 36(10), pp.1079–1083.

McConnell, S.K., 1995. Constructing the cerebral cortex: neurogenesis and fate determination. *Neuron*, 15(4), pp.761–768.

Merkle, F.T. & Alvarez-Buylla, A., 2006. Neural stem cells in mammalian development. *Current opinion in cell biology*, 18(6), pp.704–709.

Merkle, F.T. et al., 2004. Radial glia give rise to adult neural stem cells in the subventricular zone. *Proc Natl Acad Sci U S A*, 101(50), pp.17528–17532.

Meroni, G. & Diez-Roux, G., 2005. TRIM/RBCC, a novel class of “single protein RING finger” E3 ubiquitin ligases. *Bioessays*, 27(11), pp.1147–1157.

Mirzadeh, Z. et al., 2008. Neural stem cells confer unique pinwheel architecture to the ventricular surface in neurogenic regions of the adult brain. *Cell stem cell*, 3(3), pp.265–278.

Mirzadeh, Z., Coates, P.W., et al., 2010a. Cilia organize ependymal planar polarity. *The Journal of neuroscience : the official journal of the Society for Neuroscience*, 30(7), pp.2600–2610.

Mirzadeh, Z., Doetsch, F., et al., 2010b. The subventricular zone en-face: wholemount staining and ependymal flow. *Journal of visualized experiments : JoVE*, (39).

Moss, E.G., 2007. Heterochronic genes and the nature of developmental time. *Current Biology*, 17(11), pp.R425–34.

Moss, E.G., Lee, R.C. & Ambros, V., 1997. The cold shock domain protein LIN-28 controls developmental timing in C. elegans and is regulated by the lin-4 RNA. *Cell*, 88(5), pp.637–646.

Muresan, V. et al., 1993. Gamma-tubulin in differentiated cell types: localization in the vicinity of basal bodies in retinal photoreceptors and ciliated epithelia. *Journal of Cell Science*, 104 (Pt 4), pp.1229–1237.

Neumüller, R.A. et al., 2008. Mei-P26 regulates microRNAs and cell growth in the Drosophila ovarian stem cell lineage. *Nature*, 454(7201), pp.241–245. Available at: http://eutils.ncbi.nlm.nih.gov/entrez/eutils/elink.fcgi?dbfrom=pubmed&id=18528333&retmode=ref&cmd=prlinks.

Nimmo, R.A. & Slack, F.J., 2009. An elegant miRror: microRNAs in stem cells, developmental timing and cancer. *Chromosoma*, 118(4), pp.405–418.

Nishimura, Y. et al., 2006. Ciliated Cells Differentiated from Mouse Embryonic Stem Cells. *Stem cells (Dayton, Ohio)*, 24(5), pp.1381–1388.

O'farrell, F. et al., 2008. Regulation of the Drosophila lin-41 homologue dappled by let-7 reveals conservation of a regulatory mechanism within the LIN-41 subclade. *Developmental dynamics : an official publication of the American Association of Anatomists*, 237(1), pp.196–208.

Paez-Gonzalez, P. et al., 2011. Ank3-dependent SVZ niche assembly is required for the continued production of new neurons. *Neuron*, 71(1), pp.61–75.

Papaioannou, V.E. & Behringer, R.R., 2011. Early Embryonic Lethality in Genetically Engineered Mice: Diagnosis and Phenotypic Analysis. *Veterinary pathology*.

Pasquinelli, A.E. et al., 2000. Conservation of the sequence and temporal expression of let-7 heterochronic regulatory RNA. *Nature*, 408(6808), pp.86–89.

Pasquinelli, A.E. et al., 2003. Expression of the 22 nucleotide let-7 heterochronic RNA throughout the Metazoa: a role in life history evolution? *Evolution & development*, 5(4), pp.372–378.

Pfenninger, C.V. et al., 2007. CD133 is not present on neurogenic astrocytes in the adult subventricular zone, but on embryonic neural stem cells, ependymal cells, and glioblastoma cells. *Cancer research*, 67(12), pp.5727–5736.

Pfenninger, C.V. et al., 2011. Prospectively isolated CD133/CD24-positive ependymal cells from the adult spinal cord and lateral ventricle wall differ in their long-term in vitro self-renewal and in vivo gene expression. *Glia*, 59(1), pp.68–81.

Plasterk, R.H.A., 2006. Micro RNAs in animal development. *Cell*, 124(5), pp.877–881.

Poteete, A.R., 2001. What makes the bacteriophage lambda Red system useful for genetic engineering: molecular mechanism and biological function. *FEMS microbiology letters*, 201(1), pp.9–14.

Reinhart, B.J. et al., 2000. The 21-nucleotide let-7 RNA regulates developmental timing in Caenorhabditis elegans. *Nature*, 403(6772), pp.901–906.

Reymond, A. et al., 2001. The tripartite motif family identifies cell compartments. *The EMBO journal*, 20(9), pp.2140–2151.

Reynolds, B.A. & Weiss, S., 1996. Clonal and population analyses demonstrate that an EGF-responsive mammalian embryonic CNS precursor is a stem cell. *Developmental Biology*, 175(1), pp.1–13.

Reynolds, B.A. & Weiss, S., 1992. Generation of neurons and astrocytes from isolated cells of the adult mammalian central nervous system. *Science*, 255(5052), pp.1707–1710.

Reynolds, B.A., Tetzlaff, W. & Weiss, S., 1992. A multipotent EGF-responsive striatal embryonic progenitor cell produces neurons and astrocytes. *The Journal of neuroscience : the official journal of the Society for Neuroscience*, 12(11), pp.4565–4574.

Richards, L.J., Kilpatrick, T.J. & Bartlett, P.F., 1992. De novo generation of neuronal cells from the adult mouse brain. *Proc Natl Acad Sci U S A*, 89(18), pp.8591–8595.

Rodriguez, A. et al., 1996. Identification of immune system and response genes, and novel mutations causing melanotic tumor formation in Drosophila melanogaster. *Genetics*, 143(2), pp.929–940.

Roush, S. & Slack, F.J., 2008. The let-7 family of microRNAs. *Trends in cell biology*, 18(10), pp.505–516.

Rybak, A., 2009. *Expression and function of the let-7 microRNA during stem cell specification and development of the CNS*.

Rybak, A. et al., 2008. A feedback loop comprising lin-28 and let-7 controls pre-let-7 maturation during neural stem-cell commitment. *Nature cell biology*, 10(8), pp.987–993.

Rybak, A. et al., 2009. The let-7 target gene mouse lin-41 is a stem cell specific E3 ubiquitin ligase for the miRNA pathway protein Ago2. *Nature cell biology*, 11(12), pp.1411–1420.

Sanz-Ezquerro, J.J. & Tickle, C., 2000. Autoregulation of Shh expression and Shh induction of cell death suggest a mechanism for modulating polarising activity during chick limb development. *Development (Cambridge, England)*, 127(22), pp.4811–4823.

Sauer, F.C., 1935. Mitosis in the neural tube. *Journal of Comparative Neurology*, 62(2), pp.377–405.

Schulman, B.R.M., Esquela-Kerscher, A. & Slack, F.J., 2005. Reciprocal expression of lin-41 and the microRNAs let-7 and mir-125 during mouse embryogenesis. *Developmental dynamics : an official publication of the American Association of Anatomists*, 234(4), pp.1046–1054.

Schwamborn, J.C., Berezikov, E. & Knoblich, J.A., 2009. The TRIM-NHL protein TRIM32 activates microRNAs and prevents self-renewal in mouse neural progenitors. *Cell*, 136(5), pp.913–925.

Sempere, L.F. et al., 2003. Temporal regulation of microRNA expression in Drosophila melanogaster mediated by hormonal signals and broad-Complex gene activity. *Developmental Biology*, 259(1), pp.9–18.

Sempere, L.F. et al., 2002. The expression of the let-7 small regulatory RNA is controlled by ecdysone during metamorphosis in Drosophila melanogaster. *Developmental Biology*, 244(1), pp.170–179.

Shen, Q. et al., 2008. Adult SVZ stem cells lie in a vascular niche: a quantitative analysis of niche cell-cell interactions. *Cell stem cell*, 3(3), pp.289–300.

Shen, Q. et al., 2004. Endothelial cells stimulate self-renewal and expand neurogenesis of neural stem cells. *Science*, 304(5675), pp.1338–1340.

Slack, F.J. & Ruvkun, G., 1998. A novel repeat domain that is often associated with RING finger and B-box motifs. *Trends in biochemical sciences*, 23(12), pp.474–475.

Slack, F.J. et al., 2000. The lin-41 RBCC gene acts in the C. elegans heterochronic pathway between the let-7 regulatory RNA and the LIN-29 transcription factor. *Molecular cell*, 5(4), pp.659–669.

Smirnova, L. et al., 2005. Regulation of miRNA expression during neural cell specification. *The European journal of neuroscience*, 21(6), pp.1469–1477.

Smithies, O. et al., 1985. Insertion of DNA sequences into the human chromosomal beta-globin locus by homologous recombination. *Nature*, 317(6034), pp.230–234.

Sokol, N.S. et al., 2008. Drosophila let-7 microRNA is required for remodeling of the neuromusculature during metamorphosis. *Genes & development*, 22(12), pp.1591–1596.

Sonoda, J., 2001. Drosophila Brain Tumor is a translational repressor. *Genes & development*, 15(6), pp.762–773.

Spassky, N. et al., 2005. Adult ependymal cells are postmitotic and are derived from radial glial cells during embryogenesis. *The Journal of neuroscience : the official journal of the Society for Neuroscience*, 25(1), pp.10–18.

Stanford, W.L., Cohn, J.B. & Cordes, S.P., 2001. Gene-trap mutagenesis: past, present and beyond. *Nat Rev Genet*, 2(10), pp.756–768.

Stegmüller, J. & Bonni, A., 2010. Destroy to create: E3 ubiquitin ligases in neurogenesis. *F1000 Biology Reports*, pp.1–5.

Sugawara, A. et al., 2006. Current status of chromosomal abnormalities in mouse embryonic stem cell lines used in Japan. *Comparative medicine*, 56(1), pp.31–34.

Sun, X., Mariani, F.V. & Martin, G.R., 2002. Functions of FGF signalling from the apical ectodermal ridge in limb development. *Nature*, 418(6897), pp.501–508.

Tavazoie, M. et al., 2008. A specialized vascular niche for adult neural stem cells. *Cell stem cell*, 3(3), pp.279–288.

Thomas, K.R., Deng, C. & Capecchi, M.R., 1992. High-fidelity gene targeting in embryonic stem cells by using sequence replacement vectors. *Molecular and cellular biology*, 12(7), pp.2919–2923.

Thompson, S. et al., 2011. Identification of a novel Bcl-2-interacting mediator of cell death (Bim) E3 ligase, tripartite motif-containing protein 2 (TRIM2), and its role in rapid ischemic tolerance-induced neuroprotection. *The Journal of biological chemistry*, 286(22), pp.19331–19339.

Thrower, J.S. et al., 2000. Recognition of the polyubiquitin proteolytic signal. *The EMBO journal*, 19(1), pp.94–102.

Torok, M. & Etkin, L.D., 2001. Two B or not two B? Overview of the rapidly expanding B-box family

of proteins. *Differentiation*, 67(3), pp.63–71.

Valencia-Sanchez, M.A. et al., 2006. Control of translation and mRNA degradation by miRNAs and siRNAs. *Genes & development*, 20(5), pp.515–524.

Vella, M.C. et al., 2004. The C. elegans microRNA let-7 binds to imperfect let-7 complementary sites from the lin-41 3'UTR. *Genes & development*, 18(2), pp.132–137.

Wightman, B. et al., 1991. Negative regulatory sequences in the lin-14 3'-untranslated region are necessary to generate a temporal switch during Caenorhabditis elegans development. *Genes & development*, 5(10), pp.1813–1824.

Wightman, B., Ha, I. & Ruvkun, G., 1993. Posttranscriptional regulation of the heterochronic gene lin-14 by lin-4 mediates temporal pattern formation in C. elegans. *Cell*, 75(5), pp.855–862.

Winter, J. et al., 2009. Many roads to maturity: microRNA biogenesis pathways and their regulation. *Nature cell biology*, 11(3), pp.228–234.

Wu, L. & Belasco, J.G., 2005. Micro-RNA regulation of the mammalian lin-28 gene during neuronal differentiation of embryonal carcinoma cells. *Molecular and cellular biology*, 25(21), pp.9198–9208.

Wu, Y. et al., 2009. High-efficient FLPo deleter mice in C57BL/6J background. *PloS one*, 4(11), p.e8054.

Wulczyn, F.G. et al., 2011. miRNAs Need a Trim : Regulation of miRNA Activity by Trim-NHL Proteins. *Advances in experimental medicine and biology*, 700, pp.85–105.

Yan, Q. et al., 2005. CART: an Hrs/actinin-4/BERP/myosin V protein complex required for efficient receptor recycling. *Molecular biology of the cell*, 16(5), pp.2470–2482.

Yang, D.H. & Moss, E.G., 2003. Temporally regulated expression of Lin-28 in diverse tissues of the developing mouse. *Gene expression patterns : GEP*, 3(6), pp.719–726.

Yokoyama, S. et al., 2008. Dynamic gene expression of Lin-28 during embryonic development in mouse and chicken. *Gene expression patterns : GEP*, 8(3), pp.155–160.

Yu, D. et al., 2000. An efficient recombination system for chromosome engineering in Escherichia coli. *Proc Natl Acad Sci U S A*, 97(11), pp.5978–5983.

Yu, X. et al., 2008. Foxj1 transcription factors are master regulators of the motile ciliogenic program. *Nature genetics*, 40(12), pp.1445–1453.

Zamore, P.D., 2002. Evidence that siRNAs Function as Guides, Not Primers, in the Drosophila and Human RNAi Pathways. pp.1–12.

Zeng, Y., Yi, R. & Cullen, B.R., 2003. MicroRNAs and small interfering RNAs can inhibit mRNA expression by similar mechanisms. *Proc Natl Acad Sci U S A*, 100(17), pp.9779–9784.

Zhang, Y. et al., 1998. A new logic for DNA engineering using recombination in Escherichia coli. *Nature genetics*, 20(2), pp.123–128.

Zhao, C., Deng, W. & Gage, F.H., 2008. Mechanisms and functional implications of adult neurogenesis. *Cell*, 132(4), pp.645–660.

Zhou, A.-X., Hartwig, J.H. & Akyürek, L.M., 2010. Filamins in cell signaling, transcription and organ development. *Trends in cell biology*, 20(2), pp.113–123.